

TRABAJO ESPECIAL DE GRADO

IMPLEMENTATION OF POWER FLOW CALCULATIONS FOR DISTRIBUTION SYSTEMS – APPLICATION TO WEAKLY MESHED, UNBALANCED AND HARMONIC CASES

Prof. Guía: Gianfranco Chicco.

Presentado ante la Ilustre
Universidad Central de Venezuela
por la Br. Elyka Abello R.
para optar al Título de
Ingeniero Electricista.

Caracas, 2011

*A mis padres,
quienes con su apoyo, amor y sabiduría
me han guiado por los caminos de la vida
que me trajeron hasta aquí.*

Acknowledgements

I would like to thank the three institutions that made this amazing experience possible: Universidad Central de Venezuela for giving me the opportunity to finish my career in Italy; Politecnico di Torino for receiving me in a very kindly way and giving me the tools needed to complete my career; Fondo de Investigación y Desarrollo de las Telecomunicaciones for the trust and the investment they made in me. A special thanks goes to Professor Gianfranco Chicco, who guided me and helped me through this project.

Then I would like to thank my family who made me the person I am today. Nana, Kaki and Jose, who were an essential part in my child development; Kael, pioneer in every stage of life, he has been and always will be an example to follow; my father and my mother, reason and heart, always together, thank you for your unconditional love, support, advice and teachings, without them I would not have been successful in my life; and Tomás, without his support and help I could not have made this project possible.

I also would like to thank the other part of my family, those ones that I found in Torino: Peppe, Elka and Tomás Chile, thank you for being there listening and encouraging me in the most critical moments, Scuzza, Ani, Jacopo, Jonnahtan and the Diegos, thank you all for your unconditional support and your invaluable friendship, I hope it will remain over the years.

I also want to thank those friends and family in Venezuela: Jody, Orlando, Héctor and Francisco, you were a very important part of all that I have learned in the UCV; Balam, thank you for your help, it arrives just in time; Carlos and Alfredo, two great teachers that helped and supported me in critical moments of my life.

All of you in one way or another helped me in the most difficult moments of my career or joined me in the happier moments of these years.

Elyka Abello

**IMPLEMENTATION OF POWER FLOW
CALCULATIONS FOR DISTRIBUTION SYSTEMS –
APPLICATION TO WEAKLY MESHED,
UNBALANCED AND HARMONIC CASES**

Prof. Guía: Gianfranco Chicco. Tesis. Caracas. UCV. Facultad de Ingeniería. Escuela de Ingeniería Eléctrica. Ingeniero Electricista. Opción: Potencia. Institución: Politécnico di Torino. 2010.

Palabras claves: flujo de potencia; backward/forward sweep; armónicas; redes radiales; redes débilmente malladas; sistemas de distribución.

Resumen. En este trabajo especial de grado se implementó el algoritmo del *backward/forward sweep* (BFS) como método para resolver redes radiales o débilmente malladas, como es normalmente la estructura de los sistemas de distribución. Dicho método utiliza las características típicas de estas topologías de redes para simplificar las ecuaciones del sistema y así optimizar el tiempo consumido para encontrar la solución de la red. Sin embargo, este tipo de métodos presenta particulares problemas con los límites de convergencia que han sido estudiados para el análisis de sistemas eléctricos sin presencia de componentes armónicas. En este trabajo se amplió el estudio y se identificaron los límites de convergencia del método en presencia de componentes armónicas, mediante la implementación de dos variantes del BFS aplicadas a una red trifásica desbalanceada en presencia de cargas no lineales. La implementación se realizó mediante la programación en Matlab[®] de los algoritmos estudiados y su aplicación a tres redes de prueba, con la posterior verificación de los resultados obtenidos.

Contents

Acknowledgements	iv
1 Introduction	1
2 Harmonic Distortion	4
2.1 Harmonic Sources	5
2.1.1 Nonlinear Voltage-Current Sources	6
2.1.2 Line-Commutated Solid State Converters	6
2.1.3 High Frequency Sources	8
2.1.4 Non-Harmonic Sources	9
2.2 Effects of Harmonic Presence in the Power Networks	10
2.2.1 Effects on Power System Quantities	11
2.2.2 Effects on System Components	13
2.2.3 Resonance	17
2.3 Voltage Quality Standards	21
2.3.1 IEEE Standard 519-1992	21
2.3.2 IEC 61000	26

2.3.3	EN 50160	30
3	Power System Analysis	32
3.1	Distribution System Analysis	33
3.1.1	Backward-Forward Sweep	34
3.1.2	Weakly Meshed Network Treatment	41
3.2	Harmonic Analysis	43
3.2.1	Direct Harmonic Solutions	45
3.2.2	Iterative Harmonic Analysis	47
4	Components Modeling	49
4.1	Modeling At Fundamental Frequency	49
4.1.1	Transmission Lines	49
4.1.2	Transformers	57
4.1.3	Spot Loads	60
4.1.4	Distributed Loads	62
4.2	Modeling For Harmonic Studies	63
4.2.1	Transmission Lines	63
4.2.2	Transformers	66
4.2.3	Linear Loads	67
4.2.4	Non-Linear Loads	72
5	Methodology	80

6	Results and Discussion	84
6.1	Description of the Methods	84
6.1.1	Load Flow at the Fundamental Frequency	85
6.1.2	Harmonic Analysis Method 1	88
6.1.3	Harmonic Analysis Method 2	95
6.2	Convergence for Harmonic Analysis Methods Based on Backward/Forward Sweep Technique	95
6.3	Application of the Methods	100
6.3.1	Fundamental Power Flow	100
6.3.2	Harmonic Power Flow	103
6.3.3	Weakly Meshed Networks	108
6.4	Power Flow Results	113
6.4.1	Load Flow at the Fundamental Frequency	113
6.4.2	Harmonic Analysis Method 1	113
6.4.3	Harmonic Analysis Method 2	116
6.4.4	Fundamental Power Flow for a Weakly Meshed Single Phase Network	117
6.5	Comparison of the Methods	119
7	Conclusions and Recommendations	121
A	Test System	123
A.1	For Harmonic Analysis	123
A.2	For Weakly Meshed Networks	126

B Power Flow Results	127
B.1 Fundamental Power Flow Results	127
B.2 Harmonic Power Flow Results	132
B.2.1 Method 1	132
B.2.2 Method 2	160
B.3 Fundamental Power Flow Results for Weakly Meshed Network	170
 Bibliography	 175

List of Tables

2.1	Low-voltage distortion limits [57].	23
2.2	Basis for harmonic current limits [57]	23
2.3	Current distortion limits for general distribution, subtransmission and transmission systems [57]	24
2.4	Total demand distortion (TDD) limits [57]	25
2.5	Harmonic voltage distortion limits in percent of V_n [57]	26
2.6	Compatibility levels for individual harmonics in the low-voltage network according to IEC 61000-2-2.	27
2.7	Harmonic current limits for class A equipment according to IEC 61000-2-2.	28
2.8	Harmonic current limits for class C equipment according to IEC 61000-2-2.	28
2.9	Harmonic current limits for class D equipment according to IEC 61000-2-2.	28
2.10	Harmonic current limits according to IEC 61000-3-4.	29
2.11	Compatibility levels for harmonic Voltages (in percent of fundamental) for LV and MV systems according to IEC 61000-3-6.	29
2.12	Planning levels for harmonic Voltages (in percent of fundamental) for MV systems according to IEC 61000-3-6.	30

2.13 Planning levels for harmonic Voltages (in percent of fundamental) for HV and EHV systems according to IEC 61000-3-6.	30
2.14 Limits for total harmonic distortion according to IEC 61000-3-4.	31
2.15 Harmonic Voltages limits at the supply terminals according to EN 50160.	31
4.1 Submatrices of Three-Phase Transformer Connections	60
6.1 Resistive system working in a point previous to the maximum power transfer: $R_{load} = 2\text{p.u.}$ $R_{line} = 1\text{p.u.}$	96
6.2 System in the point of maximum power transfer: $R_{load} = R_{line} = 1\text{p.u.}$.	97
6.3 Resistive system after the maximum power transfer: $R_{load} = 1\text{ p.u.}$ $R_{line} = 2\text{ p.u.}$	97
6.4 Sistem working in a point previous resonance condition: $Z_{load} = -j^2\text{ p.u.}$ $Z_{line} = j\text{ p.u.}$	98
6.5 Sistem in resonance condition: $Z_{load} = -jp.u.$ $Z_{line}^* = j\text{ p.u.}$	99
6.6 Sistem working in a point after the resonance condition: $Z_{load} = -j\text{ p.u.}$ $Z_{line} = j^2\text{ p.u.}$	100
6.7 Power flow results for the 13 node network without harmonic sources. .	113
6.8 Bus voltages for the 13 node network without harmonic sources	114
6.9 Branch currents for the 13 node network without harmonic sources . . .	114
6.10 Active power losses for the 13 node network without harmonic sources.	115
6.11 Bus voltages in p.u. at each harmonic order for the 4 node test feeder with harmonic sources, obtained with the method 1.	115
6.12 Branch currents in amperes at each harmonic order for the 4 node test feeder with harmonic sources, obtained with the method 1.	116
6.13 Active power losses for the 4 node test feeder with harmonic sources, obtained with the method 1.	116

6.14	Active power losses for the 4 node test feeder with harmonic sources, obtained with the method 2.	117
6.15	Bus voltages in p.u. at each harmonic order for the 4 node test feeder with harmonic sources, obtained with the method 2.	117
6.16	Branch currents in amperes at each harmonic order for the 4 node test feeder with harmonic sources, obtained with the method 2.	118
6.17	Branch currents obtained with the application of BFS to a weakly meshed single phase network without harmonic sources.	119
6.18	Bus voltages obtained with the application of BFS to a weakly meshed single phase network without harmonic sources and comparison with the PowerWorld's solution.	119
A.1	Load specification for harmonic analysis test system.	123
A.2	Shunt capacitors bank specification for harmonic analysis test system.	124
A.3	Transformer data for harmonic analysis test system.	124
A.4	Lines specification for harmonic analysis test system.	124
A.5	Harmonic current magnitude as % of fundamental component and phase angles with respect to voltage.	125
A.6	Load specification for the single phase weakly meshed test system.	126
A.7	Lines impedance data for the single phase weakly meshed test system.	126

List of Figures

2.1	Example of a current distorted by a non linear load [15].	5
2.2	Distorted waveform and its components [15].	5
2.3	The six-pulse line-commutated converter.	7
2.4	Typical configurations of (a) AC/DC motor drives (b) DC motor drive and (c) the HVDC link.	8
2.5	Power factor for the (a) sinusoidal case and (b) nonsinusoidal case.	13
2.6	Simplified distribution system with parallel resonance [15].	18
2.7	Simplified distribution system with series resonance [57].	19
2.8	Frequency response of a system with series resonance [15].	20
2.9	Simple circuit for hand calculations [57].	20
3.1	Example of the node labeling in a radial network	34
3.2	Example of a path: $path(11) = \{1,3,7,8,11\}$	35
3.3	Two-node system.	40
3.4	V(P) curve for the two-node system [7].	41
3.5	(a) Weakly meshed network (b) Breakpoint representation using nodal current injections	42
3.6	Three phase breakpoint representation using nodal current injections	44

3.7	Network decomposition for the direct solution approach.	46
3.8	Structure diagram of the direct solution.	47
3.9	Structure diagram of the iterative solution.	48
4.1	Conductors and images geometrical configuration.	51
4.2	Representation of the impedances for a four-wire wye line segment. . .	52
4.3	Equivalent Pi-Line Model	54
4.4	Three-phase transformer	58
4.5	Uniformly distributed loads.	62
4.6	Exact lumped load model.	63
4.7	Overhead Line Model	64
4.8	Three-limb transformer	67
4.9	Magnetic equivalent circuit for a three-phase transformer	68
4.10	Load Models: (a) A (b) B (c) C and (d) D	71
4.11	Transfer functions: (a) $G_{\phi,dc}$ and (b) $G_{\phi,ac}$	74
4.12	Various types of ASD configuration: (a) VSI and PWM and (b) CSI . .	76
4.13	Generic converter circuit for ASD	76
4.14	Harmonic equivalent circuit for ASDs	77
4.15	Measured impedance of a synchronous motor [24]	79
5.1	One line diagram of the unbalanced test system.	81
5.2	(a) One line diagram of the single phase test system for weakly meshed network treatment and (b) its implementation in PowerWorld.	83
6.1	Example of the branch labeling in a radial network	85

6.2	Example of a two node resistive circuit.	96
6.3	Example of a two node equivalent circuit for harmonic analysis.	98
6.4	Flow chart of the power flow for fundamental component of a radial distribution network.	101
6.5	Flow chart of the harmonic power flow for radial distribution systems.	105
6.6	Flow chart of the method 1.	106
6.7	Flow chart of the method 2.	107
6.8	Flow chart of the load flow for weakly meshed distribution systems (I).	110
6.9	Flow chart of the load flow for weakly meshed distribution systems (II).	111
6.10	Presentacion.	112
6.11	One line diagram of the single phase test system after the cut of the breakpoint.	118
A.1	IEEE 4 node test feeder.	123
A.2	Pole Configuration.	124
A.3	Weakly Meshed Test System.	126

Chapter 1

Introduction

The concept of power quality is certainly not a new concern, but it is a subject that each day brings more and more interest for the power industry. Some of the main reasons for this fact are the growing numbers of power electronic devices in the network which increase the harmonic currents injected in the transmission and distribution power system, the increase of microprocessor-based controls and other devices more sensitive to power quality variations, the end users increased awareness of the power quality issues, and in some cases, the deregulation of the utility has complicated the power quality problems because of the possibility of the agencies to exploit the laws regarding the flow of money instead of the physical laws of power flow [15]. So nowadays a lot of resources and efforts are being devoted to the researches in the power quality fields.

The term of “power quality” can be defined as the capacity of an electrical power system to feed loads without problems and without damages, which is linked to the quality of the supply voltage. It also can be defined as the ability to function without creating problems and without reducing the efficiency of the power system, which is linked to the quality of the waveform of the current. Both definitions are strictly related to the waveforms of the system voltage and currents. In other words, power quality is strongly linked to the harmonic levels existing in the power system, called “harmonic distortion”. In addition to the overheating and high losses problems in the network components, the harmonic distortion may introduce a resonance condition in the system, generating over currents or over voltages situations that can be very harmful.

Standards on harmonics have been developed by various international organizations, such as the IEEE Standard 519-1992 [57], the IEC 61000 and the EN50160. The principal scope of these standards is to unify the harmonic distortion limits to ensure a good compatibility between the system equipment and the end-use equipment. These

limits are expressed in terms of the individual harmonic voltage distortion, the total voltage distortion (THD) or the total demand distortion (TDD). If the system already exists, the evaluation of the voltage limits or the index has to be done based of measurements done to the network components. The IEEE Standard 519-1992 [57] provides a guideline on the measuring procedures. If instead the system is planned or new, the harmonic source have to be characterized using manufacturer's data and the harmonic distortion levels have to be calculated on the basis of a model of the system. The system operating condition is obtained with a power flow calculation.

Power flow analysis, also known as load flow analysis, typically gives the voltage magnitudes and angles at all nodes of the feeder, the active and reactive power flow in each line section, the ranch currents specified in magnitude and angle, or magnitude and power factor, the power loss in each line section, the total feeder active and reactive power inputs, the total feeder power losses and the loads actual active and reactive power consumption. In its simplest form, the power flow is applied to a single phase system or a single phase equivalent of a three phase balanced system. However, in recent years, with the proliferation of large capacity unbalanced loads including electric locomotives, electric arc furnaces, unbalances among the three phases in power systems have become ever more significant. Under such conditions, the errors obtained applying a single phase equivalent power flow can become unacceptably large to be ignored, making a three-phase unbalanced load flow calculation required for the distribution system analysis. It is well known that the distribution system are more affected by the unbalances of the power networks than the transmission system, due to the nature of the loads, the existing of single and double phase cables and the fact that the unbalances do not compensate each others. Added to this fact, there is the unbalance due to the harmonic distortion. The theoretical analysis shows that in a three phase system even if the nonlinear characteristics in each phase are the same, as the nonlinear characteristic may be the function of the voltage over the nonlinear element and/or current through it, the instantaneous parameters in three-phase circuit are unbalanced because the instantaneous voltages across each phase are different [11]. Therefore, is clear the choice of three phase power flow in the case of harmonic analysis, especially in distribution networks.

Commercial programs have been developed to apply special techniques for harmonic analysis and improve the obtained results compared with the application of fundamental frequency analysis programs to harmonic studies. Among the most important of these computer tools, the following ones may be mentioned: the Network Frequency Response Analysis Program (1975), the first commercial computer program specifically designed to automate analysis of harmonic flows on large-scale systems; the McGraw-Edison Harmonic Analysis Program (1984), written in Fortran for micro-computers, includes an interactive graphical output; the V-HARM program, the one written expressly for the PC environment; the SuperHarm program, the recent version of the V-HARM written in C++ language for the Microsoft Windows environment; the

CYMHARMO program, actually written in a mixture of Fortran and C languages; and the NEPLAN program, which licensed version allows the harmonic analysis for three phase networks. Harmonic problems can also be solved on electromagnetic transient analysis programs, such as EMTP, but usually this results in less efficient solutions [15].

All programs mentioned above are private and need licenses to be used, limiting the students and particular researches to perform harmonic analysis. Free demo version of some softwares can be obtained by institutions, but usually this kind of version does not works with three phase systems. There is where the main objective of this project takes validity: to develop a simple and more accessible harmonic analysis program that could be used in future works or researchers. This objective was reached with a series of m files written in Matlab[®] from MathWorks[™], which can be easily modified according to the case of study and the data available.

Different three phase harmonic power flow method have been studied and applied in computer tools for harmonic analysis in both time and frequency domain. References [5], [39], [42], [47] and [49] are some examples of application of Newton's methods to harmonic analysis. However, none of these methods take into account the special characteristics of a distribution networks, such as is radial or weakly meshed structure, large number of nodes to be represented and high R/X ratios of the feeders. Authors of reference [45] propose a novel method based on backward/ forward sweep technique, which takes advantages of the particular structure of the distribution networks. Because of the lack of documentation in this specific area (distribution network harmonic analysis) this work was dedicated to the implementation of two methods based on backward/forward sweep techniques, verifying the advantages and the range of validity of these approaches.

Chapter 2 presents more clearly the general and specific objectives of this work; chapter 3 is an introduction to the harmonic distortion problem, its sources, its causes and the actual standards to limit them; chapter 4 describes power system analysis techniques in fundamental or harmonic frequencies, and its application to the case of interest; chapter 5 describes the principal models of the network components for fundamental and harmonic analysis; chapter 6 is a description of the methodology used to reach the objective; chapter 7 describes the methods applied, the programs made and the results obtained when applying these programs to some test networks; chapter 8 discuss the results obtained; and chapter 9 presents the final conclusions and recommendations of this project.

Chapter 2

Harmonic Distortion

In a power system there can be nonlinear devices, in which the current is not proportional to the applied voltage. When this situation is verified, even if the applied voltage is a perfectly sinusoidal waveform, the resulting current is distorted, as shown in Figure 2.1. According to Fourier [17], if the distorted waveform is periodic, like the one shown in Figure 2.2, it can be written as a sum of pure sine waves in which the frequency of each sinusoid is an integer multiple of the fundamental frequency of the distorted wave, known as *Fourier Series*. Each sinusoidal component is called a *harmonic* of the fundamental. Even if there are a few cases where the distortion is random, most distortion are periodic with components whose frequency is an integer of the power system fundamental frequency, or presents very slow changes between one cycle and the next one. Therefore, the Fourier series concept can be applied toward analyzing harmonic problems. Usually the system is analyzed separately at each harmonic order and then, if necessary, the complete output waveform can be computed. This simplifies a lot the analysis of power systems with harmonic distortion, in contrast to computing everything in time domain, where the nonlinearities may complicated every calculation that has to be made.

This chapter describes principal causes and effects of having harmonic voltages or currents into a power system. It also summarizes the current international existing standards set up to prevent the malfunction of the systems and/or its components.

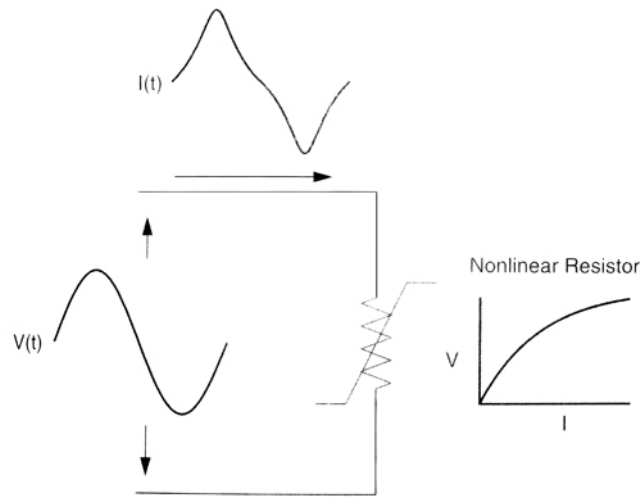


Figure 2.1: Example of a current distorted by a non linear load [15].

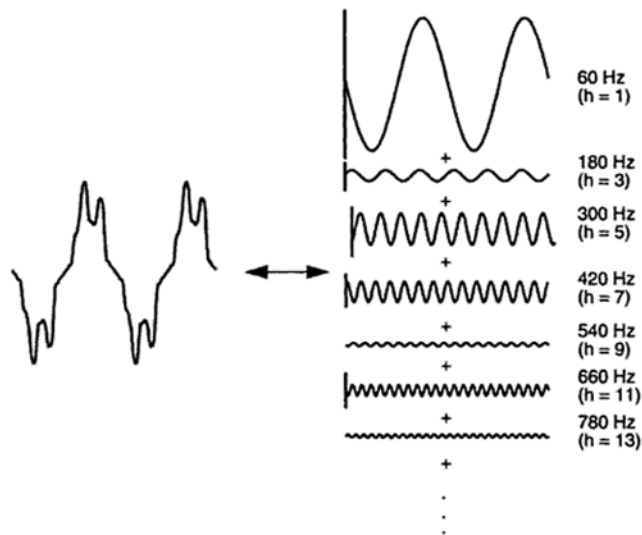


Figure 2.2: Distorted waveform and its components [15].

2.1 Harmonic Sources

In power systems operation, every nonlinear device is a potential harmonic source. Usually the harmonic sources can be divided into four main categories [24]:

- Nonlinear Voltage-Current Sources.
- Line-Commutated Solid State Converters.

- High Frequency Sources.
- Non-Harmonic Sources.

This section briefly describes each category and it contain some examples of the most common devices that generate harmonic distortion in power networks. Chapter 4 explain with more details the models used to evaluate their effect in the power networks.

2.1.1 Nonlinear Voltage-Current Sources

For these type of devices, the relationship between the voltage and the current is a nonlinear curve. The most common source in this category is transformers (due to their nonlinear magnetization characteristics), fluorescent and other gas discharge lighting devices, and other devices such as arc-furnaces. For some equipment such as core-and-coil ballasted fluorescent lights, the relationship can be relatively constant over a reasonable working range. In other cases, like the transformers, it can be very complex if hysteresis characteristics of the magnetic materials are considered. In the case of arc-furnaces the voltage-current relationship has a time-dependent variation (depending on the stage of melt) and a random variation. The harmonic currents generated by these devices are affected more by the waveforms and peak values of supply voltages than those generated by electronic switching devices.

2.1.2 Line-Commutated Solid State Converters

Line-commutated solid-state converters are the electronic power converters supplied from the ac system in which the switching of devices is synchronized to the zero-crossings of the ac voltage or its fundamental component. Generally a periodic steady state exists. Under ideal conditions the devices switch in an identical way during the positive or negative half-cycles and thus only odd-harmonic components exists, according to the Fourier series theory [17]. Compared to the nonlinear voltage-current devices, harmonic currents generated from converters are less sensitive to supply voltage distortion. Harmonic current source models are therefore commonly used to represent these devices. The phase angles of the current sources are functions of the supply voltage phase angle and they must be modeled adequately for harmonic analysis involving more than one source. Typically, devices utilizing line-commutated solid state converters include static var compensator, HVDC link and dc drives.

Static var Compensators

Static Var Compensator (SVC) are devices designed to provide the reactive power required to control dynamic voltage swings under various system conditions and improve the power system transmission and distribution performance. These devices normally have large Mvar ratings and are connected to high voltage transmission systems. Therefore, the harmonic currents generated from SVCs may affect a large number of customers and equipment. Common SVC-related harmonic studies tend to represent the device in detail, taking into account factors as firing-angle dependent harmonic generation and supply voltage unbalance.

Three-phase Static Power Converters

The introduction of this type of converters has caused a significant increase in harmonic-generating loads. The most common is the six-pulse bridge rectifier type (Figure 2.3). It is widely used as the front end for HVDC terminals, dc drives and adjustable speed drives. Typical circuit configurations for these devices are shown in Figure 2.4. The two types of commonly adopted converter circuits are the thyristor and the rectifier bridges. The first is usually used in HVDC links, current-source ac drives, and dc drives, while the second is normally seen in voltage-source and PWM ac drives. Because of the nature of the bridge connection there is no generation of zero sequence harmonics from the converter, even when the supply voltage is unbalanced or distorted [24].

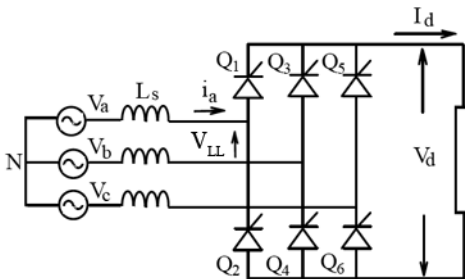


Figure 2.3: The six-pulse line-commutated converter.

The three basic components in the most common types of ac motor drives are the converter section (front-end), the inverter section, and the dc circuit that connects the two sections [31]. The converter section changes the 60/50 Hz line voltage into dc voltage through a switching process that will inject harmonic currents into the power system. The dc circuit is called the dc link. The DC current also contains harmonic ripples, due to the conversion process, which can also penetrate the power system. The inverter section is used to change the dc voltage into adjustable frequency of voltage to

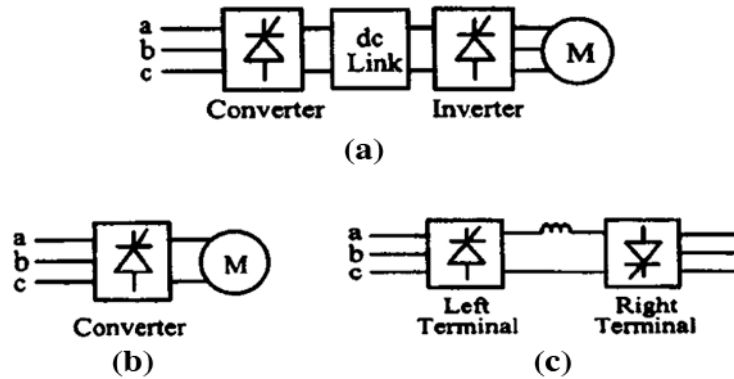


Figure 2.4: Typical configurations of (a) AC/DC motor drives (b) DC motor drive and (c) the HVDC link.

ac motor. The inverter can introduce additional ripples into the dc link current, which means injecting harmonic currents into the supply system side. In general, the extent and the frequency of inverter-produced harmonic distortions are largely a function of inverter design and motor parameters.

Single-phase Static Power Converters

These converters are commonly found in electronic equipment (computers and TVs), small adjustable speed drives, battery chargers and other rectifier and inverter applications. The most common single phase power supply consists of a capacitively filtered rectifier followed by different types of regulating stages. Such a supply draws pulses of current corresponding to periods of time in each half-cycle where the line voltage exceeds the capacitor voltage [24]. The spectrum consists of all odd harmonics with magnitudes which depend on the shape of the pulse. This is a huge difference between three-phase and single-phase converters, because the latter includes third-harmonics currents, which usually are the largest components of harmonics. These devices can be represented individually in power network harmonic studies as harmonic current sources.

2.1.3 High Frequency Sources

Some systems use high frequency switching to achieve greater flexibility in the power conversion. Electronic ballast may fall into this category. Using them in fluorescent lighting is a technique for improving current waveshape and power factor, thus

minimizing filter requirements and minimizing switching losses. Distortion is created at the switching frequency which is generally above 20 kHz. Normal techniques can be applied to reduce the low frequency harmonics, however high frequency distortion is usually not a problem because it cannot, generally, penetrate far into the system.

2.1.4 Non-Harmonic Sources

There exist several power electronic systems which produce distortion at frequencies that are not integer multiples of the fundamental frequency, commonly known as *interharmonic frequencies*. The sum of two or more pure sine waves with different frequencies not integer multiple of the fundamental frequency does not necessarily result in a periodic waveform. Therefore, these kind of waveforms do not have a Fourier series representation. Impacts of interharmonics are similar to those of harmonics, such as filter overloading, overheating, ripple, voltage fluctuation and flicker. However, solving interharmonic problems is more difficult, especially when the frequencies are random in time, like those in induction furnaces [15].

Some of the most common harmonic sources that may generate interharmonics are explained below.

Cycloconverters

Cycloconverters are devices that use static switches to convert a constant frequency fixed voltage source of ac power to a variable, lower frequency, controlled voltage output. Typical current absorbed by these devices is distorted by three different components: harmonics (components at integer multiples frequencies of the fundamental frequency) from symmetrical phase-angle triggering sequences, interharmonics at frequencies below of the fundamental frequency from any “integral” triggering; and other nonharmonic frequencies arising from a specific triggering sequence designed for a specific frequency [13]. This converter, having a fixed output frequency, produces distortion at fixed frequencies.

Doubly Fed Machine Drives

Doubly fed machines are a class of wound-rotor induction machines in which the stator is typically fed from the utility supply, while the rotor is fed by a variable voltage, lower power, and variable frequency electronic source. In these machines, the rotor

currents will be of the slip frequency [24]. With electronic converters supplying the rotor windings, the winding currents carries the harmonics of the slip frequency, which are coupled through the air gap to the stator and causes currents in the stator winding. These currents have frequencies different from the stator harmonics frequencies. The major problem related to this kind of nonlinear loads is the fact that the frequency of these currents, resulting from slip frequency harmonics, will vary with the rotor speed. Therefore, a system resonance at any frequency will be excited for some particular operating speed.

Adjustable Speed Drivers

Adjustable speed drives (ASD) may inject non-harmonic currents into the power system. There are two ways an ASD can generate harmonic currents [51]. First it is the converter operation which injects harmonic currents into the supply system by an electronic switching process. Second is the inverter operation, which can introduce additional ripples into the DC link current that can penetrate into the supply system side. The magnitude and the frequency of inverter-caused ripples depend on inverter design and motor parameters.

2.2 Effects of Harmonic Presence in the Power Networks

The degree of harm that harmonic presence can cause to a power network is determined by the susceptibility of the system components, load or power source to them. The least susceptible equipments are those whose primary function is in heating, as in an oven or furnace. In this case, the harmonic energy is generally utilized and hence is quite tolerable. The most susceptible type of equipment is that whose design or constitution assumes a perfect sinusoidal fundamental input. These equipments can be frequently found in the areas of communication or data processing application. Other equipments can be affected merely by the dielectric thermal or voltage stress, which causes premature aging of electrical insulation.

This section is dedicated to explain how the harmonic distortion may affect the principal components in a power system and the system as a whole.

2.2.1 Effects on Power System Quantities

Power system quantities such as rms values, power and power factor are normally defined for the fundamental frequency in a pure sinusoidal condition. When harmonic distortion exists in a power system, the hypothesis of sinusoidal condition is no longer valid and many of the simplifications used for the fundamental frequency analysis do not apply and the common equations for power, rms values or power factor have to be adjusted.

For a perfectly sinusoidal wave, it is known that the rms values of voltage and current are given by:

$$V_{rms} = V_1 = \frac{\hat{V}_1}{\sqrt{2}} \quad (2.1)$$

$$I_{rms} = I_1 = \frac{\hat{I}_1}{\sqrt{2}} \quad (2.2)$$

where \hat{V}_1 and \hat{I}_1 are the maximum value of voltage and current waveforms, respectively. In a non sinusoidal condition, the distortion waveform is made of the sum of diverse sinusoidal waveforms and the rms values are given by:

$$V_{rms} = \sqrt{\sum_{h=1}^{h_{max}} * V_h^2} \quad (2.3)$$

$$I_{rms} = \sqrt{\sum_{h=1}^{h_{max}} I_h^2} \quad (2.4)$$

where V_h and I_h are the rms values of the waveform at the h th harmonic component.

The active power P can be computed as the average of the product of the instantaneous voltage and the instantaneous current:

$$P = \frac{1}{T} * \int_0^T v(t) * i(t) * dt \quad (2.5)$$

Equation 2.5 is valid for both sinusoidal and nonsinusoidal conditions. Instead, Equation (2.6) indicates the average active power only for the fundamental frequency. In the nonsinusoidal case it must include the contributions of all harmonics. However, the voltage distortion in power systems is usually very low (less than 5%). Equation (2.6) can be used to compute the active power regard less of how distorted is the current [15].

$$P = V_1 * I_1 * \cos(\theta_1) = S_1 * \cos(\theta_1) \quad (2.6)$$

where θ_1 is the angle between voltage and current at the fundamental frequency.

Similar approximations between power computations at the fundamental frequency and the total power of the distorted waveform cannot be made for the reactive and complex power. These two quantities are greatly influenced by the distortion. There is some disagreement as to define the reactive power Q of the distorted waveforms. However to size shunt capacitors it is used the component at the fundamental frequency (Equation (2.7)). In fact, it is more important to determine the active power P and apparent power S_1 than the reactive one. P defines the actual power that is expended, dissipated or consumed by the load to perform real work, while S_1 defines the capacity that power system requires to deliver P at the fundamental frequency.

$$Q_1 = V_1 * I_1 * \sin(\theta_1) = S_1 * \sin(\theta_1) \quad (2.7)$$

The apparent power S for both cases, sinusoidal or nonsinusoidal, can be written as Equation (2.8).

$$S = V_{rms} * I_{rms} \quad (2.8)$$

Even if this general equation could be applied to both cases, there is actually an important difference regarding the components of this apparent power. For a perfectly sinusoidal waveform, S can also be written as Equation (2.9). Instead, in a nonsinusoidal case, the apparent power is described according to Equation (2.10), where D represents all the cross products of voltage and current at different frequencies, which yield no average power [15].

$$S_1 = \sqrt{P_1^2 + Q_1^2} \quad (2.9)$$

$$S = \sqrt{P^2 + Q^2 + D^2} \quad (2.10)$$

where P and Q can be calculated as the sum of the real and imaginary parts of the apparent power at each harmonic [29]:

$$P = \sum_{h=1}^{h_{max}} \text{Re}\{V_h * I_h\} \quad (2.11)$$

$$Q = \sum_{h=1}^{h_{max}} \text{Im}\{V_h * I_h\} \quad (2.12)$$

The term Q in Equations (2.12) and (2.10) is called “reactive voltamperes” and it is used for a mathematical quantity which should not be confused with power [48]. It

does not possess the conservation property of a power, then the term “reactive power” is not used in order to avoid confusion with actual power.

The percentage of power expended for its intended uses can be measured by the power factor (PF). In the sinusoidal case there is only one angle between the voltage and the current and the power factor can be computed as the cosine of this angle (Equation (2.13)), commonly known as the *displacement power factor*. In the nonsinusoidal case, the power factor cannot be defined as the cosine of the phase angle, instead it has to be compute from the contribution of all frequencies to the active power (Equation (2.14)). In this latter case it is called *true power factor*.

$$pf = \frac{P_1}{S_1} = \cos(\theta_1) \quad (2.13)$$

$$pf = \frac{P}{S} \quad (2.14)$$

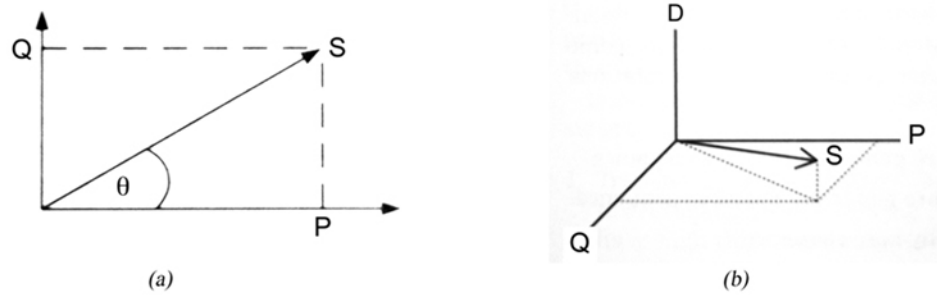


Figure 2.5: Power factor for the (a) sinusoidal case and (b) nonsinusoidal case.

The IEEE Trial-Use Standard 1459-2000 beside the terms explained below, defines the non-fundamental apparent power [20]:

$$N = \sqrt{S^2 - P^2} \quad (2.15)$$

2.2.2 Effects on System Components

Power Cables

The flow of nonsinusoidal current in a conductor will cause additional heating due to the fact that the actual rms value of the current would be greater than the expected value. This is due to two frequency-dependent phenomena: the “skin effect” and the

“proximity effect”. As a result of these two effects, the effective ac resistance is raised above the dc resistance specially for larger conductors. Therefore the losses in the cable increases due to two reasons: the increase of the I_{rms} and the higher R_{AC} . In Equation (2.16) it can be noticed that the second term of the sum doesn't exist for pure sinusoidal waveforms.

$$P_{LOSS} = R_{AC} * I_{rms}^2 = R_1 * I_1^2 + \sum_{h=2}^{h_{max}} (R_h * I_h^2) \quad (2.16)$$

where:

I_h is the rms value of the current at the h th harmonic order.
 $R_h > R_1$

In four-wired distribution systems, the existence of the triplen harmonic currents in a balanced system means a high current level flowing by the neutral wire. This current could become greater than the current flowing through, overloading the neutral wire. If the harmonic distortion level is particularly high, would needed a derating of the cable.

Transformers

There are three major effects that a harmonic distortion has on transformers:

- Increase on the rms current value which leads to an increase of conductor losses.
- Increase of eddy currents that are proportional to the square of the frequency.
- Increase of core losses, due to the increase of eddy currents in the core lamination.

The three effects mentioned above result in one final effect which is the increase of the transformer temperature. This additional heating can be critical when the current distortion is very high. As a general rule, when current distortion exceeds 5% the transformer is a candidate for derating [15]. Guidelines for transformer derating are detailed in the ANSI/IEEE Standard CS57.110-1998, *Transformer Capability When Supplying Nonsinusoidal Load Currents* [57].

Motors and Generators

Rotating machines (induction and synchronous) may suffer the harmonic current effects in many ways:

- An increased iron and copper losses at the harmonic frequencies leads to overheating and reduction of efficiency.
- Possible rise to a higher audible noise emission compared to a sinusoidal excitation.
- Production of a resultant flux distribution in the air gap which can cause or enhance a phenomena called cogging (refusal to start smoothly) or crawling (very high slip) in induction motors.
- Harmonic pairs, such as the fifth and seventh harmonics, that may create mechanical oscillations, in case of turbine-generator combination or in motor-load system. If the frequency of a mechanical resonance exists close to the frequency of the electrical stimulus, high-stress mechanical forces can develop [57].
- Harmonic voltage will induce a corresponding harmonic current in the stator of the machine. If the machine is connected to a six-pulse converter, there won't even be harmonics; each of the existing harmonics being a positive or negative sequence symmetrical component of the total current. These currents will induce additional heating in the stator windings.
- Harmonic currents flowing in the rotor are induced by the magnetomotive force in the air gap due to the harmonic currents in stator and may result into rotor heating and pulsating or reduced torque.

The sum effect of harmonics is a reduction in efficiency (typically 0.9-0.95 times the one of pure sinusoidal waves) and life expectancy of the machinery. According to the IEEE Standard 519-1992 there is no need to derate motors if the total harmonic distortion (section 2.3.1) is below the 5% limit and 3% for each individual harmonic.

Capacitors

Harmonic distortion in capacitors may cause an increase of temperature and higher dielectric stress, but the major concern arising from the use of capacitors in a power system with harmonic pollution is the possibility of system resonance. This effect imposes voltages and currents that are considerably higher than otherwise would be the case without resonance.

Electronic Equipment

Power electronic equipment is often dependent upon accurate determination of voltage zero crossings or other aspects of the voltage wave shape. Harmonic distortion can result in shifting of the voltage zero crossing or the point at which one phase-to-phase voltage becomes greater than another phase-to-phase voltage, causing the malfunctioning of many kinds of electronic circuit controls.

Other types of electronic equipment can be affected by the transmission of ac supply harmonics through the equipment power supply or by magnetic coupling of harmonics into equipment components.

Metering

In general, nonlinear loads tend to inject power back onto the supply system and linear loads absorb harmonic power due to the distortion in the voltage. This may lead to a negative error at harmonic frequencies for measurements made with induction disk devices, such as watt-hour meters. The worst errors occur when the total current at the metering site is greatly distorted (10-15%), fortunately the distortion at the total plant load is not that distorted as individual loads currents [57]. Therefore, the metering error is frequently small.

Switchgear and Relaying

As for other types of equipment, harmonic currents can increase heating and losses in switchgear, thereby reducing steady-state current carrying capability and shortening the life of some insulating components [57]. This can lead to a derating of fuses and other equipments. There are currently no standards for the level of harmonic currents that switching devices or fuses are required to interrupt or to carry, but in general, harmonic levels required to cause misoperation of relays are greater than those for other kind of devices, usually distortion factors of 10-20% are required to cause problems in relay operation.

Communication Circuits

The presence of harmonic currents or voltages in utility distribution system or within distribution system facility can produce magnetic and electric fields that could

interfere with communication systems. Voltages induced in parallel conductors often fall within the bandwidth of nominal voice communications, specially those between the 9th and 24th harmonic.

Triplen harmonics are especially troublesome in four-wire systems because they will circulate in the neutral circuit, which has the greatest exposure with the communication circuits.

2.2.3 Resonance

System resonances can be of two natures:

- **Parallel Resonance**

Parallel resonance occurs when the system inductive reactance and capacitive reactance are equal at some frequency, called the *resonant frequency* (Equation (2.17)). If the combination of capacitor banks and the system inductance result in a parallel resonance near one of the characteristic harmonics generated by the nonlinear load, that harmonic current will excite the circuit, causing an amplified current to oscillate, swapping the energy stored in the inductance with the energy storage in the capacitance, and vice versa. In other words, the voltage and currents at this frequency continue to persist at very high values, causing most of the harmonic distortion problems in power systems.

$$f_p = \frac{1}{2 * \pi} * \sqrt{\frac{1}{L_{eq}} - \frac{R^2}{4 * L_{eq}^2}} \quad (2.17)$$

where R and X_{eq} are the systems equivalent resistance and inductance.

At the resonant frequency, the parallel combination of the equivalent inductance and capacitance as seen from the harmonic current source becomes very large [15]. This impedance Z_p will depend on the value of the quality factor (Q) of the resonant circuit (Equation (2.18)). The value of the quality factor depends on the location of the power system where it is measured and it can vary from less than 5, on a distribution feeder, or more than 30, on the secondary bus of a large step-down transformer.

$$Z_p = \frac{X_C * (X_{Leq} + R)}{R} \approx \frac{X_{Leq}^2}{R} = \frac{X_C^2}{R} = Q * X_{Leq} = Q * X_C \quad (2.18)$$

$$Q = \frac{X_L}{R} = \frac{X_C}{R} \quad (2.19)$$

During the parallel resonance the harmonic current flowing in the capacitor bank or into the power system will be magnified Q times, causing capacitor failure, fuse blowing or transformer overheating.

$$I_{resonance} = \frac{V_p}{X_C} = \frac{V_p}{X_{Leq}} = Q * I_h \quad (2.20)$$

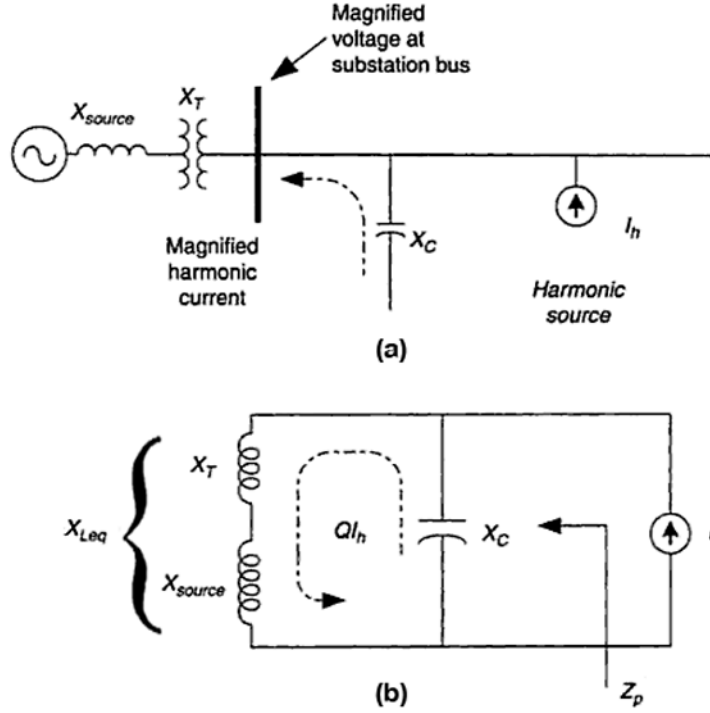


Figure 2.6: Simplified distribution system with parallel resonance [15].

Usually the values of L_{eq} and C are not available to compute the analysis of a power system, so it is used one of the following equations to calculate the resonant harmonic based on fundamental frequency impedances and ratings:

$$h_r = \sqrt{\frac{X_C}{X_{SC}}} \quad (2.21)$$

$$h_r = \sqrt{\frac{MVA_{SC}}{Mvar_{CAP}}} \quad (2.22)$$

$$h_r \approx \sqrt{\frac{kVA_{tx} * 100}{kvar_{CAP} * Z_{tx}}} \quad (2.23)$$

where:

X_C is the capacitor reactance.

X_{SC} is the system short-circuit reactance.

MVA_{SC} is the system short-circuit complex power in MVA.

MVA_{CAP} is the capacitor rated reactive power in Mvar.

kVA_{tx} is the complex power rating of the step-down transformer in kVA.

Z_{tx} is the stem-down transformer impedance in percentage.

$kvar_{CAP}$ is the reactive power rating of capacitor bank in kvar.

• **Series Resonance**

There are some instances where a shunt capacitor and the inductance of a transformer or distribution line may be seen by the nonlinear load as a series LC circuit (Figure 2.8). If the resonant frequency corresponds to a characteristic harmonic frequency of the harmonic source, the LC circuit will attract a large portion of the harmonic current generated in the distribution system. This may result in magnified and highly distorted voltage at the capacitor terminals:

$$V_C = \frac{X_C}{|j * X_T + j * X_C + R|} * V_h \approx \frac{X_C}{R} * V_h \quad (2.24)$$

where V_h is the harmonic voltage corresponding to the harmonic source I_h and R is the resistance of the resonant circuit usually small compared to the reactance.

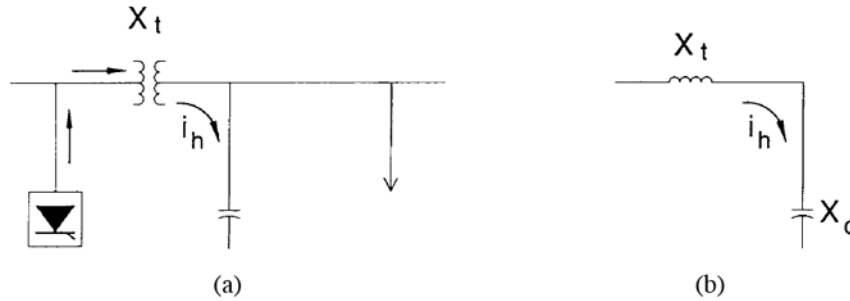


Figure 2.7: Simplified distribution system with series resonance [57].

In many systems with potential series resonance problems, parallel resonances also arise due to the circuit typology. The resulting parallel resonant frequency is always smaller than its series resonant frequency due to the source inductance contribution [15]. In the example shown in Figure 2.8 the resonance frequencies can be calculated as follows:

$$hr_{parallel} = \sqrt{\frac{X_C}{X_T + X_{source}}} \quad (2.25)$$

$$hr_{series} = \sqrt{\frac{X_C}{X_T}} \quad (2.26)$$

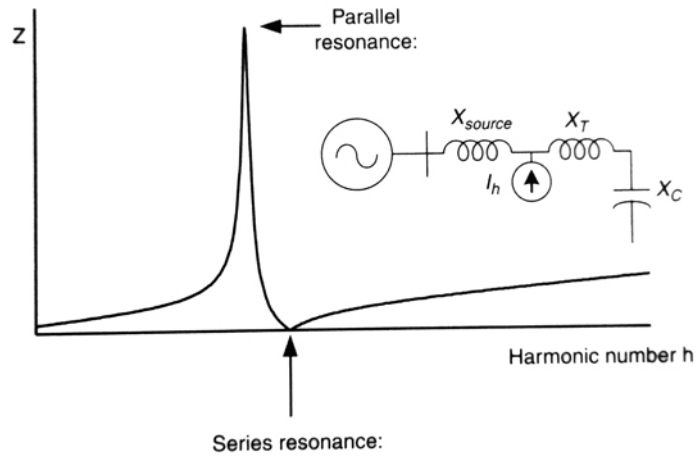


Figure 2.8: Frequency response of a system with series resonance [15].

After reviewing the effects of system resonance in power networks, it comes straightforward the conclusion that the system resonant condition, either in series or parallel, is the most significant way in which the harmonic distortion can affect a power network, not only because it could generate over voltages or over currents, but also because it magnifies the harmful effects of harmonic components into equipments, mentioned in the previous section. Therefore, it is important to be able to analyze the system frequency response characteristics and to avoid system resonance problems.

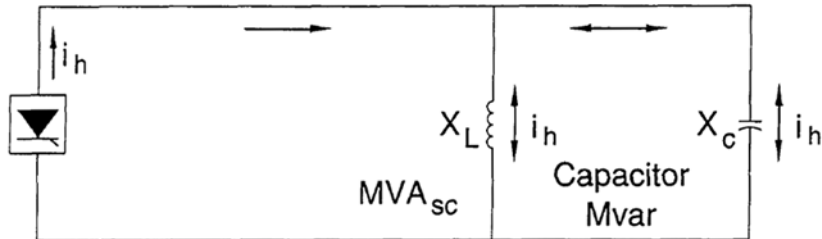


Figure 2.9: Simple circuit for hand calculations [57].

The IEEE Standard 519-1992 [57] recommends that if a system can be reduced to the circuit shown in Figure 2.9, the system frequency response can be manually calculated applying Equation (2.21), (2.22) or (2.23), depending on the data available. Instead, if the system to be analyzed is more complicated, computer simulations are usually required.

Computer programs usually are able to perform analyses including:

1. Frequency scans for system response

2. Response to multiple harmonic sources
3. Multiphase, unbalanced system solutions

The most common method employed in a computer program for harmonic analysis is a direct solution of the admittance matrix at multiple frequencies. With this type of solution, nonlinear devices are modeled as ideal voltage sources or current sources at the harmonic frequencies. Another approach that has been used for harmonic simulations has been termed harmonic load flow [57]. The load flow equation formulation uses the power constraints at the load and source nodes.

2.3 Voltage Quality Standards

2.3.1 IEEE Standard 519-1992

Harmonic currents produced by non-linear loads mentioned in previous sections, can give rise to voltage and current harmonic distortion in many places of the system. Therefore, efforts are made to limit harmonic distortions in the power networks. The IEEE Standard 519-1992 [57] proposes a participation of both parts of the system: the end users, by limiting the harmonic current injection, and the utilities, by not accentuating the harmonic currents. The limits can be established at the point of common coupling (PCC), a point of metering, or any point as long as both the utility and the consumer can either access the point for direct measurement of the harmonic indices meaningful to both or can estimate the harmonic indices at point of interference (POI) through mutually agreeable methods. The point of common coupling is defined as a point between end user or customer and the utility system where another customer can be served [15].

Recommended Limits for End Users

According to IEEE Standard 519-1992, good harmonic indices are characterized as follows:

1. The values given by the harmonic indices should be physically meaningful and strongly correlated to the severity of the harmonic effects.
2. It should be possible to determine by measurements whether or not the limits of the harmonic indices are met.

3. Harmonic indices should be simple and practical so that they can be widely used with ease.

However, the harmonic effects can change substantially depending on the characteristics of the equipment affected. Therefore, the severity of the harmonic effects imposed on all types of equipment cannot be perfectly correlated to a few simple indices. Moreover, the harmonic characteristics of the utility circuit seen from the PCC often are not known accurately. Thus, the indices are not enough by themselves and strict adherence to the recommended harmonic limits will not always prevent problems from arising. Then always good judgments are required to complete the analysis.

The consumer task are to confirm:

1. That power factor correction capacitors or harmonic filters are not being overstressed by excessive harmonics.
2. The absence of series or parallel resonance.
3. That the level of harmonics at PCC and utilization points is not excessive.

Based on the characteristics mentioned before, the recommended harmonic indices are: depth of notches, total notch area, and distortion of bus voltage distorted by commutation notches (low-voltage systems), individual and total voltage distortion, and individual and total current distortion.

Individual and total voltage distortion

The total harmonic distortion (THD) is used to define the effect of harmonics on the power system voltage [57]. It is used in low-voltage, medium-voltage, and high-voltage systems. It is expressed as a percent of the fundamental and is defined as follows:

$$THD = \sqrt{\frac{\text{sum of all squares of amplitude of all harmonic voltages}}{\text{square of the amplitude of the fundamental voltage}}} * 100\% \quad (2.27)$$

$$THD = \frac{\sqrt{\sum_{h=2}^{h_{max}} V_h^2}}{V_1} * 100\% \quad (2.28)$$

The total harmonic distortion factor (THD) and the notch area of the line-to-line voltage at PCC should be limited as shown in Table 2.1.

Table 2.1: Low-voltage distortion limits [57].

	Special Applications	General System	Dedicated System
THD (voltage)	3 %	5 %	10 %
Notch Area ($V.\mu s$)	16 400	22 800	36 500

Individual and total current distortion

The current distortion limits are developed with the scope of limit is the harmonic injection from individual customers so that they will not cause unacceptable voltage distortion levels for normal system characteristics and limit the overall harmonic distortion of the system voltage supplied by the utility.

The harmonic voltage distortion on the system is function of the total injected harmonic current and the system impedance at each of the harmonic frequencies. The total injected harmonic current will depend, naturally, on the number of individual customers injecting harmonic currents and the size of each customer. Therefore, the IEEE Standard 519-1992 establishes the limits depending on the customer size. Larger customers have more stringent limits because they represent a larger portion of the total system load. Table 2.2 shows the individual harmonic current limits expressed in percent of this maximum load (demand) current. The customer size is expressed as the ratio of the short-circuit current capacity, at the customers point of common coupling with the utility, to the customer's maximum load current.

Table 2.2: Basis for harmonic current limits [57]

SCR at PCC	Maximun Individual Frequency Voltage Harmonic (%)	Related Assumption
10	2.5-3.0	Dedicated system
20	2.0-2.5	1-2 large customers
50	1.0-1.5	Few relatively large customers
100	0.5-1.0	5-10 medium size customers
1000	0.05-0.10	Many small customers

The current distortion limits shown in Table 2.2 were developed assuming some diversity between the harmonic currents injected by different customers. It means that injection currents of different harmonic orders were assumed with differences in the phase angles, or differences in the harmonic injection vs. time profiles for each end costumer or group of customers. If individual customers meet the current distortion

limits, and there is not sufficient diversity between individual customer harmonic injections, then it may be necessary to implement some form of filtering on the utility system to limit the voltage distortion levels.

More specific limits for general distribution, subtransmission and transmission systems are shown in Table 2.3. They are also expressed in percent of the maximum load current I_L and divided by the size of the system, expressed as the ratio of the short-circuit current capacity, at the PCC, to the customer’s maximum load current. There are listed just the limits for the characteristics (odd) harmonics, the amplitudes of the noncharacteristic harmonic orders are less than 25% of the limits specified.

Table 2.3: Current distortion limits for general distribution, subtransmission and transmission systems [57]

I_{SC}/I_L	$h < 11$	$11 \leq h < 23$	$17 \leq h < 23$	$23 \leq h < 35$	$35 \leq h$
$V_n \leq 69kV$					
< 20	4.0	2.0	1.5	0.6	0.3
20 – 50	0.7	3.5	2.5	1.0	0.5
50 – 100	10.0	4.5	4.0	1.5	0.7
100 – 1000	12.0	5.5	5.0	2.0	1.0
> 1000	15.0	7.0	6.0	2.5	1.4
$69kV < V_n \leq 161kV$					
< 20	2.0	1.0	0.75	0.3	0.15
20 – 50	3.5	1.75	1.25	0.5	0.25
50 – 100	5.0	2.25	2.0	0.75	0.35
100 – 1000	6.0	2.75	2.5	1.0	0.5
> 1000	7.5	3.5	3.0	1.25	0.7
$V_n > 161kV$					
< 50	2.0	1.0	0.75	0.3	0.15
≥ 50	3.0	1.50	1.15	0.45	0.22

The limits listed in Table 2.3 are recommended as system design values for the “worst case” in normal operation (conditions lasting longer than one hour). For shorter periods, during start-ups or unusual conditions, the limits may be higher and can be obtained multiplying the values of the table by 1.5. Also if the limits are being applied to systems with harmonic-producing loads consisting of phase shift transformers or converters with pulse numbers (q) higher than six, the limits for the characteristic harmonic orders are increased by a factor equal to $\sqrt{q/6}$.

Usually, in term of current speaking, instead of use the THD indice, is defined

the total demand distortion (TDD). The load current may vary significantly according to the load, thus an index defined as the THD, where the denominator is the actual amplitude of the fundamental component, can also vary giving not reliable results. As in example, if the load current is small, the THD will be large, even if there is not that much of harmonic distortion. To avoid this problem, the TDD is defined with respect to the fundamental component of the maximum demand load current at the PCC (I_L). This current can be calculated as the average of the maximum monthly demand currents for the previous 12 month or it can be estimated in case of lack of information. Equation 2.29 shows the mathematical definition of the TDD and table 2.4 the maximum levels of TDD proposed by [57].

$$TDD = \frac{\sqrt{\sum_{h=2}^{h_{max}} I_h^2}}{I_L} * 100\% \quad (2.29)$$

Table 2.4: Total demand distortion (TDD) limits [57]

I_{SC}/I_L	$V_n \leq 69kV$	$69kV < V_n \leq 161kV$	$V_n > 161kV$
< 20	5.0	2.5	2.5
20 – 50	8.0	4.0	2.5
50 – 100	12.0	6.0	3.75
100 – 1000	15.0	7.5	3.75
> 1000	20.0	10.0	3.75

Recommended Limits for Utilities

Harmonic evaluations on the utility system are done to determinate the condition of the voltage distortion for all customers. The limits to establish the acceptability or not of the THD are shown in Table 2.5 and, as in Table 2.3, defined to be used as system design values for the “worst case” for normal operation (conditions lasting longer than one hour). For shorter periods, during start-ups or unusual conditions, the limits may be exceeded by 50%.

An important difference between the limits recommended by [57] for end users and those recommended for utilities is in the definition of the THD. In the second case is expressed as a function of the nominal system rms voltage (V_n) rather than of the fundamental frequency voltage of the fundamental frequency voltage magnitude at the time of measurement. This allows the evaluation of the voltage distortion with respect to fixed limits rather than limits that fluctuates with the system voltage (the same advantage as the TDD for the current distortion evaluation).

Table 2.5: Harmonic voltage distortion limits in percent of V_n [57]

Bus voltage at PCC	Individual harmonic voltage distortion (%)
$V_n \leq 69kV$	5.0
$69kV < V_n \leq 161kV$	2.5
$V_n > 161kV$	1.5

2.3.2 IEC 61000

The International Electrotechnical Commission (IEC) has defined a category of electromagnetic compatibility (EMC) standards that deal with power quality issues. It is divided in six parts:

1. IEC 61000-1-x: General.
2. IEC 61000-2-x: Environment.
3. IEC 61000-3-x: Limits.
4. IEC 61000-4-x: Testing and measurement techniques.
5. IEC 61000-5-x: Installation and mitigation guidelines.
6. IEC 61000-6-x: Miscellaneous.

The parts related to the harmonic distortion are IEC 61000-2 and IEC 61000-3. This section focuses on the standards dealing with harmonic of these specific parts.

IEC 61000-2-2

Defines the compatibility levels for individual harmonics in the low-voltage network: up to 240 V for single-phase systems and 415V for three-phase systems. The levels are shown in Table 2.6 given as a percentage of the fundamental component. They are not rigid and can be exceeded in a few exceptional conditions.

Table 2.6: Compatibility levels for individual harmonics in the low-voltage network according to IEC 61000-2-2.

Not multiple of 3		Multiple of 3		Even Order	Harmonic Voltage (%)
Odd Order	Harmonic Voltage (%)	Odd Order	Harmonic Voltage (%)		
5	6	3	5	2	2
7	5	9	1.5	4	1
11	3.5	15	0.3	6	0.5
13	3	21	0.2	8	0.5
17	2	>21	0.2	10	0.2
19	1.5			12	0.2
23	1.5			>12	0.2
25	1.5				
>25	$0.2+1.3*25/h$				

IEC 61000-3-2

Defines limits for harmonic current emission from equipment absorbing currents up to 16 A. The limits are established in a way to ensure that the voltage in the public network satisfies the compatibility limits defined in IEC 61000-2-2. The equipment are divided in four classes and the limits are defined for each one of them:

- Class A: balances three-phase equipment and all other equipments that doesn't falls in any other category.
- Class B: portable tools.
- Class C: lighting equipment.
- Class D: equipment with and input power of less than 600 W and input current with a characteristic waveform well specified in the standard.

IEC 61000-3-4

Analog to IEC 61000-3-2 but defines the harmonic currents emission for equipments working with inputs currents values between 16 A and 75 A.

Table 2.7: Harmonic current limits for class A equipment according to IEC 61000-2-2.

Odd order h	Max. permissible harmonic current order (A)	Even order h	Max. permissible harmonic current order (A)
3	2.3	2	1.08
5	1.14	4	0.43
7	0.77	6	0.3
9	0.4	8 to 40	$0.23 \cdot 8/h$
13	0.21		
11 to 39	$0.15 \cdot 15/h$		

Table 2.8: Harmonic current limits for class C equipment according to IEC 61000-2-2.

Harmonic order h	Max. permissible harmonic current order I_h/I_1 (%)
2	2
3	$30 \cdot (\text{circuit power factor})$
5	10
7	7
9	5
11 to 39	3

IEC 61000-3-6

Specifies limits of harmonic current emission for equipment connected to medium-voltage ($1\text{kV} \leq V_n \leq 35\text{kV}$) and high-voltage supply systems ($35\text{ kV} \leq V_n \leq 130$

Table 2.9: Harmonic current limits for class D equipment according to IEC 61000-2-2.

Harmonic order h	Max. permissible harmonic current	
	per watt (mA/W)	(A)
2	3.40	2.30
5	1.90	1.14
7	1.00	0.77
9	0.50	0.40
13	0.35	0.33
11 to 39	$3.86/h$	See Table 2.7

Table 2.10: Harmonic current limits according to IEC 61000-3-4.

Harmonic order h	Max. permissible harmonic current order I_h/I_1 (%)	Harmonic order h	Max. permissible harmonic current order I_h/I_1 (%)
3	21.6	19	1.1
5	10.7	21	0.6
7	7.2	23	0.9
9	3.8	25	0.8
11	3.1	27	0.6
13	2.0	29	0.7
15	0.7	31	0.7
17	1.2	33	0.6

kV). Two kind of levels are defined in this standard: compatibility levels and planning levels. The compatibility level is usually established empirically so that the equipment is compatible with its environment can be achieved the 95% of the time. Planning levels are design criteria or levels specified by the utility company, they are more stringent than compatibility levels.

Table 2.11: Compatibility levels for harmonic Voltages (in percent of fundamental) for LV and MV systems according to IEC 61000-3-6.

Not multiple of 3		Multiple of 3		Even Order	Harmonic Voltage (%)
Odd Order	Harmonic Voltage (%)	Odd Order	Harmonic Voltage (%)		
5	6	3	5	2	2
7	5	9	1.5	4	1
11	3.5	15	0.3	6	0.5
13	3	21	0.2	8	0.5
17	2	>21	0.2	10	0.5
19	1.5			12	0.2
23	1.5			>12	0.2
25	1.5				
>25	$0.2 + 1.3 * 25/h$				

Table 2.12: Planning levels for harmonic Voltages (in percent of fundamental) for MV systems according to IEC 61000-3-6.

Not multiple of 3		Multiple of 3		Even Order	Harmonic Voltage (%)
Odd Order	Harmonic Voltage (%)	Odd Order	Harmonic Voltage (%)		
5	5	3	4	2	1.6
7	4	9	1.2	4	1
11	3	15	0.3	6	0.5
13	2.5	21	0.2	8	0.4
17	1.6	>21	0.2	10	0.4
19	1.2			12	0.2
23	1.2			>12	0.2
25	1.2				
>25	$0.2 + 0.5*25/h$				

Table 2.13: Planning levels for harmonic Voltages (in percent of fundamental) for HV and EHV systems according to IEC 61000-3-6.

Not multiple of 3		Multiple of 3		Even Order	Harmonic Voltage (%)
Odd Order	Harmonic Voltage (%)	Odd Order	Harmonic Voltage (%)		
5	2	3	2	2	1.6
7	2	9	1	4	1
11	1.5	15	0.3	6	0.5
13	1.5	21	0.2	8	0.4
17	1	>21	0.2	10	0.4
19	1			12	0.2
23	0.7			>12	0.2
25	0.7				
>25	$0.2 + 0.5*25/h$				

2.3.3 EN 50160

Is an European standard designed to meet the supply quality requirements for European utilities. It defines harmonic voltage limits at the customer's supply terminal or in public low-voltage ($230\text{ V} \leq V_n \leq 1\text{ kV}$) and medium-voltage ($1\text{ kV} \leq V_n \leq 35\text{ kV}$) electricity distribution systems under normal operating conditions. The limits

Table 2.14: Limits for total harmonic distortion according to IEC 61000-3-4.

	THD (%)
Compatibility levels for LV and MV systems	8
Planning levels for MV systems	6.5
Planning levels for HV and EHV systems	6.5

are defined as a percentage of the fundamental component for the firsts 40 harmonics, higher-order harmonics are too small and results irrelevant as references values. Is established as a limit to the total harmonic distortion of the supply voltage, including harmonic up to 40 order, should not exceed 8%.

Table 2.15: Harmonic Voltages limits at the supply terminals according to EN 50160.

Not multiple of 3		Multiple of 3		Even Order	Harmonic Voltage (%)
Odd Order	Harmonic Voltage (%)	Odd Order	Harmonic Voltage (%)		
5	6	3	5	2	2
7	5	9	1.5	4	1
11	3.5	15	0.3	6 to 24	0.5
13	3	21	0.2		
17	2				
19	1.5				
23	1.5				
25	1.5				

Chapter 3

Power System Analysis

The most important and basic tool in the field of power system engineering is the load-flow or power-flow analysis. It is used in the operational as well as planning stages. Typically the data known prior to the analysis are the three-phase voltages of the slack node or nodes (the substation in the distribution system case) and the complex power of all the loads and model of the system components and loads. Sometimes, the input complex power supplied to the feeder from the substation is also known. From these data, the load-flow analysis of a feeder can determine the following by phase and total three-phase parameters:

- Voltage magnitudes and angles at all nodes of the feeder.
- Active and reactive power flow in each line section.
- Branch currents specified in magnitude and angle, or magnitude and power factor.
- Power loss in each line section.
- Total feeder active and reactive power inputs.
- Total feeder power losses.
- Loads actual active and reactive power consumption.

Since the invention and widespread use of digital computers, many methods for solving the load-flow problem have been developed. Most of the methods have built up for transmission systems analysis. The most widely used are the Newton-Raphson based ones or its derivations, like the fast decoupled method. The power-flow analysis of a distribution feeder is similar to that of an interconnected transmission system.

However, distribution networks having special features need a different approach for their load flow analysis.

When the system is in presence of several nonlinear loads, it can be necessary to carry out a harmonic load flow to be able to determine the distortion level in the system and the damages that it can produce to the system components, with the aim of developing accurate solution to the problems that may arise. The increase of power electronic devices in the last decades is making this kind of analysis an important and every day more frequently used tool.

The methods used in this project is a harmonic load flow to be applied in distribution systems, therefore this chapter will be centered on the description of this kind of network analysis.

3.1 Distribution System Analysis

The principal characteristics that distinguish a distribution network from the transmission system are:

1. Large number of nodes to be represented.
2. High R/X ratios of the feeders.
3. Unbalanced multiphase loads, therefore unbalanced system operation.
4. Radial Structure.

The first two characteristics are the ones that make the Newton-Raphson approaches difficult to apply in distribution systems. The unbalanced operation of the system make more complex the analysis because it requires more accurate three-phase models of the system components instead of per phase equivalent ones. The last characteristic mentioned, the radial structure, is actually a positive one that simplifies the analysis. Even if the network have not a totally radial or three structure, there are techniques to apply these methods to a weakly meshed network that are explained in section 3.1.2.

The first approaches to solve the problems of the distribution networks analysis and take advantage of its radial structure were based on a direct solution, using the impedance matrix of the unbalanced network and the Z_{bus} Gauss method, as in [19] and [10]. These methods have the advantage over Newton-Raphson that they don't need to calculate a Jacobian matrix at each iteration, but the much more simple Y_{bus}

matrix. Also, if the only voltage specified bus in the system is the slack bus, its rate of convergence is comparable to the Newton-Raphson approach. Subsequently, other techniques were developed, some of them based on the classical Newton-Raphson approach [52], others in a phase decoupled method [54]. But over the years, there is one method that has emerged to prove its effectiveness in the analysis of radial distribution systems compared to the traditional Gauss–Seidel and Newton–Raphson methods [28]. It is the backward/forward sweep method, that some authors have even called it to be “the most efficient and fast for solving the load flow of radial distribution systems” [30]. This method models the distribution network as a tree with the slack bus being the root. Primarily the backward sweep step sums either the line currents or power flows from the extremities to the root. Then, the forward sweep calculates the voltage drop at each branch, providing updates to the voltage profile based on the current estimates of the flows.

The proposed method in this project is based on the backward/forward sweep technique, therefore this is centred in the description of this specific method and its application to radial and weakly meshed networks.

3.1.1 Backward-Forward Sweep

The first step to apply the backward/forward sweep method is to define the structure of the network, by labeling correctly each branch and each node. It will be adopted the same nomenclature as in reference [7].

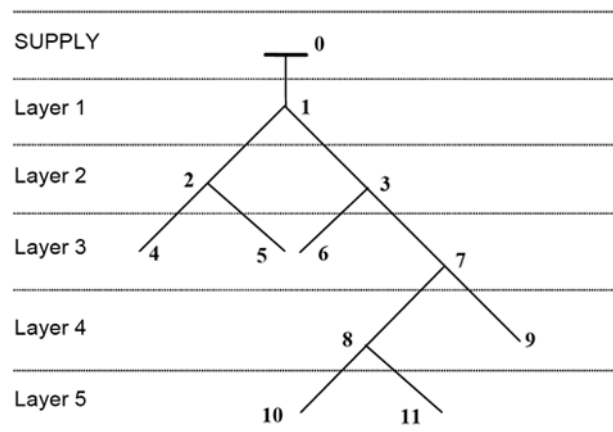


Figure 3.1: Example of the node labeling in a radial network

In a radial network composed by $n + 1$ nodes being fed at a constant feeding voltage, the node where is applied the constant voltage is denominated the root node and labeled

as *node 0*. The other nodes are numbered sequentially in ascending order proceeding from layer to layer, as shown in Figure 3.1. For each *i*th node, is defined the *path(i)* as the ordered list of the nodes encountered starting from the root (not included) and moving to the *i*th node (Figure 3.2). It can be seen that any path from the root node to a terminal node encounters nodes numbered in the ascending order. Furthermore, each node belongs to a layer, which represents the position of the node in the network and its value is equal to the dimension of the *i*th path. Each branch starts from the sending bus and is identified by the number of its unique ending bus, that will be always in a higher level. The branches are numbered beginning from the the root node and are identified by the number of its unique ending bus, i.e. the branch between *node 3* and *node 7* is the *branch #7*.

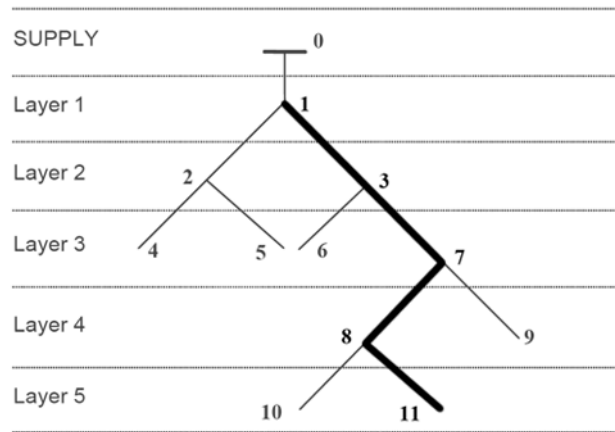


Figure 3.2: Example of a path: $path(11) = \{1,3,7,8,11\}$

The next step is to define the node-to branch incidence matrix \mathbf{L} and its inverse $\mathbf{\Gamma} = \mathbf{L}^{-1}$. As the root node is not included, both matrix will have dimensions $n \times n$. The criterion to fill the \mathbf{L} matrix is to assume for each branch a conventional value 1 for the sending bus and -1 for the ending bus, in mathematical terms:

$$l_{ij} = \begin{cases} -1 & \text{if } i=j \\ 1 & \text{if } j = \text{sending bus} \\ 0 & \text{otherwise} \end{cases} \quad (3.1)$$

where l_{ij} is the generic component of the \mathbf{L} matrix. The generic component γ_{ij} of the $\mathbf{\Gamma}$ matrix is defined by:

$$l_{ij} = \begin{cases} -1 & \text{if } j \in path(i) \\ 0 & \text{otherwise} \end{cases} \quad (3.2)$$

In the absence of mutual coupling between branches, it is possible to build the matrix $\mathbf{\Gamma}$ directly by visual inspection, without inverting the matrix \mathbf{L} . With a proper arrangement of the computational program, it is also possible to avoid the storage of the elements of the matrices \mathbf{L} and $\mathbf{\Gamma}$ [7].

For the system in Figure 3.1, the two matrices are written as follows:

$$\mathbf{L} = \begin{bmatrix} -1 & 0 & 0 & 0 & 0 & 0 & 0 & 0 & 0 & 0 & 0 \\ 1 & -1 & 0 & 0 & 0 & 0 & 0 & 0 & 0 & 0 & 0 \\ 1 & 0 & -1 & 0 & 0 & 0 & 0 & 0 & 0 & 0 & 0 \\ 0 & 1 & 0 & -1 & 0 & 0 & 0 & 0 & 0 & 0 & 0 \\ 0 & 1 & 0 & 0 & -1 & 0 & 0 & 0 & 0 & 0 & 0 \\ 0 & 0 & 1 & 0 & 0 & -1 & 0 & 0 & 0 & 0 & 0 \\ 0 & 0 & 1 & 0 & 0 & 0 & -1 & 0 & 0 & 0 & 0 \\ 0 & 0 & 0 & 0 & 0 & 0 & 1 & -1 & 0 & 0 & 0 \\ 0 & 0 & 0 & 0 & 0 & 0 & 1 & 0 & -1 & 0 & 0 \\ 0 & 0 & 0 & 0 & 0 & 0 & 0 & 1 & 0 & -1 & 0 \\ 0 & 0 & 0 & 0 & 0 & 0 & 0 & 1 & 0 & 0 & -1 \end{bmatrix} \quad (3.3)$$

$$\mathbf{\Gamma} = \begin{bmatrix} -1 & 0 & 0 & 0 & 0 & 0 & 0 & 0 & 0 & 0 & 0 \\ -1 & -1 & 0 & 0 & 0 & 0 & 0 & 0 & 0 & 0 & 0 \\ -1 & 0 & -1 & 0 & 0 & 0 & 0 & 0 & 0 & 0 & 0 \\ -1 & -1 & 0 & -1 & 0 & 0 & 0 & 0 & 0 & 0 & 0 \\ -1 & -1 & 0 & 0 & -1 & 0 & 0 & 0 & 0 & 0 & 0 \\ -1 & 0 & -1 & 0 & 0 & -1 & 0 & 0 & 0 & 0 & 0 \\ -1 & 0 & -1 & 0 & 0 & 0 & -1 & 0 & 0 & 0 & 0 \\ -1 & 0 & -1 & 0 & 0 & 0 & -1 & -1 & 0 & 0 & 0 \\ -1 & 0 & -1 & 0 & 0 & 0 & -1 & 0 & -1 & 0 & 0 \\ -1 & 0 & -1 & 0 & 0 & 0 & -1 & -1 & 0 & -1 & 0 \\ -1 & 0 & -1 & 0 & 0 & 0 & -1 & -1 & 0 & 0 & -1 \end{bmatrix} \quad (3.4)$$

The root node is defined by the following known parameters:

- \bar{V}_0 : root node voltage. Usually it is assumed the angle of the root voltage as reference for the system, leading to $\bar{V}_0 = V_0 * e^{j*0}$.
- \bar{I}_0 : net current injected in the root node.
- \bar{Y}_{S0} : total shunt admittance due to the shunt line parameters and to the equivalent admittance of the load connected to the root node.

The electrical variables at every node different to the root node are the following vectors:

- $\mathbf{v} = [\bar{V}_1, \dots, \bar{V}_i, \dots, \bar{V}_n]^T$: node voltages.

- $\mathbf{i}_S = [\bar{I}_{S1}, \dots, \bar{I}_{S2}, \dots, \bar{I}_{Sn}]^T$: total shunt currents. Includes the currents absorbed by shunt line admittances and the load currents.
- $\mathbf{S}_L = [\bar{S}_{L1}, \dots, \bar{S}_{L2}, \dots, \bar{S}_{Ln}]^T$: complex load powers.

In addition, are defined the branch currents vector and the diagonal impedance matrix as follows:

- $\mathbf{i}_B = [\bar{I}_{B1}, \dots, \bar{I}_{B2}, \dots, \bar{I}_{Bn}]^T$: branch currents circulating in the series line impedance.
- $\mathbf{Z}_B \in C^{n,n}$: containing the series impedance of the branches.
- $\mathbf{Y}_B = \mathbf{Z}_B^{-1} \in C^{n,n}$: containing the series admittance of the branches.
- $\mathbf{Y}_S \in C^{n,n}$: containing the total shunt admittance at each node, due to the contribution of the shunt line parameters and of the equivalent load admittance, that depends on the equivalent load model (detailed explanation can be find in section 4.1.3).

Once the system is defined according to the conventional parameters for the method and the initial bus voltage vector is defined, the solution method can be applied. The backward/forward sweep method for the load-flow computation is an iterative method in which, at each iteration, two computational stages are performed [7]:

- Backward Current Sweep:

At each k th iteration, the shunt currents ($\mathbf{i}_S^{(k)}$) are computed on the basis of the voltage vector at the previous iteration ($\mathbf{v}^{(k-1)}$):

$$\mathbf{i}_S^{(k)} = f(\mathbf{v}^{(k-1)}) \quad (3.5)$$

The branch currents are calculated as the summation of the injection currents from the receiving bus toward the sending bus of the feeder:

$$\mathbf{i}_B^{(k)} = \mathbf{\Gamma}^T * \mathbf{i}_S^{(k)} \quad (3.6)$$

where the $\mathbf{\Gamma}^T$ matrix serves as a filter applied to the shunt currents vector to consider for each branch, only the current injections located in the path from that node and to the root.

- Forward Voltage Sweep:

Once the branch currents are known, the bus voltages can be calculated from the sending bus toward the receiving bus on the feeder. They are updated on the basis of the voltage at the root node and of the voltage drops on the distribution lines evaluated using the branch current obtained in the backward stage:

$$\mathbf{v}^{(k)} = \mathbf{1} * \bar{V}_0 - \mathbf{\Gamma} * \mathbf{Z}_B * \mathbf{i}_B^{(k)} \quad (3.7)$$

where $\mathbf{1}$ is a $n \times 1$ vector composed of all unity terms.

The backward and forward stages are repeated iteratively, until the stop criterion is reached. This criterion is expressed in Equation (3.8), which means that the difference between the load voltages computed at the current iteration and at the previous iteration has to be lower than a specified tolerance (ε). If the stop criterion is not reached after the maximum number of iteration established, the method could be diverging. Considerations on the convergence of the backward/forward sweep method are illustrated in [7].

$$\max_i \left\{ \frac{|\bar{V}_i^{(k+1)} - \bar{V}_i^{(k)}|}{|\bar{V}_i^{(k)}|} \right\} < \varepsilon \quad \text{for } i = 1, \dots, n \quad (3.8)$$

Every node current is calculated as a function of corresponding node voltage computed at the previous iteration, therefore if Equation (3.6) and Equation (3.7) are combined, it can be seen that every bus voltage is also a function of the corresponding node voltage computed at the previous iteration:

$$\mathbf{v}^{(k)} = \mathbf{1} * \bar{V}_0 - \mathbf{\Gamma} * \mathbf{Z}_B * \mathbf{\Gamma}^T * \mathbf{i}_S^{(k)} \quad (3.9)$$

$$\mathbf{i}_S^{(k)} = g(\mathbf{v}^{(k-1)}) \quad (3.10)$$

$$\mathbf{v}^{(k)} = f(\mathbf{v}^{(k-1)}) \quad (3.11)$$

From Equation (3.11) can be recognized the Gauss-type numerical form of the backward/forward sweep method. In a Gauss-type numerical method with an iterative process that can be written according to Equation (3.13), is known from the numerical analysis [35] that the iterative process converges if and only if:

$$\rho(\mathbf{B}) < 1 \quad (3.12)$$

$$\mathbf{x}^{(k)} = \mathbf{B} * \mathbf{x}^{(k-1)} + \mathbf{c} \quad (3.13)$$

where $\rho(\mathbf{B})$ is maximum absolute eigenvalue of the matrix \mathbf{B} . Furthermore, considering any norm $\|\mathbf{B}\|$ of the matrix \mathbf{B} consistent with a vector norm, then:

$$\rho(\mathbf{B}) \leq \|\mathbf{B}\| \quad (3.14)$$

From Equations (3.12) and Equation (3.14) a sufficient condition for convergence can be taken as:

$$\|\mathbf{B}\| < 1 \quad (3.15)$$

In the specific case of the BFS method, Equation (3.13) can be written as [7]:

$$\mathbf{v}^k = \mathbf{B}^{(k-1)} * \mathbf{v}^{(k-1)} + \mathbf{v}^{(0)} \quad (3.16)$$

$$\mathbf{B}^{(k-1)} = \mathbf{\Gamma} * \mathbf{Z}_B * \mathbf{\Gamma}^T * \mathbf{Y}_S^{(k-1)} \quad (3.17)$$

Reference [7] proposes two ranges of convergence for the method when all loads are assumed to be modeled as constant admittances, Equations (3.18) and (3.19), being the second one the less restrictive sufficient condition for convergence:

$$\|\mathbf{B}\|_1 < \|\mathbf{\Gamma}^T\|_1 * \|\mathbf{Z}_B\|_1 * \|\mathbf{\Gamma}\|_1 * \|\mathbf{Y}_S\|_1 < 1 \quad (3.18)$$

$$\|\mathbf{B}\|_1 < \|\mathbf{\Gamma}^T * \mathbf{Z}_B * \mathbf{\Gamma}\|_1 * \|\mathbf{Y}_S\|_1 < 1 \quad (3.19)$$

where:

$\|\mathbf{\Gamma}^T\|_1$ is the number of network layers, which can vary from 1 (star topology) to n (unique feeder).

$\|\mathbf{\Gamma}\|_1$ is the maximum number of buses located after any node of the system. It will be equal to n if the root node is connected to a unique node.

$\|\mathbf{Z}_B\|_1$ is the maximum magnitude of a single branch impedance.

$\|\mathbf{Y}_S\|_1$ is the maximum magnitude of a shunt admittance.

From Equation (3.18) it can be seen that any modification on the system that leads to an increase of any load, series impedance of a branch increase, number of network layers or number of network nodes, will move the solution point closer to the convergence point.

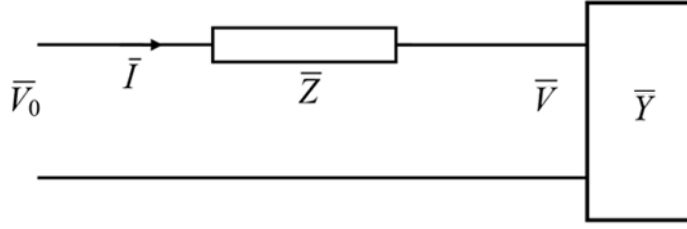


Figure 3.3: Two-node system.

In the case of a two bus system, as the one shown in Figure 3.3 the convergence condition becomes:

$$Z * Y^{(\infty)} < 1 \quad (3.20)$$

where $Y^{(\infty)}$ is the load admittance at the solution point. The limit condition $Z * Y^{(\infty)} = 1$ corresponds to the maximum power delivered to a load with given power factor. If the modulus Z of the line impedance and the power factor of the load are known, the maximum power does not depend on the type of load model (constant admittance, constant power, etc.). Thus, the convergence of the iterative method is assured for any load power up to the maximum power. Furthermore, it is not possible to converge to a solution point located on the lower branch of the V(P) curve (Figure 3.4), since all the points on the lower branch have an equivalent admittance higher than $Y^{(\infty)}$ and the condition (3.20) is not satisfied [7]. This is a very important difference with respect to other load-flow algorithms as Newton- Raphson, which can also find the solutions on the lower branch of the V(P) curve.

According to the maximum power transfer theorem, the maximum power will be delivered to the load if:

$$\begin{cases} Re \{ \bar{Z} \} = Re \left\{ \frac{1}{\bar{Y}^{(\infty)}} \right\} \\ Im \{ \bar{Z} \} = -Im \left\{ \frac{1}{\bar{Y}^{(\infty)}} \right\} \end{cases} \quad (3.21)$$

The condition mentioned before, represents the resonant operation point for the two node system. Therefore, this method has to be applied very carefully and with some modifications to analysis that includes harmonic frequencies.

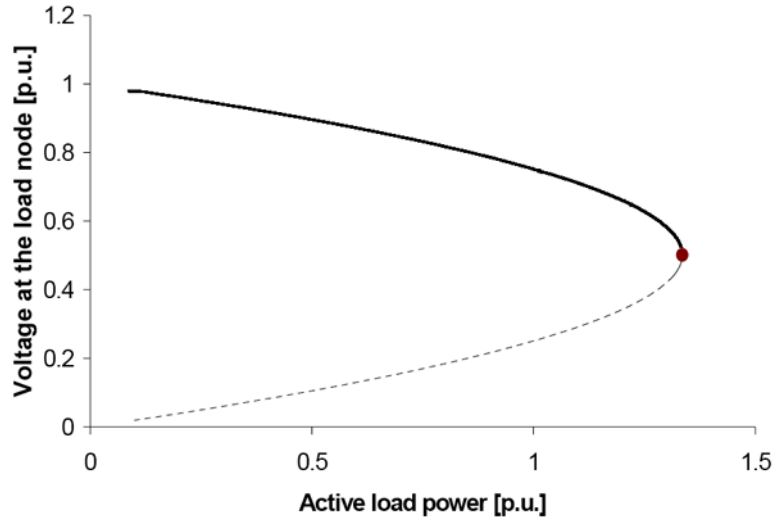


Figure 3.4: V(P) curve for the two-node system [7].

3.1.2 Weakly Meshed Network Treatment

When a distribution feeder is serving high-density load areas, it can operate with loops created by closing normal open tie switches. The radial network solution algorithm can not be directly applied to this kind of network. Nevertheless, by selecting some breakpoints in the network and following the procedure proposed in [40], it can be converted to a radial configuration and the proposed method introduced in the previous section can be applied.

The procedures consist of applying the following series of steps for each iteration:

1. Interrupt the branch currents of the loops in the network by the creation of a breakpoint in each one. This will convert the breakpoint node k in two nodes k_1 and k_2 , giving as a result a radial network.
2. Inject two currents \bar{J}_{k_1} and \bar{J}_{k_2} with equal module but opposite polarity at the two end nodes created at the breakpoint (Figure 3.5). The module of these currents will be equal to the current flowing through the branch of the original loop \bar{J}_k . This way, there will be no alteration of the network operating condition.
3. Solve the network using the backward forward sweep based method described in the previous section, considering \bar{J}_{k_1} and \bar{J}_{k_2} as current injections in their respective buses.
4. Verify that the difference between the voltages at the two nodes \bar{k}_1 and \bar{k}_2 is below an established tolerance. If it is, the procedure is finished. If it is not, a

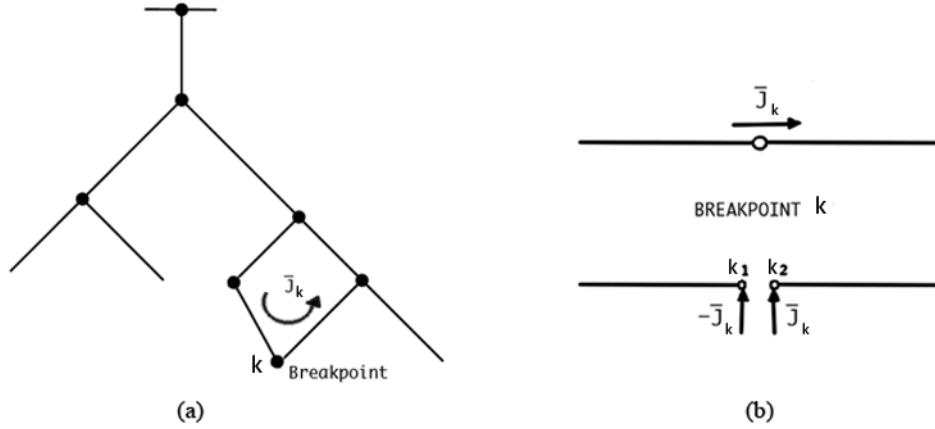


Figure 3.5: (a) Weakly meshed network (b) Breakpoint representation using nodal current injections

compensation method needs to be apply.

To calculate the values of the injection currents at the breakpoints it is used the compensation method [46]. It is an iterative method that solves the following equation system:

$$\tilde{\mathbf{V}} = \tilde{\mathbf{Z}} * \tilde{\mathbf{J}} \quad (3.22)$$

$$\begin{bmatrix} \tilde{V}_i \\ \vdots \\ \tilde{V}_k \\ \vdots \\ \tilde{V}_p \end{bmatrix} = \begin{bmatrix} \tilde{z}_{ii} & \cdots & \tilde{z}_{ik} & \cdots & \tilde{z}_{ip} \\ \vdots & \ddots & \vdots & \ddots & \vdots \\ \tilde{z}_{ki} & \cdots & \tilde{z}_{kk} & \cdots & \tilde{z}_{kp} \\ \vdots & & \vdots & \ddots & \vdots \\ \tilde{z}_{pi} & \cdots & \tilde{z}_{pk} & \cdots & \tilde{z}_{pp} \end{bmatrix} * \begin{bmatrix} \tilde{J}_i \\ \vdots \\ \tilde{J}_k \\ \vdots \\ \tilde{J}_p \end{bmatrix} \quad (3.23)$$

where \tilde{V}_k is the voltage difference between the two nodes k_1 and k_2 after the cut of the breakpoint k . The matrix $\tilde{\mathbf{Z}}$ is calculated one column at a time. Its k th column is obtained setting $\tilde{J}_k = 1 p.u.$ and all the other currents equal to zero $\tilde{J}_{i \neq k} = 0$. This corresponds to the application of 1 p.u. current at the breakpoint k with all loads and the source at the root node removed. In the absence of loads, the accurate solution of the power flow for the radial network can be reached in just one iteration. The resulting k th column is equal to the voltage difference at the breakpoints:

$$\tilde{\mathbf{Z}}_k = \tilde{\mathbf{V}} \Big|_{\tilde{J}_k=1; \tilde{J}_{i \neq k}=0} \quad (3.24)$$

Numerically, the diagonal elements of the matrix \tilde{z}_{ii} are equal to the sum of the line impedance in for all the line sections in loop i . The off-diagonal elements \tilde{z}_{ij} are nonzero only if loop i and loop j share one or more common line sections, the corresponding sign depends on the relative direction of the breakpoint current injections for loops i and j .

The impedance matrix calculated from Equation (3.24) will be constant during the following iterative process:

1. It is calculated the voltage differences vector $\tilde{\mathbf{V}}^{(m)}$ at the m th iteration. It is done solving the network with the BFS method, using the $\tilde{\mathbf{J}}^{(m-1)}$ vector calculated at the previous iteration. The initial values of the breakpoint currents are zero.
2. The convergence criterion is evaluated. If the maximum breakpoint voltage difference is within prescribed limits or the variation of this difference does not exceed a specified tolerance for NS successive iterations, exit the iterative process, if it is not continue with steps 3, 4 and 1.
3. It is calculated the incremental change in the breakpoint currents al the m th iteration ($\Delta\tilde{\mathbf{J}}^{(m)}$).

$$\tilde{\mathbf{V}}^{(m)} = \tilde{\mathbf{Z}} * \Delta\tilde{\mathbf{J}}^{(m)} \quad (3.25)$$

4. The breakpoint currents are updated :

$$\tilde{\mathbf{J}}^{(m)} = \tilde{\mathbf{J}}^{(m-1)} + \Delta\tilde{\mathbf{J}}^{(m)} \quad (3.26)$$

Figure 3.6 shows the extension of the compensation method, where compensation currents must be injected to all three phases with opposite polarity at the two end nodes, k_1 and k_2 . The procedure is the same explained above, the only difference is that matrix and vectors dimensions will be tripled.

3.2 Harmonic Analysis

The purpose of harmonic analysis is to determine the distribution of harmonic currents and voltages levels in a power system, and then calculate harmonic distortion indices. This analysis can be then used to the study of resonant conditions, harmonic filter designs of other effects of harmonics on the power system in general.

The simplest harmonic analysis can be made modeling the network as a single harmonic source in a single-phase network equivalent. This model is commonly used to

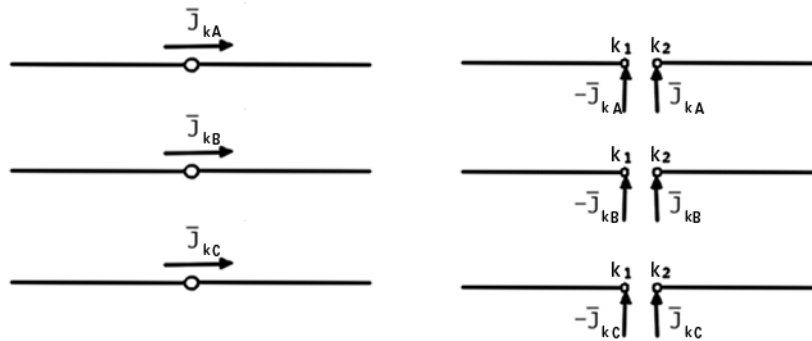


Figure 3.6: Three phase breakpoint representation using nodal current injections

derive the system harmonic impedances at the point of common coupling in filter design. However, as mentioned in the previous section, the distribution networks are in general unbalanced and may contain several harmonic sources. Therefore, the derivation of the harmonic voltages and currents existing in the network requires a multi-source three-phase harmonic analysis.

The commonly used harmonic analysis algorithms can be divided into two categories [45]. The first category is based on the transient-state analysis techniques, such as the time domain analysis and can be done based on time or frequency domain:

- **Time Domain Simulation**

The nonlinear and time-varying elements in the power system can significantly change the interaction of the harmonics with the power system. Therefore, some times for studying phenomena including non-linearity, switching operations, long-time simulations, and control systems it is necessary to use the differential equations that represent the behavior of the power system components. This results in a system of equations, usually nonlinear, that has to be solved by numerical integration.

The two most commonly used methods are the state variable and the nodal analysis. The state variable solution was the first applied to ac-dc power systems [1], but it is the nodal approach the one that has become most popular in the electromagnetic transient simulation of power system behavior because of its highly efficiency.

Once the harmonic distortions have been calculated for the steady state in the time domain, using of the Fast Fourier Transform (FFT) these can be converted into the frequency domain. This operation requires considerable time. Another problem of the time domain algorithm applied to harmonic studies is the difficulty of modeling components with distributed or frequency-dependent parameters [4].

- **Frequency Domain Simulation**

It consists of computing the harmonic current flow throughout the system for each harmonic frequency and then apply the principle of superposition. The system components are modeled to be a function of the frequency, so they have to be recalculated for each power flow made.

It is appropriate for studying phenomena such as frequency dependence, system equivalents, and frequency response at steady state.

If the harmonics generated by the nonlinear components are reasonably independent of the voltage distortion level in the a.c. system, the derivation of the harmonic sources models can be decoupled from the analysis of harmonic penetration, making a direct solution possible. This kind of solution is also called *current injection method* because most nonlinear loads have a behavior of a harmonic current sources in the system. In such cases, the expected voltage levels or the results of a fundamental frequency load flow are used to derive the current waveforms, and with them the harmonic content of the nonlinear components.

Instead, when the power rating of the non linear loads in relation to the system short circuit power is high, suppose an independency on the harmonic generated respect to the voltage distortion level in the system, may led to a vague results. In these cases, accurate results can only be obtained by iterative solution of the non linear equations that describe the steady state as a whole [4].

3.2.1 Direct Harmonic Solutions

If the calculation of the harmonic sources can be decoupled from the analysis of harmonic penetration, it is possible to apply a direct solution. It uses the expected voltage levels or the results of a fundamental frequency load flow to derive the spectrum of the currents injected by each non linear component into the linear system. Figure 3.8 shows the flow chart for the direct harmonic solution.

Taking as a valid hypothesis the superposition principle, the direct approaches divide the network in several systems that are solved one at a time:

1. Fundamental System:

All the nonlinear loads are represented as linear loads absorbing just the fundamental component of the current. Usually the model adopted is the one with fixed active and reactive power (see section 4.1.3).

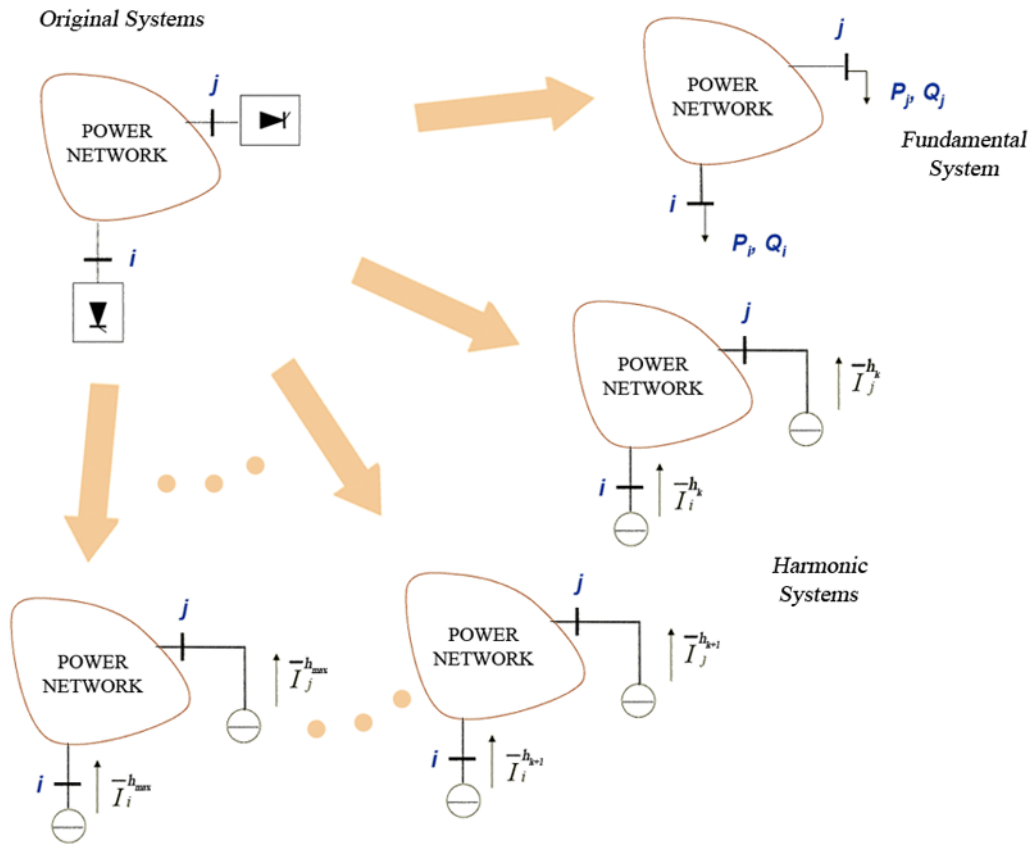


Figure 3.7: Network decomposition for the direct solution approach.

2. Harmonic Systems:

It is solved one system for each harmonic order of interest. In these systems the non linear loads are represented by a current source and the network is modeled as its equivalent Thévenin impedance. The values of the currents injected by the harmonic sources are computed in one of the following ways:

- Notice a typical current spectrum of the load, usually obtained as a table with the values of I_h/I_1 for each harmonic order, the value of the harmonic current source will be obtained multiplying the table data by the fundamental component obtained from the solution of the fundamental system.
- With specific model for each type of load. These models are usually impedances which values are frequency-dependent. The most common models are explained in section 4.2.4.

Once all the currents injections are known, the voltage distortion level can be computed from the linear system:

$$\mathbf{V}^{(h)} = \left(\mathbf{Y}^{(h)} \right)^{-1} * \mathbf{I}^{(h)} \quad (3.27)$$

where:

$\mathbf{I}^{(h)}$ is the injected currents vector for the h th harmonic.

$\mathbf{V}^{(h)}$ is the bus voltage vector for the h th harmonic.

$\mathbf{Y}^{(h)}$ is the nodal admittance matrix for the h th harmonic.

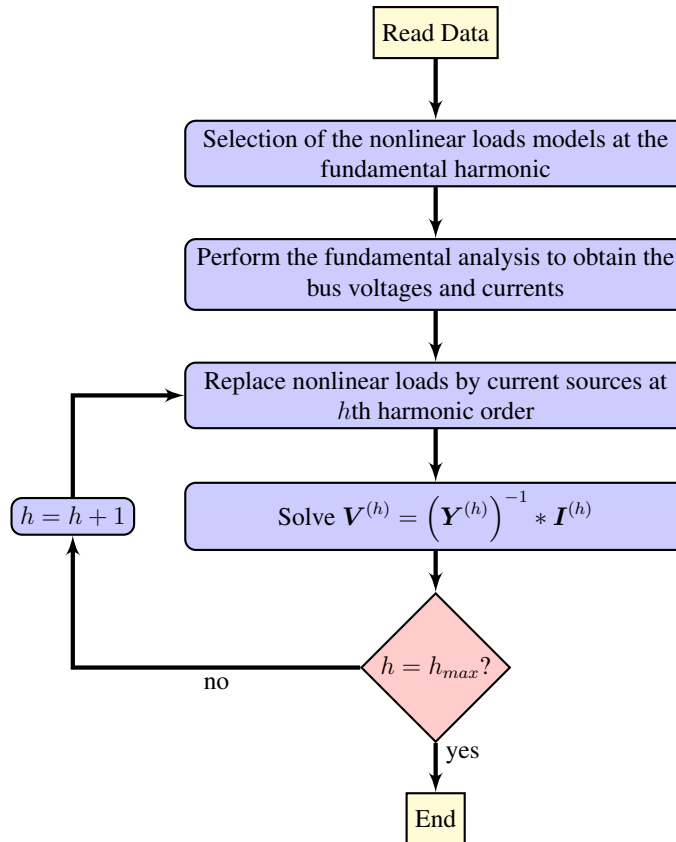


Figure 3.8: Structure diagram of the direct solution.

3.2.2 Iterative Harmonic Analysis

The increased power rating of modern HVDC and FACTS devices in relation to the short circuit power, is making that the principle of superposition frequently does not apply any more [4]. The harmonic injection from each source will be, in general, a function of the harmonic injection by the other sources and the system state. In these cases, accurate results can be only obtained by modeling the nonlinear loads coupled with the system admittance matrix, or some other more complicated expressions of the power system. Iterative algorithms, either sequentially or simultaneously, will be generally required to obtain an accurate solution.

In most of the commonly used iterative harmonic analysis, the initial estimate of harmonic current injections by the harmonic sources are determined first and the network bus harmonic voltages are computed. The estimates of the harmonic injection currents are then updated with the harmonic voltages computed in the previous iteration. This process is sequentially repeated until the convergence in the magnitude of the harmonic voltages on each bus is reached. Figure 3.9 shows the flow chart for the iterative harmonic solution.

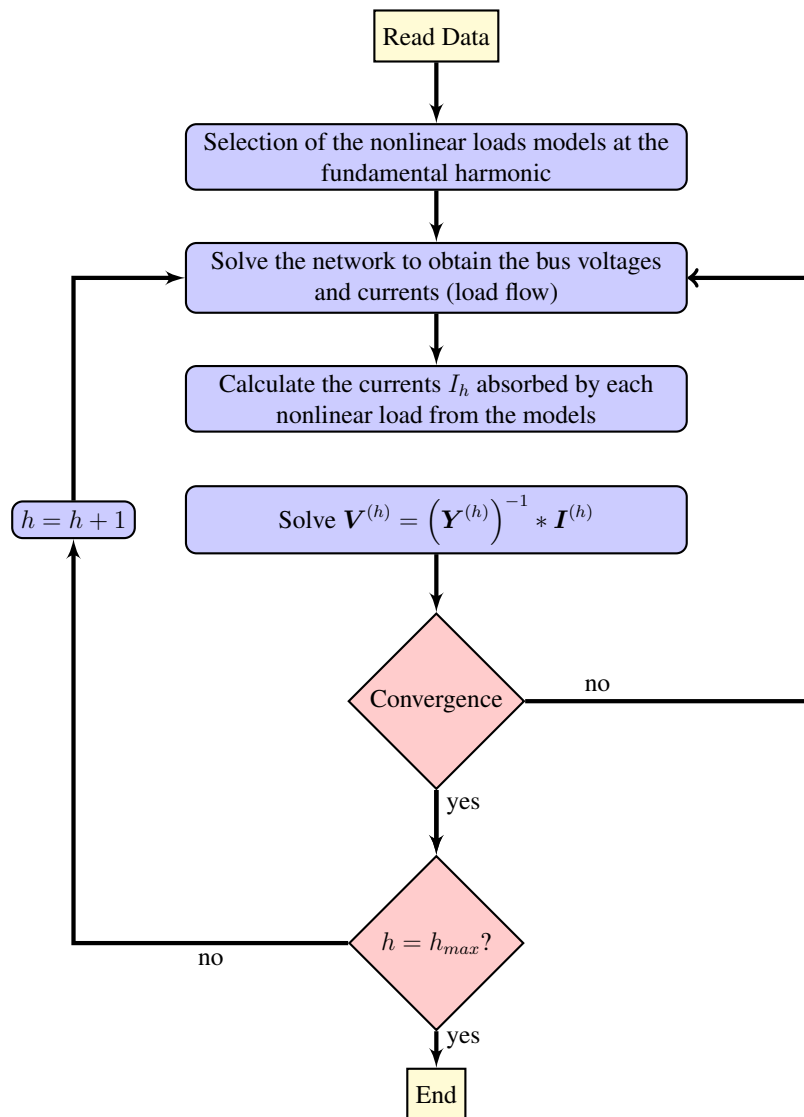


Figure 3.9: Structure diagram of the iterative solution.

Chapter 4

Components Modeling

When a power system analysis is performed, its accuracy does not depend only on the method applied to solve the equations, but a great part depends on the accuracy of a well developed model of the network. In particular, if the system under analysis has an elevate number of nonlinear loads and a further harmonic analysis is needed, the component model has to be modified according to its behavior in presence of high frequency sources.

This chapter describes the most common models used for the principal distribution system components and loads, at both fundamental and harmonic frequencies.

4.1 Modeling At Fundamental Frequency

4.1.1 Transmission Lines

Distribution feeders are unbalanced, therefore assumptions regarding spacing between conductors, conductor size and transpositions have to be avoided for better results. Assuming the earth as infinite, uniform solid with a flat upper uniform surface and constant resistivity, John Carson [8] made use of conductor images to compute the self and mutual impedances of a power line in general cases, including unbalanced cases. Equations (4.1) and (4.2) shows the final result of Carson's work.

$$\bar{z}_{ii} = r_i + 4 * \omega * P_{ii} * G + j * \left(X_i + 2 * \omega * G * \ln \left(\frac{S_{ii}}{RD_i} \right) + 4 * \omega * Q_{ii} * G \right) \quad (4.1)$$

$$\bar{z}_{ij} = 4 * \omega * P_{ij} * G + j * \left(2 * \omega * G * \ln \left(\frac{S_{ij}}{RD_j} \right) + 4 * \omega * Q_{ij} * G \right) \quad (4.2)$$

$$X_i = 2 * \omega * G * \ln \left(\frac{RD_i}{GMR_i} \right) \quad (4.3)$$

$$P_{ij} = \frac{\pi}{8} - \frac{1}{3 * \sqrt{2}} * k_{ij} * \cos(\theta_{ij}) + \frac{k_{ij}^2}{16} * \cos(2 * \theta_{ij}) * \left(0.6728 + \ln \left(\frac{2}{k_{ij}} \right) \right) \quad (4.4)$$

$$Q_{ij} = -0.0386 + \frac{1}{2} * \ln \left(\frac{2}{k_{ij}} \right) + \frac{\pi}{8} - \frac{1}{3 * \sqrt{2}} * k_{ij} * \cos(\theta_{ij}) \quad (4.5)$$

$$k_{ij} = 8.565 * 10^{-4} * S_{ij} * \sqrt{\frac{f}{\rho}} \quad (4.6)$$

where:

\bar{z}_{ii} is the self impedance of conductor i in $\Omega/mile$.

\bar{z}_{ij} is the mutual impedance between conductor i and j in $\Omega/mile$.

r_i is the resistance of conductor i in $\Omega/mile$. Typically known from a table of conductor data.

$G = 0.1609347 * 10^{-3} \Omega/mile$.

RD_i is the radius of conductor i in fts.

GMR_i is the geometric mean radius of conductor i in fts.

$\omega = 2 * \pi * f$.

f is the system frequency in Hz.

ρ is the resistivity of earth in $\Omega - m$

D_{ij} is the distance between conductors i and j in ft (Figure 4.1).

S_{ij} is the distance between conductors i and image j' in ft (Figure 4.1).

θ_{ij} is the angle between line that joins conductor i to its own image i' and the one that joins conductor i to the image j' (Figure 4.1).

Two simplifications can be made for simplify Carson's equations [25]:

$$P_{ij} = \frac{\pi}{8} \quad (4.7)$$

$$Q_{ij} = -0.03860 + \frac{1}{2} \ln \left(\frac{2}{k_{ij}} \right) \quad (4.8)$$

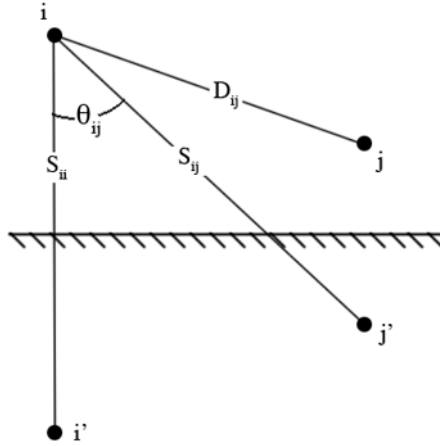


Figure 4.1: Conductors and images geometrical configuration.

Applying the previous simplifications to Equations (4.1) and (4.2), the modified Carson's equations can be obtained:

$$\bar{z}_{ii} = r_i + \pi^2 * f * G + j * 4 * \pi * f * G * \left(\ln \left(\frac{1}{GMR_i} \right) + 7.6786 + \frac{1}{2} * \ln \left(\frac{\rho}{f} \right) \right) \quad (4.9)$$

$$\bar{z}_{ij} = \pi^2 * f * G + j * 4 * \pi * f * G * \left(\ln \left(\frac{1}{D_{ij}} \right) + 7.6786 + \frac{1}{2} * \ln \left(\frac{\rho}{f} \right) \right) \quad (4.10)$$

Once computed the self and mutual impedances for a power line segment, it can be written the *primitive impedance matrix*. Equation (4.11) shown this matrix for a three-phase line consisting of m neutrals.

$$\mathbf{Z}_{prim} = \begin{bmatrix} \bar{z}_{aa} & \bar{z}_{ab} & \bar{z}_{ac} & | & \bar{z}_{an_1} & \bar{z}_{an_2} & \cdots & \bar{z}_{an_m} \\ \bar{z}_{ba} & \bar{z}_{bb} & \bar{z}_{bc} & | & \bar{z}_{bn_1} & \bar{z}_{bn_2} & \cdots & \bar{z}_{bn_m} \\ \bar{z}_{ca} & \bar{z}_{cb} & \bar{z}_{cc} & | & \bar{z}_{cn_1} & \bar{z}_{cn_2} & \cdots & \bar{z}_{cn_m} \\ \hline \bar{z}_{n_1a} & \bar{z}_{n_1b} & \bar{z}_{n_1c} & | & \bar{z}_{n_1n_1} & \bar{z}_{n_1n_2} & \cdots & \bar{z}_{n_1n_m} \\ \bar{z}_{n_2a} & \bar{z}_{n_2b} & \bar{z}_{n_2c} & | & \bar{z}_{n_2n_1} & \bar{z}_{n_2n_2} & \cdots & \bar{z}_{n_2n_m} \\ \vdots & \vdots & \vdots & | & \vdots & \vdots & & \vdots \\ \bar{z}_{n_ma} & \bar{z}_{n_mb} & \bar{z}_{n_mc} & | & \bar{z}_{n_mn_1} & \bar{z}_{n_mn_2} & \cdots & \bar{z}_{n_mn_m} \end{bmatrix} \quad (4.11)$$

In most cases, different line configurations with different numbers of wires, are used in the same system. This would lead to different orders of the primitive impedance matrix, leading to complex calculations. Therefore, the primitive impedance matrices

of all the elements of a system are reduced to the same dimensions, usually 3×3 matrix, with the self and mutual equivalent impedances for the three phases. One standard method to achieve this it is the Kron reduction [27], based on the Kirchoff laws.

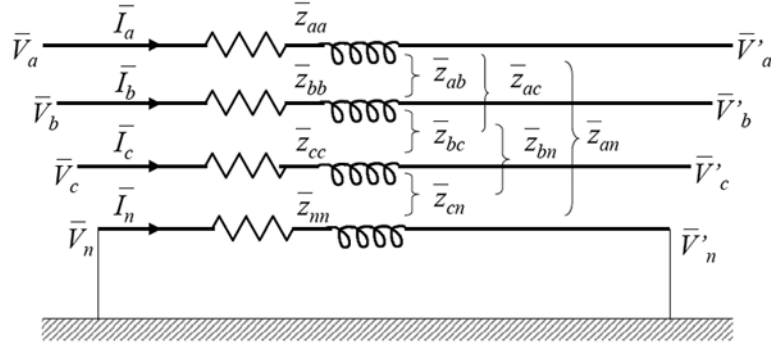


Figure 4.2: Representation of the impedances for a four-wire wye line segment.

For the four-wire multigrounded network of Figure 4.2, the Kirchoff Voltage Law can be written as:

$$\begin{bmatrix} \bar{V}_a \\ \bar{V}_b \\ \bar{V}_c \\ \bar{V}_n \end{bmatrix} = \begin{bmatrix} \bar{V}'_a \\ \bar{V}'_b \\ \bar{V}'_c \\ \bar{V}'_n \end{bmatrix} + \begin{bmatrix} \bar{z}_{aa} & \bar{z}_{ab} & \bar{z}_{ac} & \bar{z}_{an} \\ \bar{z}_{ba} & \bar{z}_{bb} & \bar{z}_{bc} & \bar{z}_{bn} \\ \bar{z}_{ca} & \bar{z}_{cb} & \bar{z}_{cc} & \bar{z}_{cn} \\ \bar{z}_{na} & \bar{z}_{nb} & \bar{z}_{nc} & \bar{z}_{nn} \end{bmatrix} * \begin{bmatrix} \bar{I}_a \\ \bar{I}_b \\ \bar{I}_c \\ \bar{I}_n \end{bmatrix} \quad (4.12)$$

To apply the Kron reduction method to this system, Equation (4.13) has to be written as :

$$\begin{bmatrix} \mathbf{V}_{abc} \\ \mathbf{V}_{ng} \end{bmatrix} = \begin{bmatrix} \mathbf{V}'_{abc} \\ \mathbf{V}'_{ng} \end{bmatrix} + \begin{bmatrix} \mathbf{z}_{ij} & \mathbf{z}_{in} \\ \mathbf{z}_{nj} & \mathbf{z}_{nn} \end{bmatrix} * \begin{bmatrix} \mathbf{I}_{abc} \\ \mathbf{I}_{ng} \end{bmatrix} \quad (4.13)$$

Kron reduction consists in adding to the equations system (4.13) the two equations 4.14 and 4.15 for the neutral voltages and then apply a series of substitutions until arrive to the final Equation (4.16). All the mathematical passages can be found in reference [25].

$$\mathbf{V}_{ng} = \mathbf{0} \quad (4.14)$$

$$\mathbf{V}'_{ng} = \mathbf{0} \quad (4.15)$$

$$\mathbf{Z}_{abc} = \mathbf{z}_{ij} - \mathbf{z}_{in} * \mathbf{z}_{nn}^{-1} * \mathbf{z}_{nj} \quad (4.16)$$

$$\mathbf{Z}' = \mathbf{Z}_{abc} = \begin{bmatrix} \bar{z}_{aa} & \bar{z}_{ab} & \bar{z}_{ac} \\ \bar{z}_{ba} & \bar{z}_{bb} & \bar{z}_{bc} \\ \bar{z}_{ca} & \bar{z}_{cb} & \bar{z}_{cc} \end{bmatrix} \quad \Omega/mile \quad (4.17)$$

The shunt admittance of a line consists of the capacitive susceptance and the conductance. The latter is usually neglected because of its small value compared to the capacitive susceptance. To calculate the shunt capacitance of overheads lines, the same concept of conductors and their images is apply, so all the distances in following equations are also referred to Figure 4.1.

For a four-wire grounded wye line, the *primitive potential coefficient matrix* can be defined as follows [25]:

$$\mathbf{P}_{prim} = \begin{bmatrix} P_{aa} & P_{ab} & P_{ac} & P_{an} \\ P_{ba} & P_{bb} & P_{bc} & P_{bn} \\ P_{ca} & P_{cb} & P_{cc} & P_{cn} \\ P_{na} & P_{nb} & P_{nc} & P_{nn} \end{bmatrix} = \left[\begin{array}{c|c} \mathbf{P}_{ij} & \mathbf{P}_{in} \\ \hline \mathbf{P}_{nj} & \mathbf{P}_{nn} \end{array} \right] \quad (4.18)$$

$$P_{ii} = 11.17689 * \ln \left(\frac{S_{ii}}{RD_i} \right) \quad (4.19)$$

$$P_{ij} = 11.17689 * \ln \left(\frac{S_{ij}}{D_{ij}} \right) \quad (4.20)$$

Applying Kron reduction to Equation (4.18):

$$\mathbf{P}_{abc} = \mathbf{P}_{ij} - \mathbf{P}_{in} * \mathbf{P}_{nn}^{-1} * \mathbf{P}_{nj} \quad (4.21)$$

The capacitance matrix is given by the inverse of the potential coefficient matrix, then the phase shunt admittance, neglecting the shunt conductance, is given by:

$$\mathbf{Y}' = \mathbf{Y}_{abc} = j * \omega * \mathbf{P}_{abc}^{-1} \quad \mu S/mile \quad (4.22)$$

For undergrounds cable lines, the field created by the charged phase conductor does not link to adjacent conductors, therefore the admittance matrix is formed only by the diagonal terms [25]. The diagonal terms for concentric neutral cables are given by Equation (4.23), while the ones for a tape-shielded cables are given by Equation (4.24).

$$y_{ii} = j * \frac{77.3619}{\ln \left(\frac{R_b}{RD_i} \right) - \frac{1}{k} * \ln \left(\frac{k * RD_s}{R_b} \right)} \quad \mu S/mile \quad (4.23)$$

where:

R_b is the radius in feet of the circle going through the center of the neutral strands.

RD_i is the radius in feet of the center phase conductor.

RD_s is the radius in feet of neutral strands.

k is the number of neutral strands.

$$y_{ii} = j * \frac{77.3619}{\ln\left(\frac{R_b}{RD_i}\right)} \mu S/mile \quad (4.24)$$

and:

R_b is the radius in feet of circle going through the center of the tape shield.

RD_i is the radius in feet of the center phase conductor.

The parameters Z' and Y' are the distributed parameters of a power line, and they usually are not applied by themselves. An equivalent pi-circuit (Figure 4.3) is introduced. The use of the equivalent pi-circuit allows to calculate voltages and currents on its ends, but no intermediate points are considered. In any relation between voltage and current in an intermediate point is desired, another equivalent pi-circuit have to be determined from this point until the end.

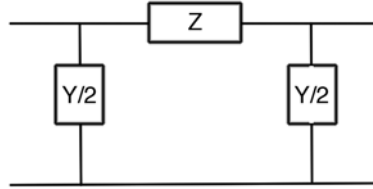


Figure 4.3: Equivalent Pi-Line Model

For short lines ($l < 150$ miles), matrices Z and Y can be obtained straightforward by multiplying Z' and Y' by the line length. However, if the lines can't be considered as short lines, the following equations have to be considered:

$$Z = Z_c * \sinh(\gamma * l) \quad (4.25)$$

$$\frac{Y}{2} = \frac{\tanh\left(\frac{\gamma * l}{2}\right)}{Z_c} \quad (4.26)$$

$$\gamma = \sqrt{z * y} \quad (4.27)$$

$$Z_c = \sqrt{\frac{z}{y}} \quad (4.28)$$

where:

Z_c is the characteristic impedance of the line (also known as surge impedance).

γ is the propagation constant.

z and y are the distributed parameters of the line.

In the case of multiconductor transmission lines, the nominal pi-series impedance and admittance per unit distance, \mathbf{Z}' and \mathbf{Y}' , are $m \times m$ matrix, with m the number of single-phase lines mutually coupled. In this case, the propagation constant is no longer a scalar but a matrix:

$$\gamma = \sqrt{\mathbf{Z}' * \mathbf{Y}'} \quad (4.29)$$

As the long-line model requires the evaluation of hyperbolic functions of this matrix, and there is no direct way of calculate \sinh or \tanh of a matrix, it has to be used the modal analysis employed in reference [18]. For a particular frequency, each mode is associated with a certain distribution of voltage and current in the conductors, a characteristic-impedance matrix and a propagation coefficient.

First it needs to expand the second order linear differential equations describing wave propagation along a single line to be used for the multiconductor lines:

$$\left[\frac{d^2 V}{dx^2} \right] = \mathbf{Z}' * \mathbf{Y}' * \mathbf{V} \quad (4.30)$$

$$\left[\frac{d^2 I}{dx^2} \right] = \mathbf{Y}' * \mathbf{Z}' * \mathbf{I} \quad (4.31)$$

After transforming the phase voltages to modal voltages with the proper transformation matrix \mathbf{T}_V , equal to the eigenvectors matrix of the $\mathbf{Z}' * \mathbf{Y}'$ product, Equations (4.30) and (4.31) can be written as:

$$\left[\frac{d^2 V_{mode}}{dx^2} \right] = \mathbf{\Lambda} * \mathbf{V}_{mode} \quad (4.32)$$

$$\left[\frac{d^2 I_{mode}}{dx^2} \right] = \mathbf{\Delta} * \mathbf{I}_{mode} \quad (4.33)$$

where $\mathbf{\Lambda}$ is the diagonal matrix of the elements of eigenvectors of the $\mathbf{Z}' * \mathbf{Y}'$ matrix. For the current equation, \mathbf{T}_I and $\mathbf{\Delta}$ are defined analog to \mathbf{T}_V and $\mathbf{\Lambda}$.

The propagation constant of each mode is the square root of the corresponding element (eigenvalue) of the $\mathbf{\Lambda}$ matrix:

$$\gamma_{mode,i} = \sqrt{\lambda_i} \quad (4.34)$$

$$\mathbf{\Lambda} = \begin{bmatrix} \gamma_1 & \cdots & \cdots & 0 \\ \vdots & \gamma_2 & & \vdots \\ \vdots & & \ddots & \vdots \\ 0 & \cdots & \cdots & \gamma_j \end{bmatrix} \quad (4.35)$$

The modal series impedance and shunt admittance must be computed from:

$$\mathbf{Z}'_{mode} = \mathbf{T}_V^{-1} * \mathbf{Z}' * \mathbf{T}_I \quad (4.36)$$

$$\mathbf{Y}'_{mode} = \mathbf{T}_I^{-1} * \mathbf{Y}' * \mathbf{T}_V \quad (4.37)$$

Once $\mathbf{Z}_{series,mode}$ and $\mathbf{Y}_{shunt,mode}$ have been calculated for each mode, \mathbf{Z}_{series} and \mathbf{Y}_{shunt} can be obtained by transforming back to the phase quantities:

$$\mathbf{Z}_{series} = \mathbf{T}_V * \mathbf{Z}' * \mathbf{T}_I^{-1} \quad (4.38)$$

$$\mathbf{Y}_{shunt} = \mathbf{T}_I * \mathbf{Y}' * \mathbf{T}_V^{-1} \quad (4.39)$$

In expanded form, Equations (4.38) and (4.39) can be written as [4]:

$$\mathbf{Z}_{eq} = l * \mathbf{Z}' * \mathbf{M} * \left[\frac{\sinh(\gamma * l)}{\gamma * l} \right] * \mathbf{M}^{-1} \quad (4.40)$$

$$\mathbf{Y}_{eq} = l * \mathbf{M} * \left[\frac{\tanh\left(\frac{\gamma * l}{2}\right)}{\frac{\gamma * l}{2}} \right] * \mathbf{M}^{-1} * \mathbf{Y}' \quad (4.41)$$

$$\left[\frac{\sinh(\gamma * l)}{\gamma * l} \right] = \begin{bmatrix} \frac{\sinh(\gamma_1 * l)}{\gamma_1 * l} & \cdots & \cdots & 0 \\ \vdots & \frac{\sinh(\gamma_2 * l)}{\gamma_2 * l} & & \vdots \\ \vdots & & \ddots & \vdots \\ 0 & \cdots & \cdots & \frac{\sinh(\gamma_j * l)}{\gamma_j * l} \end{bmatrix} \quad (4.42)$$

$$\left[\frac{\tanh\left(\frac{\gamma * l}{2}\right)}{\frac{\gamma * l}{2}} \right] = \begin{bmatrix} \frac{\tanh\left(\frac{\gamma_1 * l}{2}\right)}{\frac{\gamma_1 * l}{2}} & \dots & \dots & 0 \\ \vdots & \frac{\tanh\left(\frac{\gamma_2 * l}{2}\right)}{\frac{\gamma_2 * l}{2}} & & \vdots \\ \vdots & & \ddots & \vdots \\ 0 & \dots & \dots & \frac{\tanh\left(\frac{\gamma_j * l}{2}\right)}{\frac{\gamma_j * l}{2}} \end{bmatrix} \quad (4.43)$$

where:

\mathbf{Z}_{eq} and \mathbf{Y}_{eq} are the equivalent pi-series impedance and admittance.

\mathbf{M} is the matrix of normalized eigenvectors.

γ_j is the j th eigenvalue for $j/3$ mutually coupled circuits.

4.1.2 Transformers

Three-phase transformers are usually modeled in terms of their symmetrical components (positive, negative and zero sequence) under the assumption that the power system being studied is balanced and its components are symmetrical. As mentioned in the previous chapter, the distribution systems usually have unbalanced three-phase or mono-phase lines and loads, making the system unbalanced. As a result, the models established in positive, negative and zero sequence reference frame cannot be broken into independent sequence models and the decoupling feature of other symmetrical element models cannot be used further.

The method under study in this project is aimed to the distribution systems, therefore the transformer model presented in this section is in the a, b, c phases frame. Even if there are few methods developed to be use in asymmetrical networks with the sequence models [53], they still are the less common models applied to distribution systems.

Figure 4.4 shows the elementary circuit of a three-phase transformer showing 12-terminal coupled primitive network, consisting of three primary windings and three secondary windings mutually coupled through the transformer core. The short-circuit

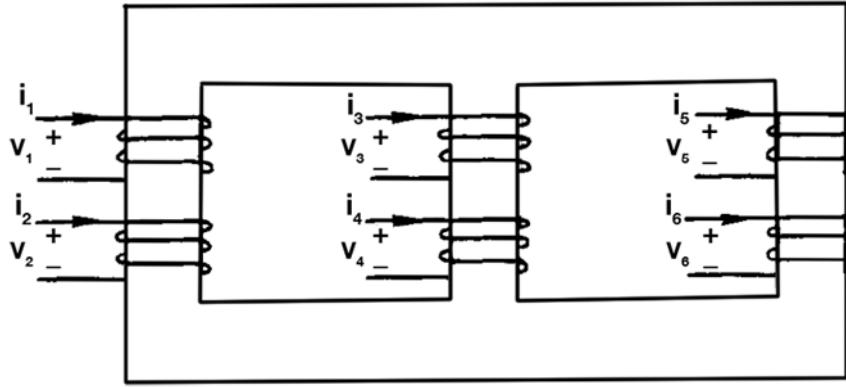


Figure 4.4: Three-phase transformer

primitive matrix for this network is:

$$\mathbf{Y}_{prim} = \begin{bmatrix} y_{11} & y_{12} & y_{13} & y_{14} & y_{15} & y_{16} \\ y_{21} & y_{22} & y_{23} & y_{24} & y_{25} & y_{26} \\ y_{31} & y_{32} & y_{33} & y_{34} & y_{35} & y_{36} \\ y_{41} & y_{42} & y_{43} & y_{44} & y_{45} & y_{46} \\ y_{51} & y_{52} & y_{53} & y_{54} & y_{55} & y_{56} \\ y_{61} & y_{62} & y_{63} & y_{64} & y_{65} & y_{66} \end{bmatrix} \quad (4.44)$$

$$\begin{bmatrix} i_1 \\ i_2 \\ i_3 \\ i_4 \\ i_5 \\ i_6 \end{bmatrix} = \begin{bmatrix} y_{11} & y_{12} & y_{13} & y_{14} & y_{15} & y_{16} \\ y_{21} & y_{22} & y_{23} & y_{24} & y_{25} & y_{26} \\ y_{31} & y_{32} & y_{33} & y_{34} & y_{35} & y_{36} \\ y_{41} & y_{42} & y_{43} & y_{44} & y_{45} & y_{46} \\ y_{51} & y_{52} & y_{53} & y_{54} & y_{55} & y_{56} \\ y_{61} & y_{62} & y_{63} & y_{64} & y_{65} & y_{66} \end{bmatrix} * \begin{bmatrix} v_1 \\ v_2 \\ v_3 \\ v_4 \\ v_5 \\ v_6 \end{bmatrix} \quad (4.45)$$

To fill the admittance matrix in Equation (4.45) it would have to be made 21 separate short circuit measurements. But if a flux symmetry is assumed, some algebraic simplifications can be done [9], obtaining :

$$\mathbf{Y}_{prim} = \begin{bmatrix} y_p & -y_m & y'_m & y''_m & y'_m & y''_m \\ -y_m & y_s & y''_m & y'''_m & y''_m & y'''_m \\ y'_m & y''_m & y_p & -y_m & y'_m & y''_m \\ y''_m & y'''_m & -y_m & y_s & y''_m & y'''_m \\ y'_m & y''_m & y'_m & y''_m & y_p & -y_m \\ y''_m & y'''_m & y''_m & y'''_m & -y_m & y_s \end{bmatrix} \quad (4.46)$$

where:

y'_m is the mutual admittance between primary coils.

y_m'' is the mutual admittance between primary and secondary coils on different cores.

y_m''' is the mutual admittance between secondary coils.

Equation (4.46) considers odds coils (1,3,5) primary windings and even coils (2, 4, 6) the secondary windings. If there are no mutual couplings the primed elements are all zero and the admittance matrix can be further simplified:

$$\mathbf{Y}_{prim} = \begin{bmatrix} y_p & -y_m & 0 & 0 & 0 & 0 \\ -y_m & y_s & 0 & 0 & 0 & 0 \\ 0 & 0 & y_p & -y_m & 0 & 0 \\ 0 & 0 & -y_m & y_s & 0 & 0 \\ 0 & 0 & 0 & 0 & y_p & -y_m \\ 0 & 0 & 0 & 0 & -y_m & y_s \end{bmatrix} \quad (4.47)$$

Equation (4.47) does not yet consider any particular connection of the three-phase transformer. The terminal pairs can still be connected in any of the six standard three-phase combinations of connections between triangle or star. If a connection matrix \mathbf{N} is defined according to Equation (4.48), after a Kron's transformation [27], the node impedance matrix can be written as in Equation (4.49).

$$\mathbf{v}_{branch} = \mathbf{N} * \mathbf{V}_{node} \quad (4.48)$$

$$\mathbf{Y}_{node} = \mathbf{N}^T * \mathbf{Y}_{prim} * \mathbf{N} \quad (4.49)$$

The node admittance matrix can be divided into four submatrices as follows:

$$\mathbf{Y}_{node} = \begin{bmatrix} \mathbf{Y}_{pp} & \mathbf{Y}_{ps} \\ \mathbf{Y}_{sp} & \mathbf{Y}_{ss} \end{bmatrix} \quad (4.50)$$

where each sub-matrix depends on the three-phase transformer connection. Table 4.1 shows the basic submatrices used in three-phase node admittance formation for the nine three-phase connections for three-phase banks, defining \mathbf{Y}_I , \mathbf{Y}_{II} and \mathbf{Y}_{III} as follows [9]:

$$\mathbf{Y}_I = \begin{bmatrix} y_t & 0 & 0 \\ 0 & y_t & 0 \\ 0 & 0 & y_t \end{bmatrix} \quad \mathbf{Y}_{II} = \frac{1}{3} * \begin{bmatrix} 2 * y_t & -y_t & -y_t \\ -y_t & 2 * y_t & -y_t \\ -y_t & -y_t & 2 * y_t \end{bmatrix} \quad (4.51)$$

$$\mathbf{Y}_{III} = \frac{1}{\sqrt{3}} * \begin{bmatrix} -y_t & y_t & 0 \\ 0 & -y_t & y_t \\ y_t & 0 & -y_t \end{bmatrix}$$

where y_t is the leakage admittance per phase in per unit. The numerical values of y_s , y_p and y_m of Equation (4.47) were assumed equal to the leakage admittance y_t due to the subtle differences in magnitude between, but if more complete information is available it can be exploited to the benefit of accuracy.

Winding Connections		Self-Admittance		Mutual Admittance	
Primary	Secondary	Y_{pp}	Y_{ss}	Y_{ps}	Y_{sp}
Y-Ground	Y-Ground	Y_I	Y_I	$-Y_I$	$-Y_I$
Y-Ground	Y	Y_{II}	Y_{II}	$-Y_{II}$	$-Y_{II}$
Y	Y-Ground				
Y	Y				
Δ	Δ				
Y-Ground	Δ	Y_I	Y_{II}	Y_{III}	Y_{III}^T
Y	Δ	Y_{II}	Y_{II}	Y_{III}	Y_{III}^T
Δ	Y				
Δ	Y-Ground	Y_{II}	Y_I	Y_{III}	Y_{III}^T

Table 4.1: Submatrices of Three-Phase Transformer Connections

If the off-nominal tap ratio between primary and secondary windings is $\alpha : \beta$, where α and β are the taps on the primary and secondary side, respectively, in per unit, then the submatrices are modified as follows [14]:

- Divide self-admittance of primary matrix by α^2
- Divide self-admittance of secondary matrix by β^2
- Divide mutual admittance matrixes by $(\alpha * \beta)$

Once the admittance matrix has been formed for a particular connection it represents a simple subsystem composed of the two buses interconnected by the transformer.

4.1.3 Spot Loads

The loads definition and modelling depends on the type of analysis desired. For example, the power-flow study of a transmission system will require a different definition than the one used for a secondary distribution feeder.

Depending on the type of load to be represented, 3 models can be defined. THis models can be seen as specific cases of the general representation with user-defined

exponents, Equations (4.52) and (4.53). Most power system analysis methods, as the backward/forward sweep, require a representation of the loads as current sources. Equations (4.54), (4.56) and (4.57) give the current source value in care of a Y connection for a constant power loads, constant impedance loads and constant current loads, respectively.

$$P = P_0 * \left(\frac{V}{V_0} \right)^\alpha \quad (4.52)$$

$$Q = Q_0 * \left(\frac{V}{V_0} \right)^\beta \quad (4.53)$$

where α and β are user-defined exponents.

• PQ Loads

The active and reactive power are assigned. It corresponds to put $\alpha = \beta = 0$ in the general model. The currents absorbed by the loads can be directly computed from:

$$\bar{I}_p = \left(\frac{\bar{S}_p}{\bar{V}_{pn}} \right)^* = \frac{|\bar{S}_p|}{|\bar{V}_{pn}|} * e^{j*(\delta_p - \theta_p)} \quad (4.54)$$

where:

$$p = 1, 2, 3$$

\bar{V}_{pn} is the line to neutral voltage of phase p calculated when solving the system.

\bar{S}_p is the complex power (assigned).

δ_p is the line to neutral voltage angle for the phase p .

θ_p is the power factor angle for phase p (assigned).

• Z Loads

The impedance module of the load is are assigned. It corresponds to put $\alpha = \beta = 2$ in the general model. Usually the given data is the complex power, therefore the first step to determine the currents absorbed by the load it is to compute the load impedance:

$$\bar{Z}_p = \frac{|\bar{V}_{assumed}|^2}{\bar{S}_p^*} = \frac{\bar{V}_{assumed}|^2}{|\bar{S}_p|} * e^{j*\theta_p} \quad (4.55)$$

$$\bar{I}_p = \frac{\bar{V}_p n}{\bar{Z}_p} = \frac{|\bar{V}_p n|}{|\bar{Z}_p|} * e^{j*(\delta_p - \theta_p)} \quad (4.56)$$

where:

$$p = 1, 2, 3$$

$V_{assumed}$ is the line to neutral voltage assumed value to calculate the impedance fixed value.

\bar{V}_{pn} is the line to neutral voltage of phase p calculated when solving the system.

\bar{S}_p is the complex power (assigned).

δ_p is the line to neutral voltage angle for the phase p .

θ_p is the power factor angle for phase p (assigned).

• **I Loads**

The current amplitude and the power factor are assigned. It corresponds to put $\alpha = \beta = 1$ in the general model. The currents module is assigned and fixed, while the angle varies depending on the voltage angle.

$$\bar{I}_p = |I_p| * e^{j(\delta_p - \theta_p)} \tag{4.57}$$

where:

$p = 1,2,3$

δ_p is the line to neutral voltage angle for the phase p .

θ_p is the power factor angle for phase p (assigned).

Non linear loads are usually represented as PQ loads when the analysis is made for the fundamental frequency. If the analysis has to be done also for harmonic frequencies, different models have to be applied. These models are described in section 4.2.

4.1.4 Distributed Loads

Many times the loads can be assumed as uniformly distributed along the line. In these cases it is not necessary to model each load in order to determinate the total voltage drop from the source end to the last load. An equivalent lumped load representation can be used.

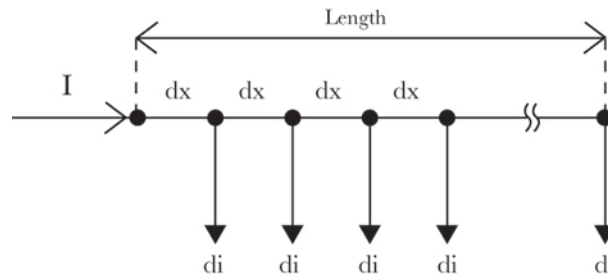


Figure 4.5: Uniformly distributed loads.

The model has to meet two characteristics: keep the total voltage drop from the source node to the last load and, at the same time, keep the total three phase power loss

down the line. Figure 4.5 shows the original load configuration, they are n uniformly loads spaced dx meters apart. The loads are supposed to be described by the assigned current model with a constant value of di . Figure 4.6 shows the exact lumped model [25], where a $2/3$ of the total line current is modeled at $1/4$ of the total length from the current to the last load, and the remaining $1/3$ of the current is modeled at the end of the line.

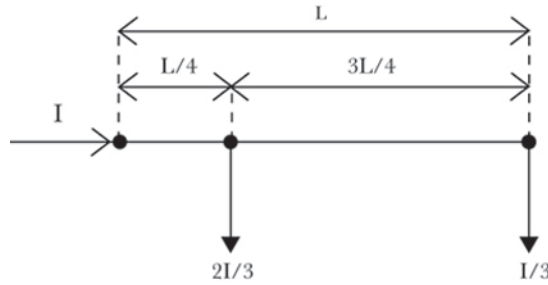


Figure 4.6: Exact lumped load model.

4.2 Modeling For Harmonic Studies

When an harmonic analysis is required adequate models for harmonic generating loads and system components must be used in order to simulate the propagation of harmonics throughout the network. If the system under analysis is a transmission one, it will require a much more complex model than a distribution systems. In this case, accurate representations for transmission lines, cables, transformers, capacitor banks, loads, and machines are required. Instead, for industrial and distribution systems, it is generally enough to model the system in detail only on the low side of the step-down transformer from the transmission system. A short-circuit equivalent at the high side of the step-down transformer is sufficient because the impedance is usually dominated by the one of the step-down transformer. On the low side of the step-down transformer, it is important to include all the buses with capacitor and large loads connected. At these lower voltage levels the capacitor banks dominate the capacitance of the lines, so it is usually acceptable to ignore the last one.

4.2.1 Transmission Lines

For low frequencies and/or short lines, a simple series impedance is a sufficient representation for lines. However, it is often important to include the shunt capacitance in the representation for lines and cables when performing studies in which frequencies above the 25th harmonic are important [57].

Overhead Lines

Typical overhead lines can be modeled by a multiphase coupled equivalent-pi circuit as shown in Figure 4.7. For balanced harmonic analysis, the model can be simplified into a single-phase pi-circuit determined from the positive sequence impedance data of the line. For unbalanced lines, more complex and specific three-phase model have to be used, as the one described in section 4.1.

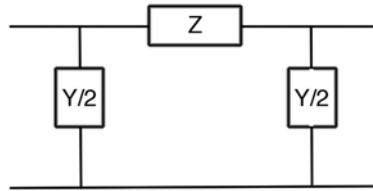


Figure 4.7: Overhead Line Model

The principal characteristic that have to be taken into account when modeling overhead lines are:

1. The frequency-dependency of the unit-length series impedance. The effects with major influence in the frequency-dependence of this parameter are the earth return effect and the conductor skin effect.
2. The distributed-parameter nature (long-line effects) of the unit-length series impedance and shunt capacitance.

The unit-length series impedance and shunt admittance parameters of the model of Figure 4.7 are calculated according to the physical arrangement of the line conductors. The series impedance Z is composed of internal and external impedance. The last one mentioned is a function of earth return condition and the frequency of interest and can be determined from Carson's formula [8] as in reference [18].

The internal resistance has to take account of the skin effect, which increase with the frequency and its influence can be very considerable. Reference [18] proposes Equation (4.58) to calculate the internal impedance of the conductor at high frequencies, assuming that the depth of penetration is very small and the current density at the surface of the conductor is proportional to the magnetic-field intensity at the surface.

$$Z_c = \frac{K * m * \rho}{r * (n + 2) * \pi} \quad (4.58)$$

$$m = \sqrt{j * \omega * \mu * l * \rho} \quad (4.59)$$

where:

- ρ is the conductor resistivity.
- μ is the conductor permeability.
- K is the conductor stranding factor.
- r is the radius of each strand.
- n is the number of strand in the outer layer
- l is the line length.

A much more simple approximation can be done according Equation (4.60) [24]:

$$R(f) = \begin{cases} (0.035 * M^2 + 0.938) * R_{dc} & \text{if } M < 2.4 \\ (0.35 * M + 0.3) * R_{dc} & \text{if } M \geq 2.4 \end{cases} \quad (4.60)$$

$$M = 0.05012 * \sqrt{\frac{f * \mu_r}{R_{dc}}} \quad (4.61)$$

where:

- μ_r is the relative permeability of the cylindrical wire (1 for non-magnetic conductors, including aluminum and copper).
- f is the frequency in Hz.
- R_{dc} is the dc resistance in Ω/km

Inclusion of the frequency-dependent effects requires the calculation of unit-length line constants for each harmonic frequency, which requires much input data for harmonic analysis programs. As the earth return effects mainly affect the zero-sequence harmonic components and the conductor skin effects mainly affect the line resistance, which in turn affects the damping level at resonance frequencies, if zero sequence harmonic penetration and damping at resonance frequencies are not of significant concern, the frequency-dependency effects may be neglected [24]. In this case, a single unit-length \mathbf{Z} matrix computed at the dominant resonance frequency is adequate.

Once obtained the unit-length parameters, matrices \mathbf{Y} and \mathbf{Z} can be calculated. If the line is short or low order harmonic are the only ones present in the analysis, the long-line effects can be ignored and the \mathbf{Y} and \mathbf{Z} matrices are the unit-length parameters multiplied by the line length. If long-line effects need to be included, the \mathbf{Y} and \mathbf{Z} matrices should be computed using the hyperbolic long-line equations (section 4.1.1).

Whether or not to include the long-line effects depends on the length of the line being modelled and the harmonics of interest. A criterion for estimate the critical line lengths where the long-line effects should be represented is presented in reference [24]:

$$l_{crit} = \frac{150}{h} \quad (4.62)$$

where l_{crit} units are miles and h is the harmonic number.

According to reference [2], at harmonic frequencies the limiting distances of transposition effectiveness are much shorter than for the fundamental frequency and can aggravate unbalance, thus it suggests that for line lengths of 250 km, for the third harmonic and 150 km, for the fifth, three-phase line model should be considered.

Underground Cables

Underground cable models are very similar to overhead line models. The long-line effects of underground cables can be represented in the same way as that used for overhead lines. In general, cables have more shunt capacitance than overhead lines. Therefore, long-line effects are more significant. An estimate of critical cable lengths (in miles) where the long-line effects should be represented according to reference [24] is:

$$l_{crit} = \frac{90}{h} \quad (4.63)$$

4.2.2 Transformers

For harmonic analysis, transformers can be modeled as an inductive reactance connected in series with a frequency-dependent resistance:

$$X_{Th} = R_T * \sqrt{h} + j * X_T * h \quad (4.64)$$

where R_T and X_T are the components of the transformer's short circuit impedance at the fundamental frequency.

Equation 4.64 ignores the magnetization non-linearities of the transformer, assuming that it normally operates within the linear region of the magnetizing characteristic. However, transformers are designed to operate very close to the limit of the linear characteristics and if they are working under a small over-excitation, their contribution to the harmonic content can be important. Therefore, if in the system to be analyzed there is a transformer over excited and all the data about its magnetizing characteristic is available, it is recommended to use a model that takes the non-linear characteristics into account. Such a model can be described by the following equations [4]:

$$\begin{bmatrix} i_1 \\ i_2 \\ i_3 \end{bmatrix} = \begin{bmatrix} k_{11} & k_{12} & k_{13} \\ k_{21} & k_{22} & k_{23} \\ k_{31} & k_{32} & k_{33} \end{bmatrix} * \begin{bmatrix} j * h * \omega & 0 & 0 \\ 0 & j * h * \omega & 0 \\ 0 & 0 & j * h * \omega \end{bmatrix}^{-1} * \begin{bmatrix} v_1 \\ v_2 \\ v_3 \end{bmatrix} + \begin{bmatrix} i_{n1} \\ i_{n2} \\ i_{n3} \end{bmatrix} \quad (4.65)$$

where $v_p = j * h * \omega * \phi_p$ for $p = 1,2,3$ and the matrix \mathbf{K} and the vector i_n are defined as:

$$\begin{aligned} k_{p1} &= d_{p1} * R_{1b} + d_{p4} * R_{1b} + d_{p6} \\ k_{p2} &= d_{p2} * R_{2b} - d_{p4} * R_{2b} + d_{p5} * R_{2b} + d_{p7} \\ k_{p3} &= d_{p3} * R_{3b} - d_{p5} * R_{3b} + d_{p8} \end{aligned} \quad (4.66)$$

$$i_p = -a_1 * d_{p1} - a_2 * d_{p2} - a_3 * d_{p3} - a_4 * d_{p4} - a_5 * d_{p5} \quad (4.67)$$

$$\begin{aligned} a_1 &= R_{1b} * \phi_{1b} + R_{6b} * \phi_{6b} - f_1(\phi_{1b}) - f_6(\phi_{6b}) \\ a_2 &= R_{2b} * \phi_{2b} + R_{7b} * \phi_{7b} - f_2(\phi_{2b}) - f_7(\phi_{7b}) \\ a_3 &= R_{3b} * \phi_{3b} + R_{8b} * \phi_{8b} - f_3(\phi_{3b}) - f_8(\phi_{8b}) \\ a_4 &= R_{1b} * \phi_{1b} + R_{4b} * \phi_{4b} - R_{2b} * \phi_{2b} - f_1(\phi_{1b}) - f_4(\phi_{4b}) + f_2(\phi_{2b}) \\ a_5 &= R_{2b} * \phi_{2b} + R_{5b} * \phi_{5b} - R_{3b} * \phi_{3b} - f_2(\phi_{2b}) - f_5(\phi_{5b}) + f_3(\phi_{3b}) \end{aligned} \quad (4.68)$$

where:

$p=1,2,3.$

R_i and ϕ_i are the reluctance and flux according to Figure 4.9.

R_{ib} and ϕ_{ib} are the reluctance and flux obtained after applying a Taylor's expansion to the magnetic equations [4].

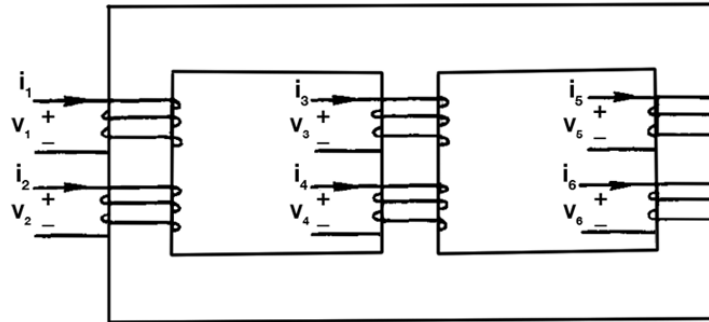


Figure 4.8: Three-limb transformer

4.2.3 Linear Loads

A distribution system supplies a number of loads conveniently distributed in circuits that connect it to the nearest distribution point. In general, a considerable number of

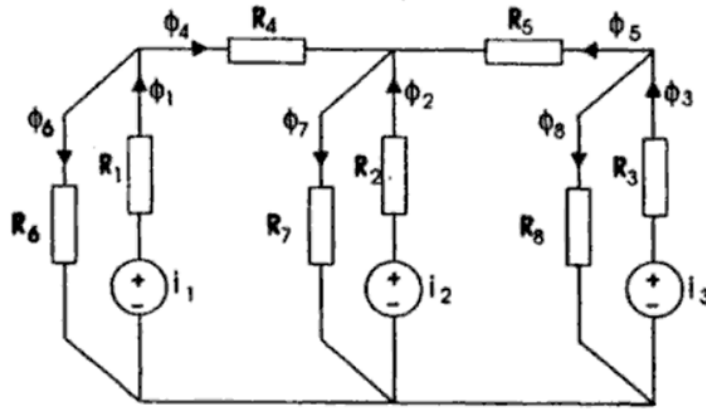


Figure 4.9: Magnetic equivalent circuit for a three-phase transformer

loads are located so close together and supplied from the main distribution point, that they can be considered as a whole and represented by a unique lumped load. If there are uniformly distributed loads, it can be used the model described in section 4.1.4 to obtain two equivalent lumped loads. In most of the cases, a simple radial system is used, whether supplying a large plant, small factory, domestic or commercial consumers.

Consumers' loads have a considerable influence on the harmonic network characteristic. They constitute the main element of the damping component and also may affect the resonance conditions, particularly at higher frequencies. Consequently, an adequate representation of the system loads is needed.

Loads are generally expressed by their active and reactive power (PQ model), which are used to calculate the equivalent impedance or current injection for load flow studies at fundamental frequency, assuming the system voltage. At harmonic frequency these values of P and Q cannot be used straightforwardly because the active power absorbed by a rotating machine does not exactly correspond to a damping value and so additional information is necessary. The four models proposed by [36] that are shown in Figure 4.10 are described below. The choice of the model has to be done according to the load characteristics and information available.

- Model A:

In some cases, the reactive power estimated may have a negligible effect at harmonic frequencies. Thus, the load is represented just by its rated active power P , considering an equivalent resistance of value R (Equation (4.69)). This representation should be used when the motor part is very small and the resistive effect is predominant, i.e. for commercial and domestic loads.

$$R = \frac{V_n^2}{P} \quad (4.69)$$

where V_n is the rated voltage at fundamental frequency.

- Model B:

This model consists of a resistance in parallel with an inductance and another resistance. The inductance L should be evaluated using an estimation of the number of motors in service, their installed unitary power (not demand) and their inverse inductance. However, this precise information on the number of motors, etc. in general is unavailable, then a fraction K of the total active power demand (P) must be used to represent the motor part. This is then multiplied by a factor that considers the installed power which should be used, for instance equal to 1.2. To calculate the equivalent inverse inductance, a factor K_1 , proportional to the severity of the starting condition should be used. Therefore, R and L of Figure 4.10.b can be calculated as follows:

$$R = \frac{V_n^2}{P * (1 - K)} \quad (4.70)$$

$$L = \frac{V_n^2}{1.2 * K * K_1 * P} \quad (4.71)$$

where K assumes values around 0.80 for industrial loads and around 0.15 for commercial and domestic loads, and K_1 is between 4 and 7.

An additional resistance representing the motor damping can be included as:

$$R_1 = \frac{L}{K_2} \quad (4.72)$$

where K_2 is a fraction of the inverse inductance or locked-rotor inductance and can assume values around 0.2.

- Model C:

When a big induction motor or group of motors are connected directly at intermediate voltage levels, like in the case of industrial plants, the motive part is better

represented by a resistance in series with the inverse inductance of the motor.

The equivalent resistance of the resistive part and the inverse inductance of the motor is estimated as in model **B**. The series resistance R_1 can be calculated as in Equation (4.73).

$$R_1 = \frac{\omega_f * L}{K_3} \quad (4.73)$$

where:

K_3 is the effective quality factor Q of the motor circuit (≈ 8)

ω_f is the fundamental frequency

Additionally, a series inductance L_T connected to R can be incorporated to represent the equivalent leakage reactance of the distribution transformers at lower voltage. It can be assumed a value of:

$$L_T = \frac{0.1 * R}{\omega} \quad (4.74)$$

- Model D:

This model was developed from experiments performed on medium voltage outputs using audio-frequency ripple-control generators at EDF (Électricité de France) [6], and has been adopted by the CIGRE (Conference Internationale des Grands Reseaux Electriques à Haute Tension) as their type-C load model, valid between 5th and 30th harmonics. The circuit suggested is a branch with an inductance in series with a resistance connected in parallel with another inductance. The estimated P and Q are used in empirical formulas, Equations (4.75) to (4.77), to calculate the equivalent impedances.

$$R = \frac{V_n^2}{P} \quad (4.75)$$

$$L_1 = \frac{0.073 * h * R}{\omega} \quad (4.76)$$

$$L_2 = \frac{h * R}{\omega * (6.7 * tg(\phi) - 0.74)} \quad (4.77)$$

$$tg(\phi) = \frac{Q}{P} \quad (4.78)$$

An alternative to model A is explained in [24], where is added a parallel inductor:

$$L = \frac{V^2}{\omega_f * Q} \quad (4.79)$$

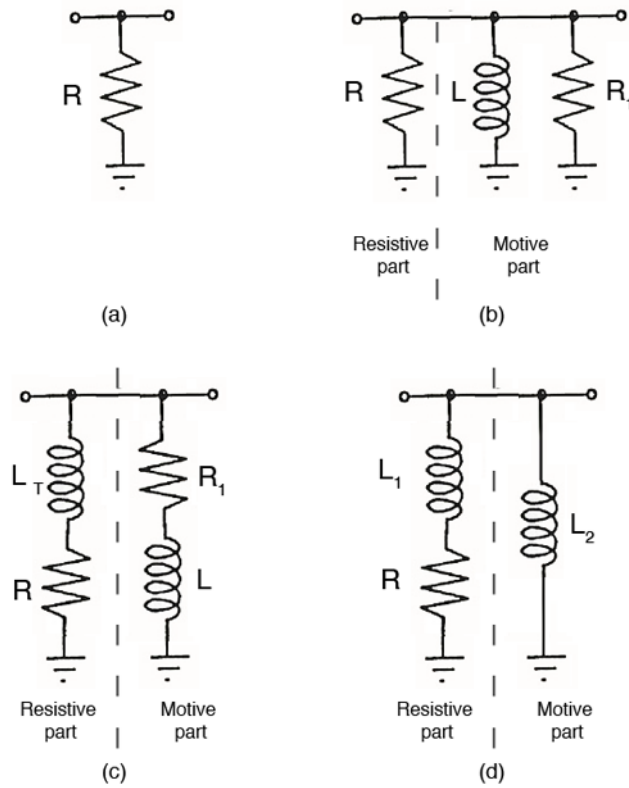


Figure 4.10: Load Models: (a) A (b) B (c) C and (d) D

This model assumes that the all reactive load is assigned to an inductor L, actually a majority of reactive power comes from induction motors, then this model is not recommended.

References [24] and [33] also proposes an alternative to model B as a parallel connection of an inductive reactance and a resistance:

$$X = j * \frac{V_n^2}{(0.1 * h + 0.9) * Q} \quad (4.80)$$

$$R = \frac{V_n^2}{(0.1 * h + 0.9) * P} \quad (4.81)$$

Latter model which usually applied in studies concerning mainly the transmission networks, where the equivalent parts of the distribution systems are specified by the consumption of active and reactive power (P and Q) at the fundamental frequency.

Reference [4] proposes a model for the predominantly passive loads (typically domestic) consisting of a series RX impedance:

$$Z = \sqrt{h} * R_f + j * X_f * h \quad (4.82)$$

where R_f and X_f are the load resistance and reactance at the fundamental frequency. The weighting coefficient \sqrt{h} varies according to the model, for instance, reference [33] uses $(0.6 * \sqrt{h})$ instead.

4.2.4 Non-Linear Loads

The non-linear loads are the harmonic sources in the system, briefly described in section 2.1. As mentioned in section 3.2, the harmonic simulation can be in frequency domain, in time domain or in both, thus also the models can vary depending on the domain used. This section will describe some of the models that have been developed for the principal types of harmonic sources.

Three-Phase Line-Commutated Converter

In general, the power electronic devices that generates harmonic currents can be modeled by using simple current source models or more complicated device-level models. The most common model is the one of a harmonic current source specified by its magnitude and phase spectrum. More detailed models are necessary if voltage distortion is significant. When this situation is considered, it is required a more sophisticated converter analysis with harmonic currents as a function of system reactance, delay angle, and commutation angle. The accuracy of converter model is considered to guarantee the convergence of the simulation.

At present, there are several techniques that have been developed for modeling of power electronic converters in harmonic simulation [21].

- Current Source Model:

Is the most common technique used for harmonic simulation and it is valid to balanced and unbalanced systems [21]. It consists of treating the converters as known sources of harmonic currents with or without including phase angle information. This is due to the fact that the converter acts as an injection current source to the system in many operational conditions. Generally, the steady-state condition is assumed. The current harmonics injected into a bus have a magnitude determined from the typical measured spectrum and rated load current for the harmonic source (Equation (4.83)).

$$I_h = I_{rated} * \frac{I_{h-sp}}{I_{1-sp}} \quad (4.83)$$

where $I_{h.sp}$ is the typical current spectrum of the source at harmonic h [24].

For harmonic studies involving just one converter, the phase angles usually are ignored and only the magnitudes are used in the harmonic simulation. When multiple converters are considered simultaneously, harmonic phase angles need to be included for taking the harmonic cancellation effect into account. It can be done using Equation (4.84) [24].

$$\theta_h = \theta_{h.sp} + h * (\theta_1 - \theta_{1.sp}) \quad (4.84)$$

where $\theta_{h.sp}$ is the typical phase angle spectrum of the source at harmonic h and θ_1 is the phase angle obtained from the load flow solution for the fundamental frequency current component.

The advantages of the current source method are that the solution can always be obtained without an iterative process and is computationally efficient. The disadvantage is that when typical harmonic spectra are used to represent the harmonic currents generated by the converter, the interaction between the network and the converter is ignored. This drives to an inadequate evaluation of cases involving nontypical operating modes, such as partial loading and excessive harmonic voltage distortions. Reference [41] suggests that the current injection model can be used carefully when the converter source voltage THD is on the order of 10% or more.

- Transfer Function Model:

This model is based on the modulation theory and small signal linearisation, that uses two transfer functions ($G_{\phi,dc}$ and $G_{\phi,ac}$) to relate the dc and ac sides of the converter when the input voltage waveform is modulated by a signal at any specified frequency [3].

The dc voltage is calculated by summing each phase voltage multiplied by its associated transfer function (Equation (4.85)). The transfer switching function $G_{\phi,dc}$ can take values between -1 and $+1$, where 0 signifies no connection of the dc side, ± 1 means connection of the dc side positive or negative bus to the phase ϕ and 0.5 is used to represent the phases during the commutation process.

$$v_d = N * \sum_{\phi} (G_{\phi,dc} * v_{\phi}) \quad (4.85)$$

where:

$\phi = 0^\circ, 120^\circ, 240^\circ$ for phases a, b, c respectively
 N is the converter transformer ratio

Similarly, the dc current can be defined as in Equation (4.86), with $G_{\phi,ac}$ values also between -1 and $+1$, but with the raises and falls during the commutation process being approximately linear transfers.

$$i_{\phi} = N * G_{\phi,ac} * i_{dc} \quad (4.86)$$

The transfer functions $G_{\phi,ac}$ and $G_{\phi,dc}$ are the sum of a basic function without commutation period and steady firing angle, a firing angle variation function (dashed line in the figure) and a commutation function. Figure 4.11 shows how these functions are calculated: the dotted line represents the basic function, then the dashed line is the function calculated taking account the firing angle variation $\Delta\alpha$, and the solid line waveform is the transfer function including the effect of a commutation period. Expressing the transfer function as a summation of these three components, simplifies the frequency spectra expressions.

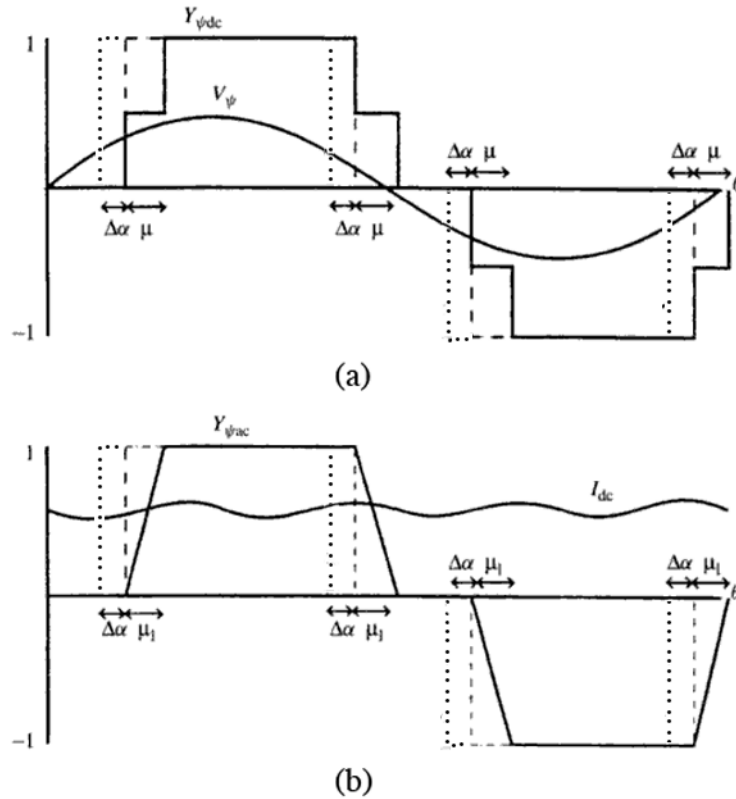


Figure 4.11: Transfer functions: (a) $G_{\phi,dc}$ and (b) $G_{\phi,ac}$

Once known the transfer functions the entire system can be solved by the harmonic coupling matrix equation [21]:

$$\begin{bmatrix} I_{ac} \\ V_{dc} \end{bmatrix} = \begin{bmatrix} A & B & E \\ C & D & F \end{bmatrix} \begin{bmatrix} V_{ac} \\ I_{dc} \\ \alpha \end{bmatrix} \quad (4.87)$$

where:

I_{ac} is the vector of the ac side sequence harmonic currents.

V_{ac} is the vector of the ac side sequence harmonic voltages.

I_{dc} is the vector of the dc side harmonic currents.

α is the firing angle.

In Equation (4.87), **A**, **B**, **C**, **D**, **E** and **F** can be regarded as sub-matrices of the converter transfer functions between associated input and output variables and are obtained by the time-domain simulation with harmonic perturbations. These matrices need to be built for each operating point considered and are then combined with the ac and dc system impedance as well as control characteristics at harmonic frequencies. If the firing angle harmonics are not considered, the only existing sub-matrices are **A**, **B**, **C** and **D**.

This model can be used either in the time or frequency domain with the incorporation of the iterative approach, eliminating the problem existing with the current source model. It has been developed for both single-phase and three-phase converters while ignoring the effects of converter controls, commutation variations, and resistance in ac network impedance [41].

Adjustable Speed Drives

Adjustable speed drives (ASD) is becoming a significant load component for power distribution systems. Modern ASDs employ power electronic devices to vary the frequency of the power supply for AC motor speed control and produce harmonics during this process. The research on the modelling of ASDs for harmonic analysis has been limited. It has been commonly assumed that a ASD can be modelled as harmonic current sources. Reference [51] proposes a general three-phase ASD model for analysing harmonic propagation in balanced and unbalanced three-phase power systems with ASDs.

- Norton-Equivalent Circuit Model:

An adjustable speed drive (ASD) can be represented with a generic three-phase bridge converter circuit of Figure 4.13. An important advantage of this circuit is that the inverter and the motor are both modelled as just one direct current source. The magnitudes and phase angles of this source should be determined from the inverter design and the motor operating conditions. Studies made on [51] have proven the validity of this model without the need to model the current source

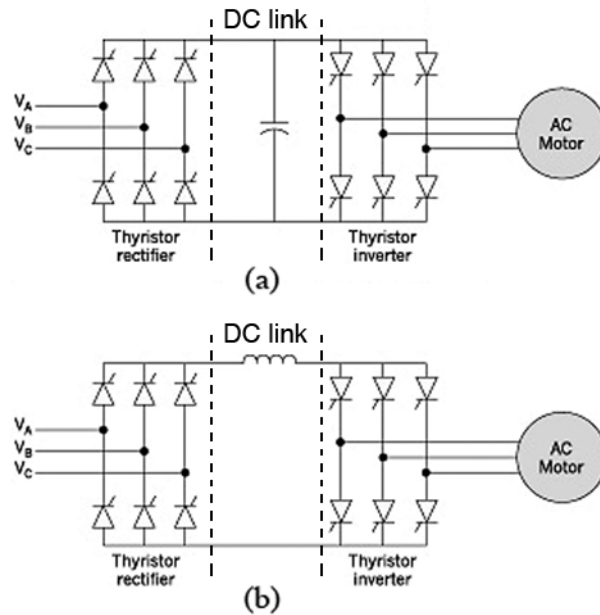


Figure 4.12: Various types of ASD configuration: (a) VSI and PWM and (b) CSI

as a harmonic source. This is because, in the case of pulse width modulation (PWM) and voltage source inverter (VSI) type ASDs, the inverter harmonics are largely bypassed by the DC link capacitor before they can penetrate into the supply system side, and in the case of current source inverter (CSI) type ASD, the series inductor serves as a large impedance to block inverter harmonics from ever getting into the converter.

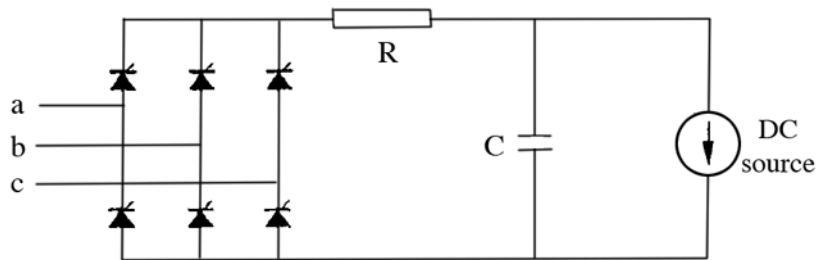


Figure 4.13: Generic converter circuit for ASD

The delta-connected final model (without consider overlaps effects) is shown in Figure 4.14, where I_h is the supply voltage-dependent harmonic current source and X_0 is an equivalent harmonic impedance. The current sources in the model are determined with a given three-phase drive terminal voltage, normally calculated from a three-phase network harmonic power flow solutions. This model

is valid under various system conditions such as supply voltage unbalance, harmonic distortions at the AC or DC side, and the asymmetry of drive parameters.

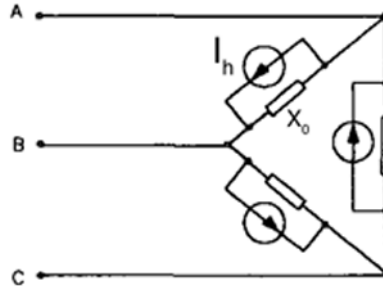


Figure 4.14: Harmonic equivalent circuit for ASDs

The input data needed to construct the described model are:

1. The firing angle of the converter thyristors: α .
 2. The direct current flowing into the inverter: I_{dc} .
 3. The DC link component parameters: R, C .
- Simplified Current Source Model:

If the parameters necessary for building the previously described model are not available, it is possible to use a more simplified current source model as described in [24]. It consists in a harmonic source with currents of low magnitude, independent of the voltage levels in the system, and a frequency spectrum of $f = 6 * f_i \pm f_0$, where f_i is the inverter frequency and f_0 is the AC system frequency. The source magnitudes are either calculated as I_1/h for the h th harmonic order or measured from a particular drive operating condition.

Rotating Machines

Synchronous machines convert negative sequence currents into third harmonic positive sequence and, in general, act as a harmonic converter. Getting to an accurate model that represents this fact is a very complex problem [38], since conversion means coupling of harmonics which otherwise would be examined separately. Therefore, generators are often represented by a single approximate impedance at each harmonic.

In synchronous and asynchronous machines, the rotating magnetic field created by stator harmonics rotates at a speed significantly higher than the rotor speed. Therefore

at harmonic frequencies the impedance approaches the negative sequence impedance. In the case of synchronous machines the inductance used for the model is usually the negative sequence impedance or the average of direct and quadrature subtransient impedances (Equation (4.88)). Induction machines are modeled with its locked rotor inductance when the subtransient characteristics are not known.

$$X_h = h * \frac{X_d'' + X_q''}{2} \quad (4.88)$$

In both, synchronous or asynchronous machines, the frequency-dependency of the resistance can be significant due to skin effects and eddy current losses. Figure 4.15 shows the negative sequence impedance of a 1100 hp synchronous motor as a function of frequency. Usually a variation of the resistance according to Equation (4.89) is taken [24].

$$R_h = h^a * R_f \quad (4.89)$$

where:

R_h is the resistance at the h frequency
 R_f is the resistance at the fundamental frequency
 a may vary between 0.5 and 1.5.

Equation (4.90) shows another way to represent the frequency-dependency of the resistance presented in [4]. This model takes into account the apparent slip at the superimposed frequency S_h .

$$R_{mh} = R_B * \left(a * k_a + \frac{b}{S_h} * k_b \right) \quad (4.90)$$

$$S_h = \frac{\pm h * \omega_s - \omega_r}{\pm h * \omega_s} \quad (4.91)$$

where:

R_B is the total motor resistance with the rotor locked.
 a is the coefficient between the stator resistance and R_B (typically 0.45)
 b is the coefficient between the rotor resistance and R_B (typically 0.55)
 k_a is the correction factor to take into account the skin effect in the stator, defined by Equation (4.92)
 k_b is the correction factor to take into account the skin effect in the rotor, defined by Equation (4.93)

$$k_a = h^\alpha \quad (4.92)$$

$$k_b = (\pm h - 1)^\alpha \quad (4.93)$$

The positive or negative signs on expressions (4.91), (4.92) and (4.93) depend on the sequence of the harmonic h , being positive for negative sequence harmonics and negative for positive sequence ones.

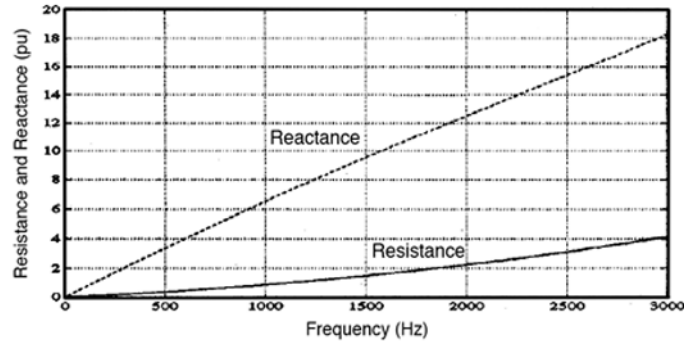


Figure 4.15: Measured impedance of a synchronous motor [24]

If the motor is connected in delta or ungrounded star, there is no way to let the zero sequence harmonic currents to flow.

Chapter 5

Methodology

The principal scope of this research was to develop a computer tool able to perform power flow calculations for distribution systems in presence of unbalances and/or harmonic distortion with radial or weakly meshed structure. The steps needed to reach this scope were:

1. Selection of language and software

Selection of language and software to be used for the implementation of the method. It was chosen Matlab[®] from MathWorks[™], due to its versatility for matrix computations. Matlab[®] uses a programming language that can be easy to learned and applied without requiring a lot of technical and programming knowledge. This is a very useful characteristic when the programmed code is implemented in power system analysis, due to the fact that power system analysis is in constant change and new components with new models are constantly required to be introduced in the studies. Therefore, a program code developed in Matlab[®] can be easily modified to introduce new components models or to adjust old ones to the data input available.

The version used to develop all the .m files is the Matlab[®] R2008a running in a MacBook with a 2.4 GHz Intel Core 2 Duo processor.

2. Selection of the method used to solve the power flow

This stage includes a research of several methods proposed to solve harmonic power flow analysis. The choice made was to use two versions of the backward/forward sweep-based methods, due to its advantages in solving radial distribution systems, compared to Newton based methods (see chapter 3). The first one is the method proposed by Teng and Chang in [45], from now on referred as “method 1”. The second one it is a simple extension of the traditional backward/forward

sweep approach (section 3.1.1), from now on referred as “method 2”. Both methods are described in section 6.1.

3. Selection of the test systems

The network selected to perform the tests of the programmed methods was the IEEE 13 Node Test Feeder [22]. It was chosen by the characteristic of been small, therefore very manageable, but at the same time offering very interesting characteristics of non-ideal distribution systems:

- Relatively highly loaded feeder for a 4.16 kV system.
- Overhead and underground lines with variety of phasing.
- Shunt capacitor banks.
- In-line transformer.
- Unbalanced spot and distributed loads.

The complete data corresponding for this system is given in [22] and was used to verify the proper operation of the power flow for the fundamental component of the network. The only difference between the actual system used and that one from [22] is the substation voltage regulator between nodes 650 and 632. To avoid the modeling of this component that was considered secondary for the analysis of the methods, it was taken the IEEE results at the exit point of this regulator as the voltages of the slack node in the actual test system used (Figure 5.1).

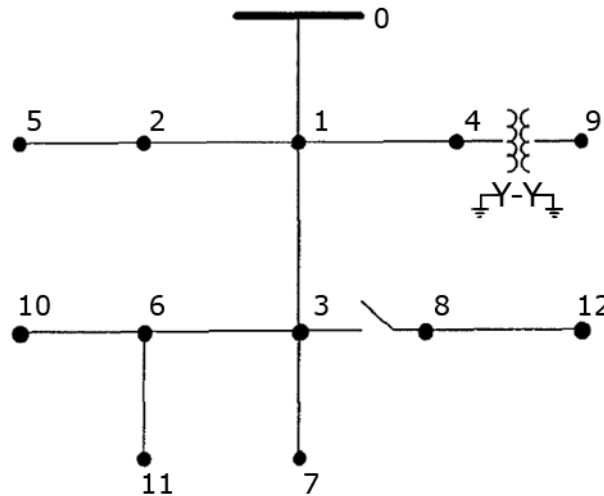


Figure 5.1: One line diagram of the unbalanced test system.

For the harmonic power flow calculations it was used a simpler the test system, the IEEE 4 Node Test Feeder. One unbalanced three phase load was assume at the end of the feeder (node 4). The complete data corresponding for this system is given in appendix A.1.

4. Implementation of the method 1 to solve the power flow calculation for a single-phase radial distribution network

It was a previous step to the actual three-phase power flow. It serves to the familiarization with the variants that method 1 proposes to the classical backward/forward sweep.

5. Implementation of the power flow calculation for a three-phase radial distribution network

In this step the program developed in the previous step 4 was expanded to the three-phase case application. It was divided in three parts:

- 5.1 Implementation of the backward/forward sweep to solve the fundamental frequency power flow: the data of the system used was the one without harmonic loads. This step includes the verification of the results obtained with the program with those given in reference [22] as the solution of the network power flow.
- 5.2 Implementation of the method 1 to solve the harmonic power flow: the data of the system used was the one with harmonic loads (appendix A.1).
- 5.3 Implementation of the method 2 to solve the harmonic power flow: with the same data and network used in the previous step it was implemented method 2 totally based on the BFS program developed and proved on step 4.

6. Comparison of method 1 and method 2 applied to the three-phase radial distribution network

Comparison of results obtained by both methods, the time employed and iteration needed by each one to solve the power flow.

7. Implementation of the power flow calculation for a single-phase weakly meshed distribution network

It was added the procedure explained in section 3.1.2 to the BFS method and then proved on a weakly meshed network. Two parts can be defined in this step:

- 7.1 Implementation of the backward/forward sweep to solve the fundamental frequency power flow for a single phase network: the network used is shown in Figure 6.11. It consist of 5 nodes, one loop and five spot loads. More specific data for the network used are in appendix A.2. Both methods were implemented and tested here.
- 7.2 Comparison of the results: the network was solved with a demo version of the commercial program PowerWorld Simulator v13 and this results were confronted to those obtained with the developed program in Matlab[®].

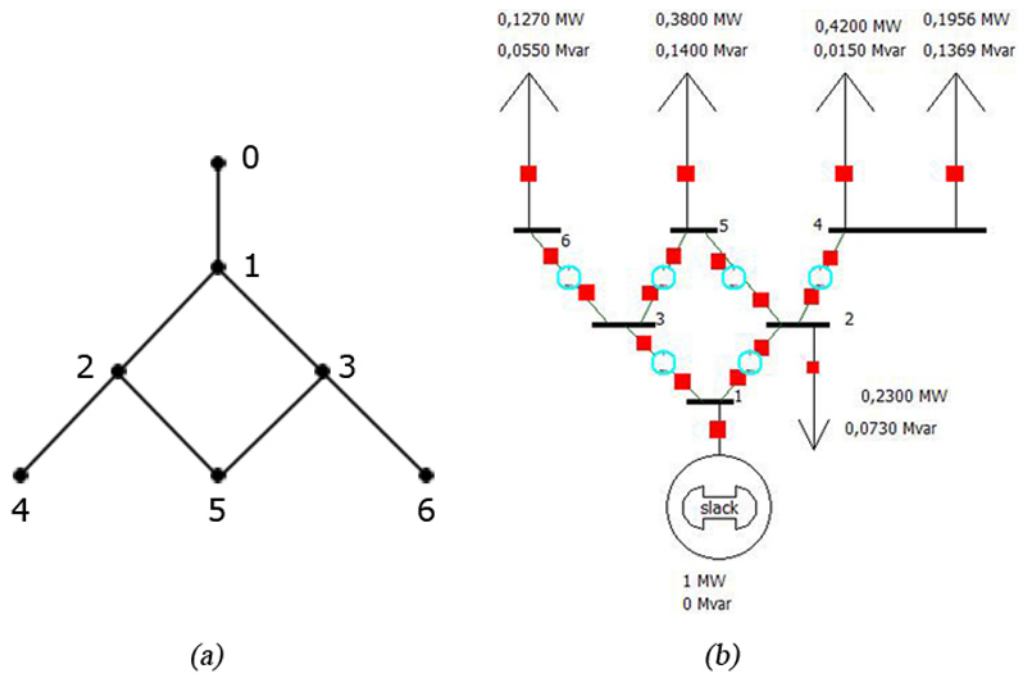


Figure 5.2: (a) One line diagram of the single phase test system for weakly meshed network treatment and (b) its implementation in PowerWorld.

Chapter 6

Results and Discussion

6.1 Description of the Methods

The two methods chosen to solve the harmonic power flow and the one used to solve the fundamental component are BFS based methods; that method takes advantage of the radial structure of the distribution systems and can be only applied on radial networks. Using the procedure described in section 3.1.2 it can be also applied to weakly meshed networks.

The first step to solve the system is the labeling of the nodes. It has to be done as described in section 3.1.1, beginning by naming the supply node at the top of the tree as “node zero” and then keeping on labeling from left to right, from top to bottom (an example is shown in Figure 3.1). Then, the branches labeling is done in a similar way, but starting the count from one instead of zero. At the end, each branch j , will finish at node j . Figure 6.1 shows the branch labeling corresponding to the example of Figure 3.1.

With the labeling finished, is possible to define the node to branch incidence matrix \mathbf{L} and its inverse $\mathbf{\Gamma}$, as described in section 3.1.1. Knowing the position of the loads and the branch incidence matrix \mathbf{L} , a coefficient vector \mathbf{A}_j can be deduced. This vector is defined by Teng and Chang [45] as the coefficient vector of harmonic currents for the branch j that consist of 1 if the corresponding bus harmonic current flows through the branch, or 0 if it doesn't flow. To be able of expand the algorithm to three-phase unbalanced systems, the $M \times 1$ vectors \mathbf{A}_j were defined as $M \times 3$ matrix, where M is the number of total loads and shunt capacitors, and each column represent the coefficient vector for the corresponding phase.

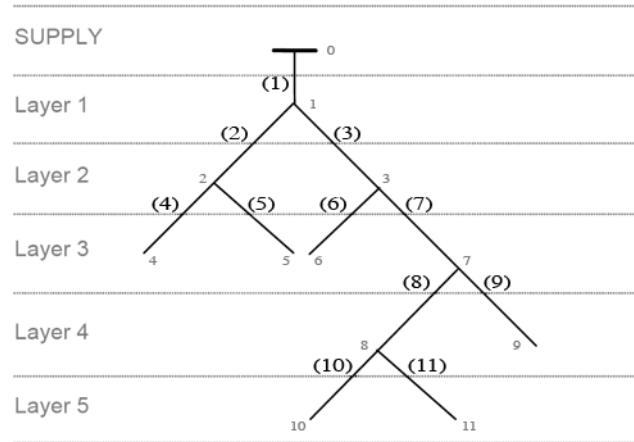


Figure 6.1: Example of the branch labeling in a radial network

Once the system has been characterized with these matrix \mathbf{L} , $\mathbf{\Gamma}$ and \mathbf{A}_j it can be done the load flow at the fundamental frequency and then the harmonic analysis, using method 1 or method 2. All processes are described in sections 6.1.1, 6.1.2 and 6.1.3.

6.1.1 Load Flow at the Fundamental Frequency

The load flow at the fundamental frequency used is a backward/forward sweep based method. It differs of the traditional BFS (section 3.1.1) by the fact that the branches current vector \mathbf{B}_j is defined by Equation (6.1) instead of Equation (3.6). This modification was made because the \mathbf{A} matrix was needed for the harmonic analysis, so it has to be calculated anyway. Then, instead of expanding the $\mathbf{\Gamma}$ matrix to the three-phase case, it has been used the one that was already available. The concept is still the same, a coefficient that records whether or not the current flows through the branch.

$$\mathbf{B}_{j,p} = \sum_{k=1}^N (A_{j,k,p} * \bar{I}_{k,p}) \quad (6.1)$$

where:

N is the total number of branches in the network

$j = 1, 2, \dots, N$

$p = 1, 2, 3$

$\mathbf{B}_{j,p}$ is the component p of the three-phase currents vector of branch j

$A_{j,i,p}$ is the (j,p) element of the \mathbf{A} matrix corresponding to branch j

$\bar{I}_{k,p}$ is the phase p element of the currents vector for the load k

$$\mathbf{B} = \begin{bmatrix} \mathbf{B}_1 \\ \vdots \\ \mathbf{B}_j \\ \vdots \\ \mathbf{B}_N \end{bmatrix} = \begin{bmatrix} \bar{B}_{1,1} \\ \bar{B}_{1,2} \\ \bar{B}_{1,3} \\ \vdots \\ \bar{B}_{j,1} \\ \bar{B}_{j,2} \\ \bar{B}_{j,3} \\ \vdots \\ \bar{B}_{N,1} \\ \bar{B}_{N,2} \\ \bar{B}_{N,3} \end{bmatrix} \quad (6.2)$$

$$\mathbf{A}_j = \begin{bmatrix} A_{j1,1} & A_{j1,2} & A_{j1,3} \\ \vdots & \vdots & \vdots \\ A_{jk,1} & A_{jk,2} & A_{jk,3} \\ \vdots & \vdots & \vdots \\ A_{jM,1} & A_{jM,2} & A_{jM,3} \end{bmatrix} \quad (6.3)$$

$$\mathbf{I} = \begin{bmatrix} \mathbf{I}_1 \\ \vdots \\ \mathbf{I}_k \\ \vdots \\ \mathbf{I}_M \end{bmatrix} = \begin{bmatrix} \bar{I}_{1,1} \\ \bar{I}_{1,2} \\ \bar{I}_{1,3} \\ \vdots \\ \bar{I}_{k,1} \\ \bar{I}_{k,2} \\ \bar{I}_{k,3} \\ \vdots \\ \bar{I}_{M,1} \\ \bar{I}_{M,2} \\ \bar{I}_{M,3} \end{bmatrix} \quad (6.4)$$

If the shunt line parameters are taken into account, the total current branch vector \mathbf{B}_{tot} is calculated as:

$$\mathbf{B}_{tot} = \mathbf{B} + \mathbf{B}L_s \quad (6.5)$$

First it is necessary to calculate the currents injected by the admittances $\mathbf{I}L_s$. If j is the node between branches x and j :

$$\mathbf{I}L_{s_j} = \frac{\mathbf{b}_j}{2} * \mathbf{V}_j + \frac{\mathbf{b}_x}{2} * \mathbf{V}_x \quad (6.6)$$

Then \mathbf{BL}_{shunt} can be calculated as:

$$\mathbf{BL}_{s_{j,p}} = \sum_{i=1}^N (-\Gamma_{i,j} * \mathbf{IL}_{s_{i,p}}) \quad (6.7)$$

where:

$$i = 1, 2, \dots, N$$

$\mathbf{BL}_{s_{j,p}}$ is the component p of the three-phase current vector of branch j due to the shunt line parameters

$$\mathbf{BL}_s = \begin{bmatrix} \mathbf{BL}_{s_1} \\ \vdots \\ \mathbf{BL}_{s_j} \\ \vdots \\ \mathbf{BL}_{s_N} \end{bmatrix} = \begin{bmatrix} \overline{BL}_{s_{1,1}} \\ \overline{BL}_{s_{1,2}} \\ \overline{BL}_{s_{1,3}} \\ \vdots \\ \overline{BL}_{s_{j,1}} \\ \overline{BL}_{s_{j,2}} \\ \overline{BL}_{s_{j,3}} \\ \vdots \\ \overline{BL}_{s_{N,1}} \\ \overline{BL}_{s_{N,2}} \\ \overline{BL}_{s_{N,3}} \end{bmatrix} \quad (6.8)$$

For the forward voltage sweep is necessary to calculate first the product between the line impedance and the branch currents:

$$\mathbf{ZI} = \mathbf{Zb} * \mathbf{B}_{tot} \quad (6.9)$$

where \mathbf{Zb} is a $(3N) \times (3N)$ matrix, composed of the 3×3 lines impedances sub-matrix on its diagonal.

$$\mathbf{Zb} = \begin{bmatrix} \mathbf{Zb}_1 & \dots & \dots & \dots & 0 \\ \vdots & \ddots & & & \vdots \\ \vdots & & \mathbf{Zb}_j & & \vdots \\ \vdots & & & \ddots & \vdots \\ 0 & \dots & \dots & \dots & \mathbf{Zb}_N \end{bmatrix} \quad (6.10)$$

$$\mathbf{Zb}_j = \begin{bmatrix} \overline{Zj}_{1,1} & \overline{Zj}_{1,2} & \overline{Zj}_{1,3} \\ \overline{Zj}_{2,1} & \overline{Zj}_{2,2} & \overline{Zj}_{2,3} \\ \overline{Zj}_{3,1} & \overline{Zj}_{3,2} & \overline{Zj}_{3,3} \end{bmatrix} \quad (6.11)$$

Then the node voltage at node j for the phase p can be calculated by:

$$\mathbf{V}_{p,j} = \bar{V}_{0,p} + \sum_{k=1}^N (\Gamma_{j,k} * \mathbf{Z} \mathbf{I}_{j,p}) \quad (6.12)$$

$$\mathbf{V} = \begin{bmatrix} \mathbf{V}_1 \\ \mathbf{V}_2 \\ \mathbf{V}_3 \end{bmatrix} = \begin{bmatrix} V_{1,1} \\ \vdots \\ \bar{V}_{1,j} \\ \vdots \\ \bar{V}_{1,N} \\ V_{2,1} \\ \vdots \\ \bar{V}_{2,j} \\ \vdots \\ \bar{V}_{2,N} \\ V_{3,1} \\ \vdots \\ \bar{V}_{3,j} \\ \vdots \\ \bar{V}_{3,N} \end{bmatrix} \quad (6.13)$$

6.1.2 Harmonic Analysis Method 1

The first harmonic analysis method studied and applied here is based on the method proposed by Teng and Chang [45], which is based on the backward/forward sweep (BFS) technique described in section 3.1.1. With the same advantages mentioned for the BFS applied to a fundamental load flow, reduced time consumption and low complexity, the problem mentioned in [45] by the authors in trying to use directly the BFS method to the harmonic analysis is that the harmonic currents absorbed by the shunt capacitors installed in distribution feeders are unknown. They solve this situation computing the currents absorbed by the shunt capacitors with an iterative technique, and then the forward/backward sweep is used to obtain the relationship between bus harmonic currents, branch currents and bus voltages of each harmonic order. In reference [45] the authors describe the method for a single-phase system. This chapter describes the expanded method for a three-phase system.

Non-linear loads are treated as current sources defined by a characteristic spectrum of amplitude and angle related to the fundamental component as described in section

4.2.4. Linear loads, can be expressed as absorbed currents in the harmonic analysis. For composite loads, non linear loads and linear loads can be treated as harmonic current sources and impedances in proportion to the specification of load composition. The value of the current consumed by the linear loads at bus i for the k th iteration can be calculated as in Equation 6.14.

$$\overline{Ih}_i^{(h,k)} = \frac{\overline{V}_i^{(h,k)}}{\overline{Z}_i^{(h)}} \quad (6.14)$$

where $Z_i^{(h)}$ is the h th harmonic equivalent impedance of the linear load at bus i , calculated with the constant impedance model.

The capacitance of the line impedance can usually be omitted in the distribution system analysis due to its small effect. Therefore, the transmission line model used is just the series impedance part of the one described in section 4.2.1. If it is necessary, the capacitance can also be considered in the proposed method.

The system harmonic current vector is divided in two parts:

$$\mathbf{I}^{(h,k)} = \begin{bmatrix} \mathbf{Ih}^{(h,k)} \\ \dots \\ \mathbf{Is}^{(h,k)} \end{bmatrix} = \begin{bmatrix} \mathbf{Ih}_1^{(h,k)} \\ \vdots \\ \mathbf{Ih}_m^{(h,k)} \\ \dots \\ \mathbf{Is}_1^{(h,k)} \\ \vdots \\ \mathbf{Is}_n^{(h,k)} \end{bmatrix} \quad (6.15)$$

$$\mathbf{Ih}_j^{(h,k)} = \begin{bmatrix} \overline{Ih}_{j,1}^{(h,k)} \\ \overline{Ih}_{j,2}^{(h,k)} \\ \overline{Ih}_{j,3}^{(h,k)} \end{bmatrix} \quad \mathbf{Is}_j^{(h,k)} = \begin{bmatrix} \overline{Is}_{j,1}^{(h,k)} \\ \overline{Is}_{j,2}^{(h,k)} \\ \overline{Is}_{j,3}^{(h,k)} \end{bmatrix}$$

where:

$\mathbf{I}^{(h,k)}$ is a $3(n + m) \times 1$ vector of the system three-phase harmonic currents.

$\mathbf{Ih}^{(h,k)}$ is a $3m \times 1$ vector of the three-phase harmonic currents contributed by linear impedance and nonlinear loads in the system.

m is the number of linear impedance and nonlinear loads in the sys-

tem.
 $\mathbf{I}S^{(h,k)}$ is a $3n \times 1$ vector of the three-phase harmonic currents absorbed by shunt capacitors.
 n is the number of shunt capacitor in the system.

A coefficient matrix \mathbf{A}_j is defined for each branch j . Analog to the Γ matrix defined for the original BFS method, this new coefficient matrix records whether the system harmonic currents flow through the j branch. If a bus harmonic current flows through the branch j , the corresponding position to the phase and node source of this current will be 1. Meanwhile, if the current doesn't flow through the branch, it will be 0.

$$\mathbf{A}_j = \begin{bmatrix} \mathbf{A}h_j \\ \cdots \\ \mathbf{A}s_j \end{bmatrix} = \begin{bmatrix} \mathbf{A}h_{j,1} \\ \vdots \\ \mathbf{A}h_{j,m} \\ \cdots \\ \mathbf{A}s_{j,1} \\ \vdots \\ \mathbf{A}s_{j,n} \end{bmatrix} \quad (6.16)$$

$$\mathbf{A}h_{j,i} = [\mathbf{A}h_{j,i.1} \quad \mathbf{A}h_{j,i.2} \quad \mathbf{A}h_{j,i.3}]$$

$$\mathbf{A}s_{j,i} = [\mathbf{A}s_{j,i.1} \quad \mathbf{A}s_{j,i.2} \quad \mathbf{A}s_{j,i.3}]$$

where:

\mathbf{A}_j is a $(n + m) \times 3$ matrix consisting of 1 and 0 only.

$\mathbf{A}h_j$ is the $m \times 3$ coefficient matrix of the harmonic currents contributed by nonlinear loads and linear impedances.

$\mathbf{A}s_j$ is the $n \times 3$ coefficient matrix of the harmonic currents contributed by shunt capacitors.

The voltage drop at branch j for the p phase can be computed from the impedance matrix of the branch j (\mathbf{Z}_j), the coefficient matrix of the branch (\mathbf{A}_j) and the current injection vector (\mathbf{I}) (Equation (6.17)).

$$\begin{aligned} \Delta \mathbf{V}_{j,p}^{(h,k)} &= \sum_{i=1}^m \left(\mathbf{Z}_{j,p}^{(h)} * \begin{bmatrix} \mathbf{A}h_{j,i.1} & 0 & 0 \\ 0 & \mathbf{A}h_{j,i.2} & 0 \\ 0 & 0 & \mathbf{A}h_{j,i.3} \end{bmatrix} * \mathbf{I}h_i \right) + \\ &+ \sum_{i=1}^n \left(\mathbf{Z}_{j,p}^{(h)} * \begin{bmatrix} \mathbf{A}s_{j,i.1} & 0 & 0 \\ 0 & \mathbf{A}s_{j,i.2} & 0 \\ 0 & 0 & \mathbf{A}s_{j,i.3} \end{bmatrix} * \mathbf{I}s_i \right) \end{aligned} \quad (6.17)$$

$$\mathbf{Z}_j^{(h)} = \begin{bmatrix} \overline{Z}_{j,11}^{(h)} & \overline{Z}_{j,12}^{(h)} & \overline{Z}_{j,13}^{(h)} \\ \overline{Z}_{j,21}^{(h)} & \overline{Z}_{j,22}^{(h)} & \overline{Z}_{j,23}^{(h)} \\ \overline{Z}_{j,31}^{(h)} & \overline{Z}_{j,32}^{(h)} & \overline{Z}_{j,33}^{(h)} \end{bmatrix} = \begin{bmatrix} \mathbf{Z}_{j,1}^{(h)} \\ \mathbf{Z}_{j,2}^{(h)} \\ \mathbf{Z}_{j,3}^{(h)} \end{bmatrix} \quad (6.18)$$

$$\mathbf{Z}_{j,p}^{(h)} = \begin{bmatrix} Z_{j,p1}^{(h)} & Z_{j,p2}^{(h)} & Z_{j,p3}^{(h)} \end{bmatrix} \quad (6.19)$$

If the drop voltages are known, the bus voltages of the system could be calculated by the forward voltage sweep (Equation (6.20)). The problem is that the vector of the currents absorbed by the shunt capacitors ($\mathbf{I} \mathbf{s}^{(h,k)}$) is unknown. The first step to calculate these unknown currents is to write the bus voltage vector as in Equation (6.21), where the voltages are related to the currents through the matrix $\mathbf{H} \mathbf{A}^{(h)}$ composed of the line impedances of the branches between the load or shunt capacitor and the nodes.

$$\mathbf{V}^{(h),k+1} = \mathbf{V}_0^{(h)} + \mathbf{V}^{(h,k)} \quad (6.20)$$

$$\mathbf{V}^{(h,k)} = -\mathbf{H} \mathbf{A}^{(h)} * \mathbf{I}^{(h,k)} \quad (6.21)$$

where:

$\mathbf{V}_0^{(h)}$ is the harmonic component of the slack.

$\mathbf{H} \mathbf{A}^{(h)}$ is the $3N \times 3(n+m)$ relationship matrix between the bus voltages and system harmonic currents.

Then, the bus voltages of shunt capacitors ($\mathbf{V} \mathbf{s}^{(h,k)}$) can be written as:

$$\mathbf{V} \mathbf{s}_p^{(h,k)} = -\mathbf{H} \mathbf{A} \mathbf{s}_p^{(h)} * \mathbf{I}^{(h,k)} \quad (6.22)$$

where:

$p=1, 2, 3$.

$\mathbf{H} \mathbf{A} \mathbf{s}^{(h)}$ is a $n \times 3(n+m)$ matrix composed of the row vectors related to the buses of shunt capacitors.

$$\mathbf{H} \mathbf{A} \mathbf{s}^{(h)} = \begin{bmatrix} \mathbf{H} \mathbf{A} \mathbf{s}_1^{(h)} \\ \mathbf{H} \mathbf{A} \mathbf{s}_2^{(h)} \\ \mathbf{H} \mathbf{A} \mathbf{s}_3^{(h)} \end{bmatrix} \quad (6.23)$$

$$\mathbf{V}_{\mathbf{s}}^{(h,k)} = \begin{bmatrix} \mathbf{V}_{\mathbf{s}_1}^{(h,k)} \\ \mathbf{V}_{\mathbf{s}_2}^{(h,k)} \\ \mathbf{V}_{\mathbf{s}_3}^{(h,k)} \end{bmatrix} \quad (6.24)$$

$$\mathbf{HAs}_p^{(h)} = \begin{bmatrix} \mathbf{HAs}_{p,1,1} & \mathbf{HAs}_{p,1,2} & \cdots & \mathbf{HAs}_{p,1,n+m} \\ \mathbf{HAs}_{p,2,1} & \mathbf{HAs}_{p,2,2} & \cdots & \mathbf{HAs}_{p,2,n+m} \\ \vdots & \vdots & \ddots & \vdots \\ \mathbf{HAs}_{p,n,1} & \mathbf{HAs}_{p,n,2} & \cdots & \mathbf{HAs}_{p,n,n+m} \end{bmatrix} \quad (6.25)$$

$$\mathbf{V}_{\mathbf{s}_p}^{(h,k)} = \begin{bmatrix} \overline{V}_{\mathbf{s}_{p,1}}^{(h,k)} \\ \overline{V}_{\mathbf{s}_{p,2}}^{(h,k)} \\ \vdots \\ \overline{V}_{\mathbf{s}_{p,n}}^{(h,k)} \end{bmatrix} \quad (6.26)$$

The components of the matrix $\mathbf{HAs}_{p,i,j}^{(h)}$ are defined by the relationship between voltage at node i (for the phase p) and currents absorbed by the shunt capacitor j (for all the three phases). It is a 1×3 vector and can be computed according to Equation 6.27.

$$\mathbf{HAs}_{p,i,j}^{(h)} = \sum_{x \in S_{ij}} \left(\mathbf{Z}_{x,p}^{(h)} * \begin{bmatrix} Ah_{x,i,1} & 0 & 0 \\ 0 & Ah_{x,i,2} & 0 \\ 0 & 0 & Ah_{x,i,3} \end{bmatrix} \right) \quad (6.27)$$

where S_{ij} is the set of branches of the phase p connected between the node i and the node of the shunt capacitor j .

The voltage at each shunt capacitors can also be written as:

$$\mathbf{V}_{\mathbf{s}_j}^{(h,k)} = \mathbf{Z}_{\mathbf{s}_j}^{(h)} * \mathbf{I}_{\mathbf{s}_j}^{(h,k)} = \begin{bmatrix} Z_{\mathbf{s}_{j,1}}^{(h)} & 0 & 0 \\ 0 & Z_{\mathbf{s}_{j,2}}^{(h)} & 0 \\ 0 & 0 & Z_{\mathbf{s}_{j,3}}^{(h)} \end{bmatrix} * \begin{bmatrix} I_{\mathbf{s}_{j,1}}^{(h,k)} \\ I_{\mathbf{s}_{j,2}}^{(h,k)} \\ I_{\mathbf{s}_{j,3}}^{(h,k)} \end{bmatrix} \quad (6.28)$$

From Equation (6.28) it can be written an expression for the shunt capacitor voltages

vector ($\mathbf{V}_s^{(h,k)}$):

$$\mathbf{V}_s^{(h,k)} = \mathbf{Z}_s^{(h)} * \mathbf{I}_s^{(h,k)} \quad (6.29)$$

where $\mathbf{Z}_s^{(h)}$ is a $3n \times 3n$ matrix with the shunt capacitor impedances placed in strategic positions to satisfy Equation (6.28) for every $j = 1, \dots, n$, as shown in Equation (6.30).

$$\mathbf{Z}_s^{(h)} = \begin{bmatrix} \mathbf{Z}_{s_{1,A}}^{(h)} & \mathbf{0} & \cdots & \cdots & \mathbf{0} \\ \mathbf{0} & \mathbf{Z}_{s_{2,A}}^{(h)} & \cdots & \cdots & \mathbf{0} \\ \vdots & \vdots & \ddots & & \vdots \\ \mathbf{0} & \mathbf{0} & \cdots & \cdots & \mathbf{Z}_{s_{n,A}}^{(h)} \\ \mathbf{Z}_{s_{1,B}}^{(h)} & \mathbf{0} & \cdots & \cdots & \mathbf{0} \\ \mathbf{0} & \mathbf{Z}_{s_{2,B}}^{(h)} & \cdots & \cdots & \mathbf{0} \\ \vdots & \vdots & \ddots & & \vdots \\ \mathbf{0} & \mathbf{0} & \cdots & \cdots & \mathbf{Z}_{s_{n,B}}^{(h)} \\ \mathbf{Z}_{s_{1,C}}^{(h)} & \mathbf{0} & \cdots & \cdots & \mathbf{0} \\ \mathbf{0} & \mathbf{Z}_{s_{2,C}}^{(h)} & \cdots & \cdots & \mathbf{0} \\ \vdots & \vdots & \ddots & & \vdots \\ \mathbf{0} & \mathbf{0} & \cdots & \cdots & \mathbf{Z}_{s_{n,C}}^{(h)} \end{bmatrix} \quad (6.30)$$

$$\mathbf{Z}_s^{(h)} = \begin{bmatrix} \mathbf{Z}_{s_{j,A}}^{(h)} \\ \mathbf{Z}_{s_{j,B}}^{(h)} \\ \mathbf{Z}_{s_{j,C}}^{(h)} \end{bmatrix} = \begin{bmatrix} Z_{j,1}^{(h)} & 0 & 0 \\ 0 & Z_{j,2}^{(h)} & 0 \\ 0 & 0 & Z_{j,3}^{(h)} \end{bmatrix} \quad (6.31)$$

where:

$$j = 1, 2, \dots, n.$$

$$\mathbf{0} = [0 \ 0 \ 0]$$

Replacing Equation (6.29) in (6.22):

$$\mathbf{Z}_s^{(h)} * \mathbf{I}_s^{(h,k)} = -\mathbf{H}\mathbf{A}\mathbf{s}^{(h)} * \mathbf{I}^{(h,k)} \quad (6.32)$$

$\mathbf{HAs}^{(h)}$ can be divided in two components. The first one (left part) is composed of the m first columns and is the one that relates the bus voltages to the currents injected by the linear impedances and nonlinear loads. The second one contains the remaining n columns, those ones that relate the bus voltages to the currents absorbed by the shunt capacitors.

$$\mathbf{HAs}^{(h)} = [\mathbf{HAsh}^{(h)} \quad | \quad \mathbf{HAss}^{(h)}] \quad (6.33)$$

Replacing Equation (6.33) in (6.34) and manipulating the expression, it can be written Equation (6.37).

$$\begin{aligned} \mathbf{Zs}^{(h)} * \mathbf{Is}^{(h,k)} &= - [\mathbf{HAsh}^{(h)} \quad | \quad \mathbf{HAss}^{(h)}] * \mathbf{I}^{(h,k)} \\ &= - \left(\mathbf{HAsh}^{(h)} * \mathbf{Ih}^{(h,k)} + \mathbf{HAss}^{(h)} * \mathbf{Is}^{(h,k)} \right) \end{aligned} \quad (6.34)$$

$$\left(\mathbf{HAss}^{(h)} + \mathbf{Zs}^{(h)} \right) * \mathbf{Is}^{(h,k)} = -\mathbf{HAsh}^{(h)} * \mathbf{Ih}^{(h,k)} \quad (6.35)$$

$$\mathbf{HLF}^{(h)} = \mathbf{HAss}^{(h)} + \mathbf{Zs}^{(h)} \quad (6.36)$$

$$\mathbf{HLF}^{(h)} * \mathbf{Is}^{(h,k)} = -\mathbf{HAsh}^{(h)} * \mathbf{Ih}^{(h,k)} \quad (6.37)$$

As $\mathbf{HLF}^{(h)}$, $\mathbf{HAsh}^{(h)}$ and $\mathbf{Ih}^{(h,k)}$ are known, from Equation (6.37) the currents absorbed by the shunt capacitors $\mathbf{Is}^{(h,k)}$ can be calculated. It can be noticed that Equation (6.37) represents a system of $3n$ linear equations, instead of solving a whole $3N$ equations system.

Once the shunt capacitors currents are known, the branch current vector \mathbf{B} (Equation (6.38)) can be calculated, the branch voltage drops (Equation (6.17)) and the bus voltages (Equation (6.21)) caused by the harmonic currents.

$$\begin{aligned} \mathbf{B}_j^{(h,k)} &= \sum_{i=1}^m \left(\begin{bmatrix} Ah_{j,i.1} & 0 & 0 \\ 0 & Ah_{j,i.2} & 0 \\ 0 & 0 & Ah_{j,i.3} \end{bmatrix} * \mathbf{Ih}_i \right) + \\ &+ \sum_{i=1}^n \left(\begin{bmatrix} As_{j,i.1} & 0 & 0 \\ 0 & As_{j,i.2} & 0 \\ 0 & 0 & As_{j,i.3} \end{bmatrix} * \mathbf{Is}_i \right) \end{aligned} \quad (6.38)$$

The iteration process for the h th harmonic order will stop if the following criterion is satisfied:

$$|V_j^{(h,k+1)} - V_j^{(h,k)}| \leq \varepsilon \quad \text{for } i = 1, 2, \dots, N \quad (6.39)$$

6.1.3 Harmonic Analysis Method 2

The second method applied is simpler than method 1 because it sees the shunt capacitors as linear loads, then calculates their currents as:

$$\overline{I_{s_j}}^{(h,k)} = \frac{\overline{V_{s_j}}^{(h,k)}}{\overline{Z_{s_j}}} \quad (6.40)$$

$$\overline{Z_{s_j}} = \frac{|\overline{V_{n_j}}|^2}{\overline{S_{n_j}}} \quad (6.41)$$

where:

$\overline{I_{s_j}}^{(h,k)}$ is the h -th harmonic current absorbed by the shunt capacitor j at the k -th iteration.

$\overline{V_{s_j}}^{(h,k)}$ is the h -th harmonic voltage at the shunt capacitor j for the k -th iteration.

$\overline{Z_{s_j}}$ is the shunt capacitor impedance.

$\overline{V_{n_j}}$ is the rated voltage of the shunt capacitor j .

$\overline{S_{n_j}}$ is the rated apparent power of the shunt capacitor j .

This method consists on applying to each harmonic order the algorithm and equations of section 6.1.1. For each harmonic order the models of the system components and loads are recalculated and then the BFS is applied.

6.2 Convergence for Harmonic Analysis Methods Based on Backward/Forward Sweep Technique

In section 3.1.1 the convergence criterion for the backward/forward sweep technique was explained in the case of a fundamental load flow. The limit condition to reach convergence in a case of a two node system is the maximum power delivery point [7]. According to the maximum power theorem this condition is for $R_{line} = R_{load}$ for purely resistive circuits and $Z_{line} = Z_{load}^*$ for RLC or LC systems.

Figure 6.2 shows a simple example of a two node circuit which resistance values varies from a condition previous to the maximum power delivery ($R_{line} < R_{load}$) to a condition after the maximum power transfer point ($R_{line} > R_{load}$). Tables 6.1, 6.2 and 6.3 show the results obtained after 10 iterations, confirming the theoretical analysis.

The circuit of Figure 6.3 represents a very simple example where can be seen that this condition can be extended to the harmonic analysis case.

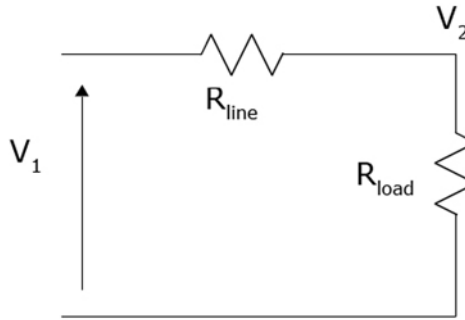


Figure 6.2: Example of a two node resistive circuit.

Table 6.1: Resistive system working in a point previous to the maximum power transfer:

$$R_{load} = 2\text{p.u. } R_{line} = 1\text{p.u.}$$

Iteration	V_c		I_c		I	
	(p.u)	(degrees)	(p.u)	(degrees)	(p.u)	(degrees)
1	0.5000	0.0000	0.2500	0.0000	1.2500	0.0000
2	1.2500	180.0000	0.6250	180.0000	0.3750	0.0000
3	0.3750	180.0000	0.1875	180.0000	0.8125	0.0000
4	0.8125	180.0000	0.4063	180.0000	0.5938	0.0000
5	0.5938	180.0000	0.2969	180.0000	0.7031	0.0000
6	0.7031	180.0000	0.3516	180.0000	0.6484	0.0000
7	0.6484	180.0000	0.3242	180.0000	0.6758	0.0000
8	0.6758	180.0000	0.3379	180.0000	0.6621	0.0000
9	0.6621	180.0000	0.3311	180.0000	0.6689	0.0000
10	0.6689	180.0000	0.3345	180.0000	0.6655	0.0000

Table 6.4 shows the solution of the circuit in a operating point previous to the resonant condition: $X_L = j$; $X_C = -j2$. It can be clearly seen that the method is converging. Instead in Tables 6.5 and 6.6, which represent resonant condition and one operating point after the resonance, the divergence situation can be noticed.

Table 6.2: System in the point of maximum power transfer: $R_{load} = R_{line} = 1\text{p.u}$

Iteration	Vc		Ic		I	
	p.u	Degrees	p.u	Degrees	p.u	Degrees
1	0.5000	0.0000	0.5000	0.0000	1.5000	0.0000
2	1.5000	180.0000	1.5000	180.0000	0.5000	180.0000
3	0.5000	0.0000	0.5000	0.0000	1.5000	0.0000
4	1.5000	180.0000	1.5000	180.0000	0.5000	180.0000
5	0.5000	0.0000	0.5000	0.0000	1.5000	0.0000
6	1.5000	180.0000	1.5000	180.0000	0.5000	180.0000
7	0.5000	0.0000	0.5000	0.0000	1.5000	0.0000
8	1.5000	180.0000	1.5000	180.0000	0.5000	180.0000
9	0.5000	0.0000	0.5000	0.0000	1.5000	0.0000
10	1.5000	180.0000	1.5000	180.0000	0.5000	180.0000

Table 6.3: Resistive system after the maximum power transfer: $R_{load} = 1\text{ p.u.}$ $R_{line} = 2\text{ p.u.}$

Iteration	Vc		Ic		I	
	p.u	Degrees	p.u	Degrees	p.u	Degrees
1	0.5000	0.0000	0.5000	0.0000	1.5000	0.0000
2	3.0000	180.0000	3.0000	180.0000	2.0000	180.0000
3	4.0000	0.0000	4.0000	0.0000	5.0000	0.0000
4	10.0000	180.0000	10.0000	180.0000	9.0000	180.0000
5	18.0000	0.0000	18.0000	0.0000	19.0000	0.0000
6	38.0000	180.0000	38.0000	180.0000	37.0000	180.0000
7	74.0000	0.0000	74.0000	0.0000	75.0000	0.0000
8	150.0000	180.0000	150.0000	180.0000	149.0000	180.0000
9	298.0000	0.0000	298.0000	0.0000	299.0000	0.0000
10	598.0000	180.0000	598.0000	180.0000	597.0000	180.0000

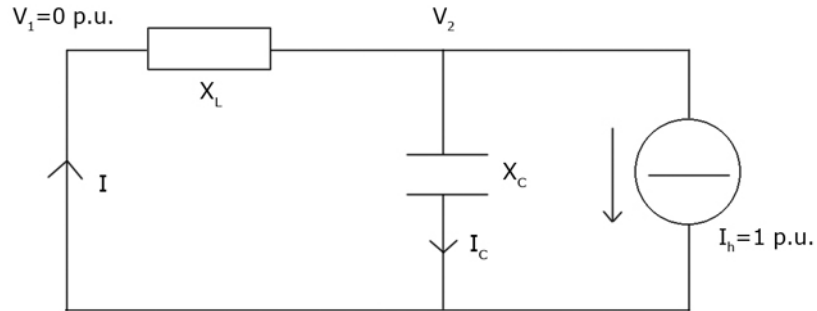


Figure 6.3: Example of a two node equivalent circuit for harmonic analysis.

Table 6.4: System working in a point previous resonance condition: $Z_{load} = -j2$ p.u.
 $Z_{line} = j$ p.u..

Iteration	Vc		Ic		I	
	p.u	Degrees	p.u	Degrees	p.u	Degrees
1	0.1000	0.0000	0.0500	90.0000	1.0012	2.8624
2	1.0012	-87.1376	0.5006	2.8624	1.5002	0.9548
3	1.5002	-89.0452	0.7501	0.9548	1.7500	0.4092
4	1.7500	-89.5908	0.8750	0.4092	1.8750	0.1910
5	1.8750	-89.8090	0.9375	0.1910	1.9375	0.0924
6	1.9375	-89.9076	0.9688	0.0924	1.9688	0.0455
7	1.9688	-89.9545	0.9844	0.0455	1.9844	0.0226
8	1.9844	-89.9774	0.9922	0.0226	1.9922	0.0112
9	1.9922	-89.9888	0.9961	0.0112	1.9961	0.0056
10	1.9961	-89.9944	0.9980	0.0056	1.9980	0.0028

Table 6.5: Sistem in resonance condition: $Z_{load} = -jp.u.$ $Z_{line}^* = j p.u.$

Iteration	Vc		Ic		I	
	p.u	Degrees	p.u	Degrees	p.u	Degrees
1	0.1000	0.0000	0.1000	90.0000	1.0050	5.7106
2	1.0050	-84.2894	1.0050	5.7106	2.0025	2.8624
3	2.0025	-87.1376	2.0025	2.8624	3.0017	1.9092
4	3.0017	-88.0908	3.0017	1.9092	4.0012	1.4321
5	4.0012	-88.5679	4.0012	1.4321	5.0010	1.1458
6	5.0010	-88.8542	5.0010	1.1458	6.0008	0.9548
7	6.0008	-89.0452	6.0008	0.9548	7.0007	0.8185
8	7.0007	-89.1815	7.0007	0.8185	8.0006	0.7162
9	8.0006	-89.2838	8.0006	0.7162	9.0006	0.6366
10	9.0006	-89.3634	9.0006	0.6366	10.0005	0.5729

Table 6.6: Sistem working in a point after the resonance condition: $Z_{load} = -j$ p.u.
 $Z_{line} = j2$ p.u.

Iteration	Vc		Ic		I	
	(p.u)	(degrees)	(p.u)	(degrees)	(p.u)	(degrees)
1	0.1000	0.0000	0.1000	90.0000	1.0050	5.7106
2	2.0100	-84.2894	2.0100	5.7106	3.0067	3.8141
3	6.0133	-86.1859	6.0133	3.8141	7.0114	3.2705
4	14.0228	-86.7295	14.0228	3.2705	15.0213	3.0529
5	30.0426	-86.9471	30.0426	3.0529	31.0413	2.9546
6	62.0825	-87.0454	62.0825	2.9546	63.0812	2.9078
7	126.1624	-87.0922	126.1624	2.9078	127.1612	2.8849
8	254.3223	-87.1151	254.3223	2.8849	255.3211	2.8736
9	510.6421	-87.1264	510.6421	2.8736	511.6409	2.8680
10	1023.2817	-87.1320	1023.2817	2.8680	1024.2804	2.8652

6.3 Application of the Methods

6.3.1 Fundamental Power Flow

The program developed in Matlab[®] consists of a set of 8 files that follow the flow chart of Figure 6.4 to solve the power flow at the fundamental component according to the method explained in section 6.1.2:

- **fundamental.m**

It is the main body of the program. It calls all the other files needed.

- **configurations.m**

It is part of the *read data* block of Figure 6.4. It contains the matrix of the line impedances and admittance in unit length (ohms per mile and μ siemens per mile, respectively) for each configuration of overhead lines or underground cables. If some configuration of lines different to those defined in [22] has to be added, they have to be introduced in this file. In this file are also assigned the components other than lines (transformers and switches) and the different kinds of connection of the loads.

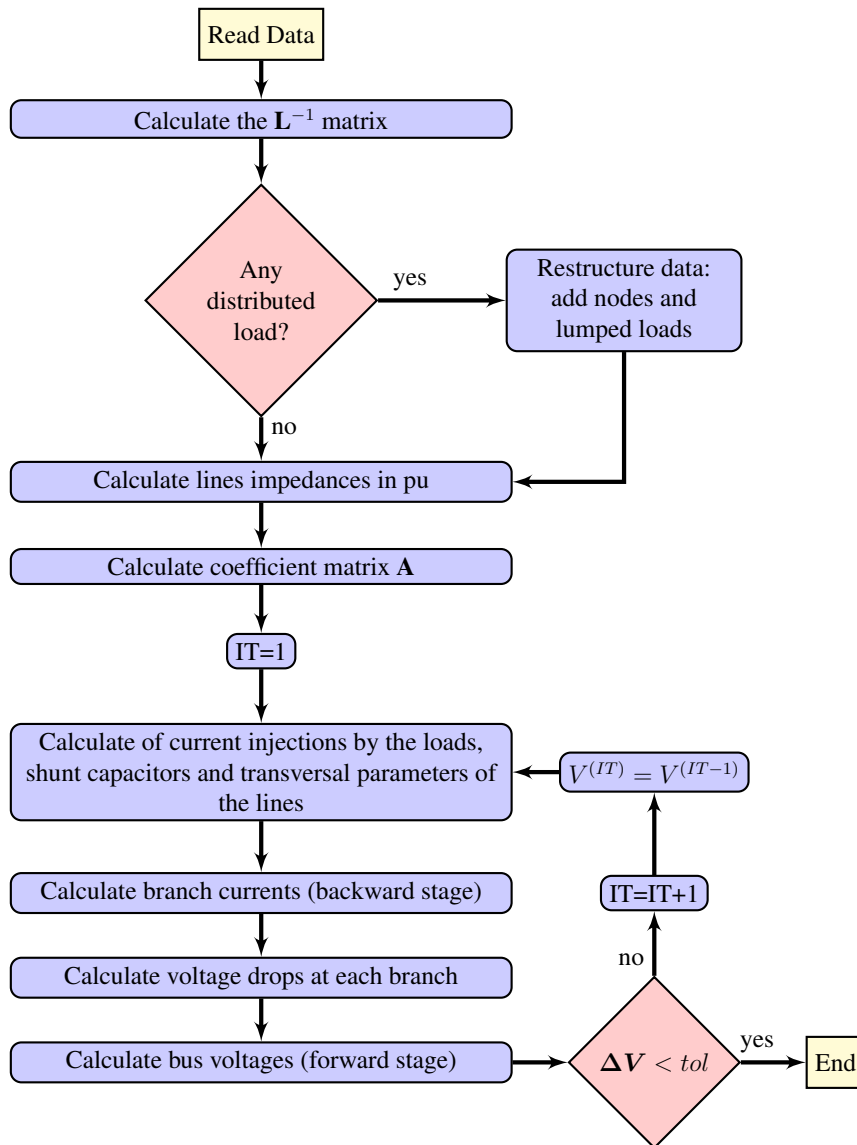


Figure 6.4: Flow chart of the power flow for fundamental component of a radial distribution network.

- **inputs.m**

It is also part of the *read data* block of Figure 6.4. Here the user can define the following parameters that describe the structure and the initial state of the network:

- Number of nodes.
- Number of shunt capacitors, spots and uniformly distributed linear loads.
- Maximum number of iterations.

- Tolerance of the variation between the maximum of the differences between bus voltage at the actual and the previous iteration.
- Slack voltages.
- Incidence matrix \mathbf{L}
- Shunt capacitors position, connection and nominal reactive power for each phase.
- Linear spot and distributed loads position, connection, model (PQ, I, Z) and nominal active and reactive power for each phase.
- Transformers position, nominal apparent power, nominal voltage levels and short circuit impedance.
- Lines data: length, configuration and ends nodes.

- **distributedLoad.m**

This file is called just if it is specified in the inputs that the number of distributed loads is not zero. It is the *restructure data* block of Figure 6.4. Its objective is to implement the model described in section 4.1.4, therefore it divides the total power into two lumped loads and adds a node to the network. This last step implies adding a row and a column to the incidence matrix \mathbf{L} .

- **genZ.m**

Based on the length and configuration of the lines, this file generates the series component of the pi-model of the lines (section 4.1.1). It also calculates the impedance of the shunt capacitors and the transformer. Actually the only model supported is the Y-grounded/Y-grounded connections, if other types of connections have to be used, it has to be modified according to section 4.1.2. All of the impedances are calculated in the p.u. system, using the base power S_{base} introduced by the user and the base voltages according to the nominal voltage levels of the transformers.

- **genA.m**

Based on the implications matrix \mathbf{L} , this file generates the coefficient matrix \mathbf{A}_i , presented in section 6.1.2, for each node i .

- **lineC.m**

It calculates the transversal parameters of the lines according to the pi-model of section 4.1.1 and the branch currents due to these parameters.

- **results.m**

It is the file responsible for organizing the output data at each iteration into tables and showing them into the Matlab command window.

6.3.2 Harmonic Power Flow

To implement the harmonic analysis of a radial distribution network, the program developed has the structure shown in Figure 6.5. The backward/forward sweep method used to solve the fundamental component of system is the same described in section 6.3.1.

The program consists of the 17 .m files briefly described below, but only 15 or 16 have to be run at the same time, depending on the method chosen.

- **method1.m / method2.m**

Can be applied one at a time, depending of the method to be used. Each one is the main body of the program. It calls all the other files needed and solves the harmonic BFS according to the method chosen.

- **configurations_h.m**

Analog to the file *configurations.m* of the fundamental power flow, but in this case it includes the typical spectrum tables of the nonlinear loads modeled as harmonic current sources.

- **inputs_c.m**

Analog to the file *inputs.m* of the fundamental power flow, but in this case it has to be specified the maximum harmonic order to include in the analysis and the composition of the loads (percentage of motive, passive and each type of nonlinear load).

- **input_LINES.m**

In this file the physical and geometrical characteristic are defined for the lines.

- **distibutedLOAD_h.m**

Analog to the file *distibutedLOAD.m* of the fundamental power flow. it is not the same file because the input matrix of the load data is defined different in the case of harmonic analysis, then it has to be adapted to this type of entry.

- **carson.m**

It is part of the *calculate lines impedances* block of Figure 6.5. It applies the Carson's equation [8] to calculate the lines impedances (see section 4.1.1).

- **genZ_h.m**

It is also is part of the *calculate lines impedances* block of Figure 6.5. It assigns to each branch the line impedance in p.u. corresponding according to its type.

- **kron.m**

It is the final part of the *calculate lines impedances* block of Figure 6.5. It applies the Kron reduction to the impedances obtained from *Rharmonic.m* to get a 3×3 matrix (see section 4.1.1).

- **genA_h.m**

Same file as *genA.m* of the fundamental power flow.

- **fundamental_h.m**

Apply the backward/forward sweep algorithm described in section 6.3.1.

- **Rharmonic.m**

It calculates the value of the lines resistance and reactance per unit length at the h -th harmonic order according to Equation (4.58).

- **Zlong_lines.m**

It is called by the main program just in case it is necessary to handle lines with the long lines equations (see sections 4.1.1 and 4.2.1).

- **results_it.m**

Organizes the bus voltages, branch currents, shunt capacitors and load currents at each iteration into tables and shows them into the Matlab command window.

- **results_h.m**

Organizes into tables the shunt capacitors and loads currents, bus voltages, branch currents, branch losses and total number of iterations made for each harmonic order and shows them into the Matlab command window. It also has a warning message that will be shown in case of reaching the maximum number of iterations, telling that the method may be diverging.

- **total_res.m**

Organizes and shows in the Matlab command window the harmonic levels of the network, that is the branch currents and bus voltage magnitudes and the total harmonic distortion (THD) levels for each node. It also shows the total system losses.

- **genHA.m**

Calculates the elements of the single phase **HA** matrix, which describe the relation between bus voltages and node currents. In the main program this file has to be called three times for a three phase system.

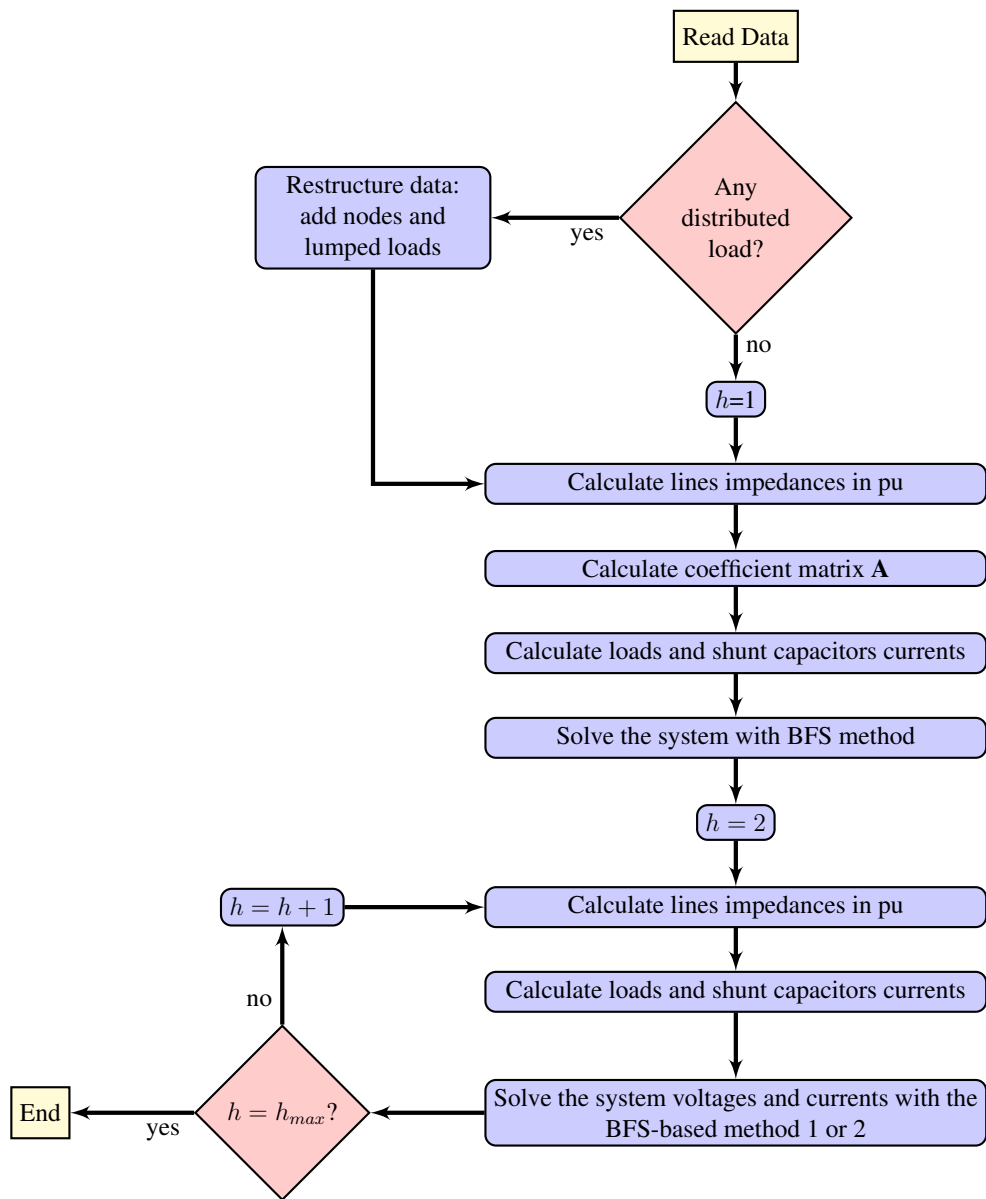


Figure 6.5: Flow chart of the harmonic power flow for radial distribution systems.

Method 1

The procedure of method 1 described in section 6.1.2 can be summarized in the flow chart of Figure 6.6.

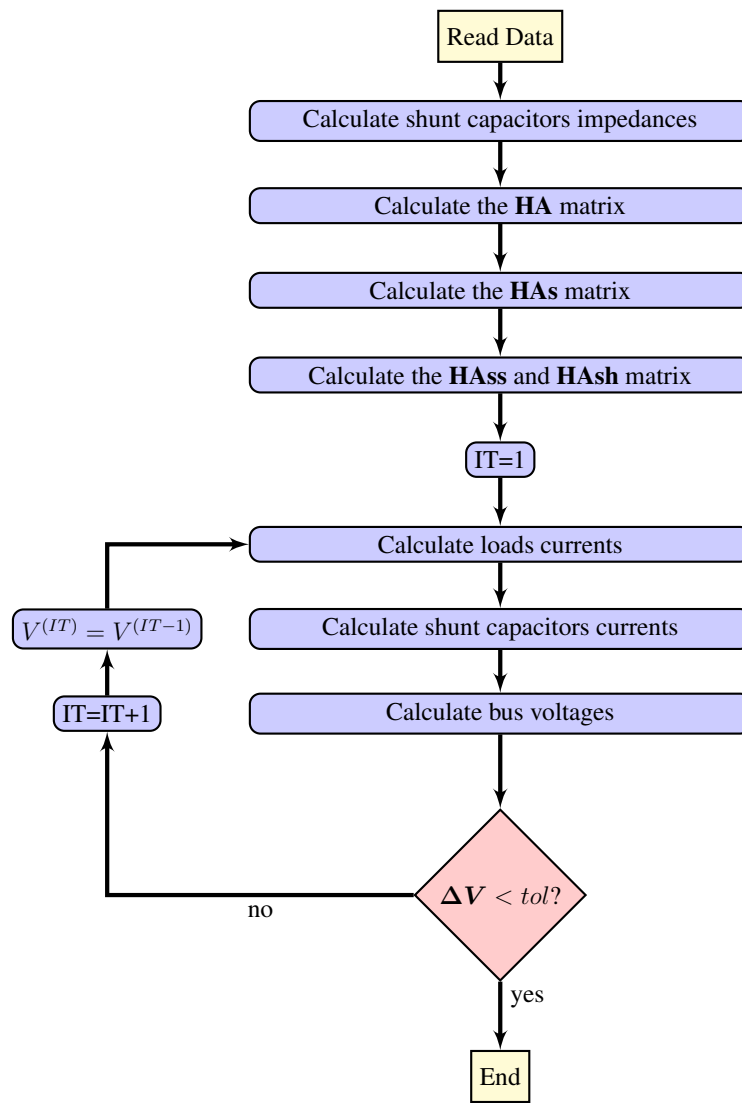


Figure 6.6: Flow chart of the method 1.

Method 2

The procedure of method 2 described in section 6.1.3 can be summarized in the flow chart of Figure 6.7.

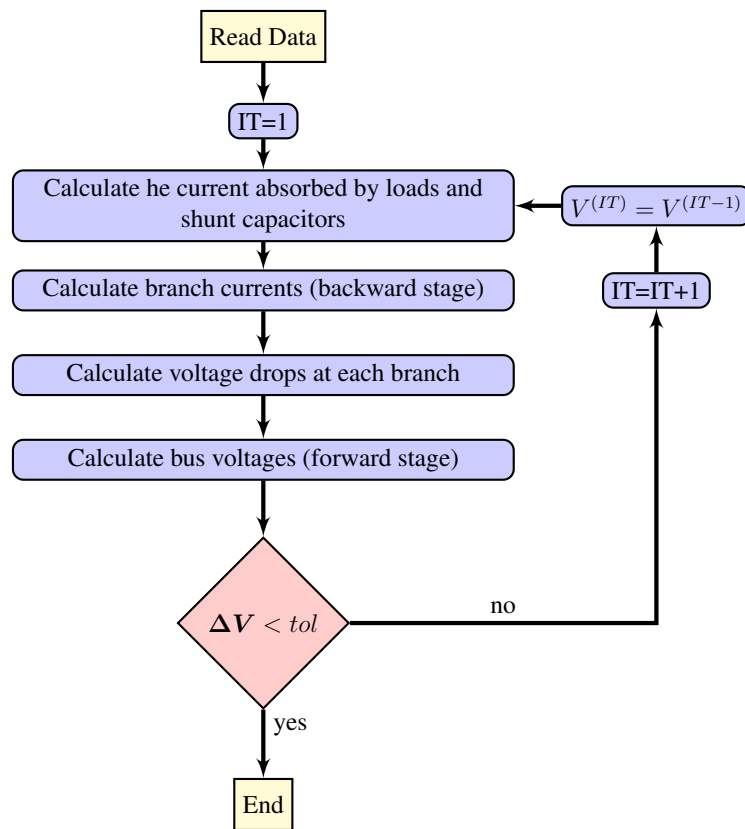


Figure 6.7: Flow chart of the method 2.

6.3.3 Weakly Meshed Networks

The procedure described in section 3.1.2 to solve weakly meshed networks with method designed to be applied in radial configurations, was implemented with 19 .m files briefly described below, but only 17 or 18 have to be run at the same time, depending on the method chosen.

- **meshedNETWORK.m**

It is the main body of the program. It calls all the other files needed.

- **M_inputs.m**

Analog to *inputs.m*, both files require the same input data. The user has to be very careful when entering the branch and node data, the following rules must be followed:

- When entering the incidence matrix **L**: if two nodes belong to the same layer, it will be taken as a “son” the one labeled with a greater number.
- The breakpoint of a loop will be the node labeled with a highest number.
- The end node of a lines has to be entered in ascending order, it means that in the first column there will be the node labeled with the smaller number.
- The line that closes the loop has to be placed at the last row of the data line matrix. If there is more that one breakpoint, the last line has to be the one with the highest breakpoint.

- **meshed.m**

This file identifies from the incidence matrix **L** if there exists any loop in the network. If there is any loop, it identifies the breakpoints as the node labeled with the highest number and breaks it into two nodes, restructuring the system data and adding two constant loads for each breakpoint to simulate the compensation currents.

- **configurations_h.m, distributedLOAD_h.m, genZ_h.m, genA_h.m, Zlong_lines.m, Rharmonic.m, lineC.m, ZSaux.m and genHA.m**

They are the same files used in the case of radial networks and described in the previous section.

- **BFS_Zmesh.m**

Solve the bus voltages of each system required to calculate the components of the matrix \tilde{Z} (see section 3.1.2).

- **MlineCZ.m**

It is called by *BFS_Zmesh.m*. It computes the contribution of the shunt parameters of the lines to the branch currents.

- **BFS_f.m**

It solves the bus voltages and branch currents for the fundamental component. It is based on the program explained in section 6.3.1.

- **BFS_h1 / BFS_h2**

Can be applied one at a time, depending of the method to be used. Each one solves the harmonic BFS according to the method chosen.

- **results_h.m**

Organizes into tables the bus voltage, branch currents, shunt capacitors and loads currents for each harmonic order and shows them into the Matlab command window. It also has a warning message that will be shown in case of reaching the maximum number of iterations, telling that the method may be diverging.

- **total_res.m**

Organizes and shows in the Matlab command window the harmonic levels of the network, which is the branch currents and bus voltage magnitudes and the total harmonic distortion (THD) levels for each node.

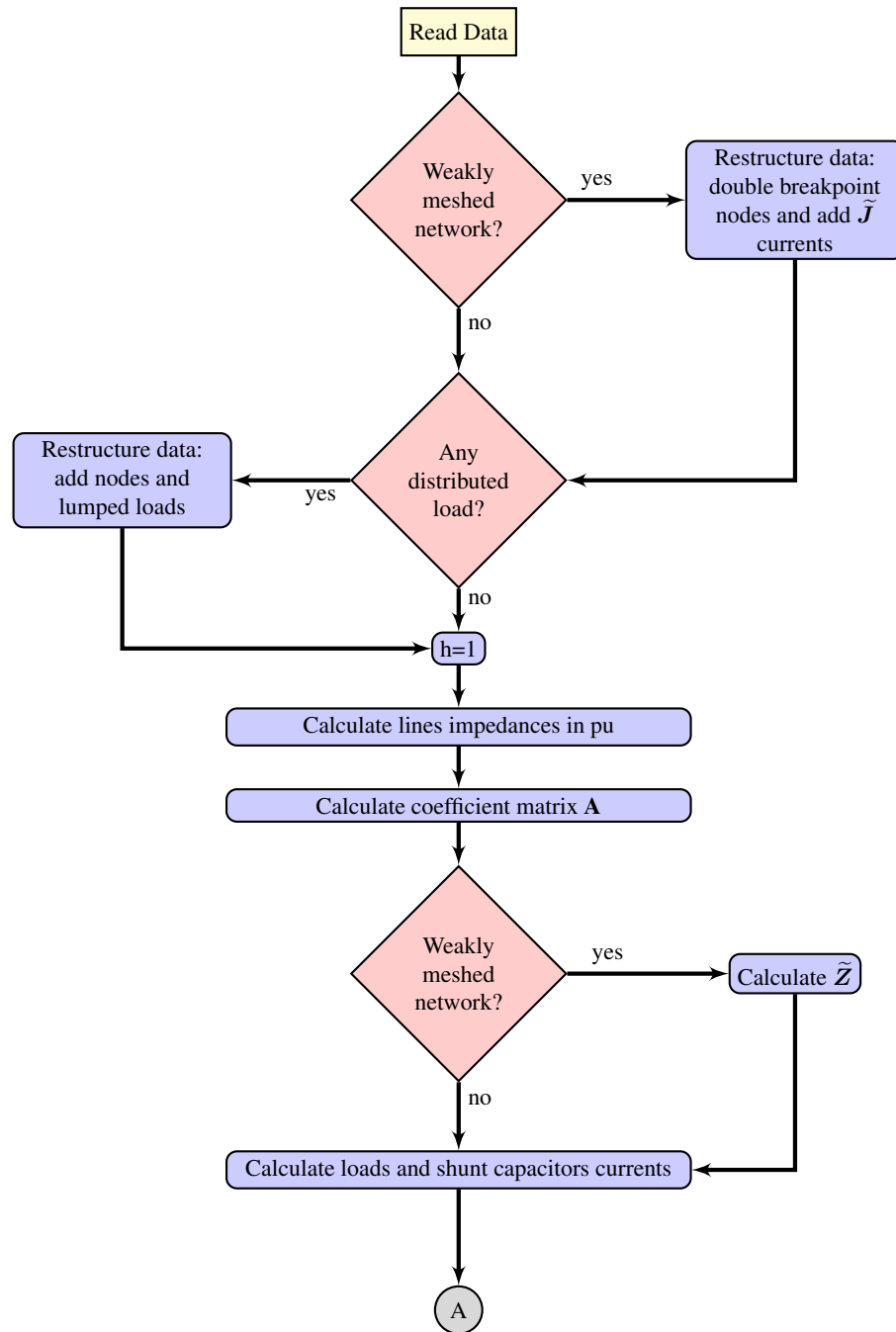


Figure 6.8: Flow chart of the load flow for weakly meshed distribution systems (I).

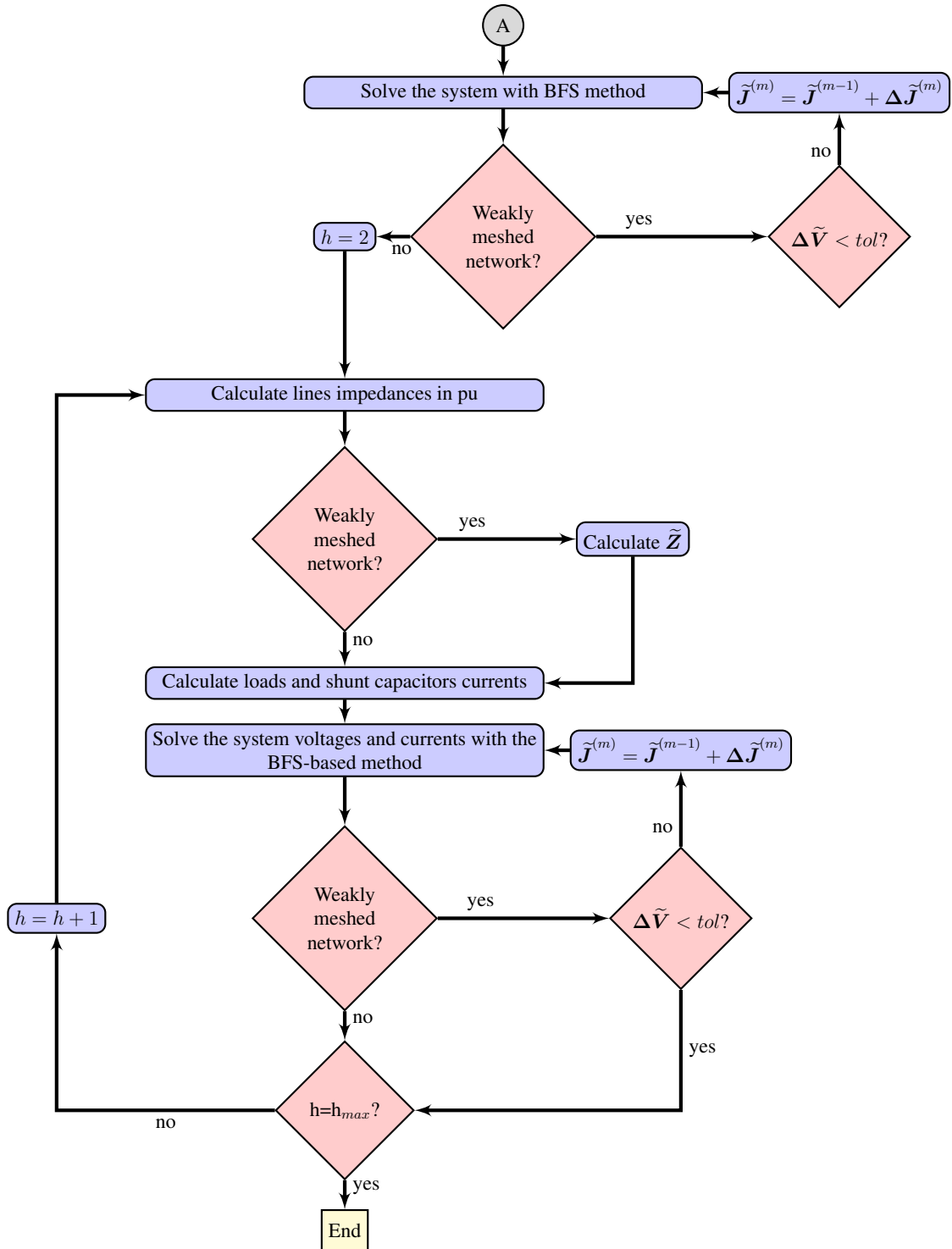


Figure 6.9: Flow chart of the load flow for weakly meshed distribution systems (II).

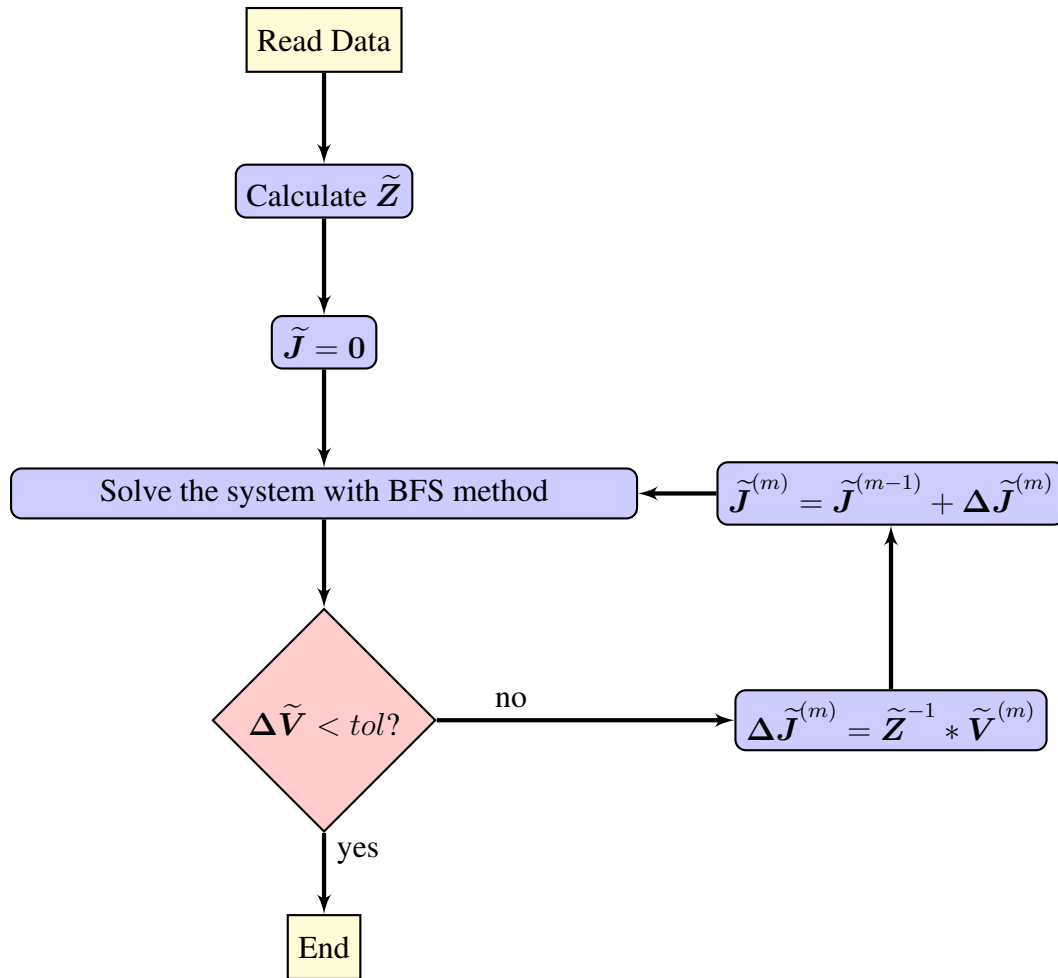


Figure 6.10: Presentacion.

6.4 Power Flow Results

6.4.1 Load Flow at the Fundamental Frequency

The most important results obtained applying the set of .m files to the network of [22] are shown in the tables below, where the “added” label is assigned to a node if it does not belong to the original system, but was added as a part of the distributed load model. The results were reached after 6 iterations in 0.479 seconds for a tolerance of 10^{-6} for the maximum difference between bus voltages of two consecutive iterations.

Comparing the results obtained with those given in [22] it can be seen that the maximum difference between the values is obtained for the total losses and it is equal to 0.07%. That means that the method programmed is have always less than 1% of error, so it can be a trustable program to solve unbalanced distribution networks for the fundamental frequency.

More specific results are shown in appendix B.1, including bus voltages, branch currents, loads currents and shunt capacitors currents, as well as the time consumed by each .m file, the system power factor and the total power consumption and losses for each phase. From the time consuming table shown in this appendix, it can be noticed that 65.76% of the time was used to print the results. This is because the results were printed for each iteration, just for documentation in case that some one need to compare this kind of results. Usually results are needed just at the end of the iterative process and the time consumed by the program will be even lower than the 0.479 s obtained here.

Table 6.7: Power flow results for the 13 node network without harmonic sources.

	kW	kvar	kVA
Feeder Total Power	3 577.1219	1 724.2883	3 971.0163
Total Power in the Branches	110.9828	324.5757	343.0256

6.4.2 Harmonic Analysis Method 1

The analysis was made for frequencies from the fundamental to the 7th harmonic. Most important results obtained applying the set of .m files to the 4 node test feeder are shown in the tables below. They were calculated for a tolerance of 10^{-5} for the maximum difference between bus voltages of two consecutive iterations and 30 maximum of iterations allowed for each harmonic order. More specific results are shown in

Table 6.8: Bus voltages for the 13 node network without harmonic sources

Bus No	IEEE Bus Name	Phase A		Phase B		Phase C	
		pu	Degree	pu	Degree	pu	Degree
1	632	1.02101	-2.4893	1.0420	-121.7200	1.0175	117.8290
2	645	–	–	1.0328	-121.8997	1.0155	117.8562
3	671	0.9900	-5.2956	1.0529	-122.3419	0.9778	116.0256
4	633	1.0180	-2.5539	1.0401	-121.7654	1.0148	117.8249
5	646	–	–	1.0311	-121.9753	1.0134	117.9014
6	684	0.9881	-5.3186	–	–	0.9758	115.9244
7	680	0.9900	-5.2956	1.0529	-122.3419	0.9778	116.0256
8	692	0.9900	-5.2956	1.0529	-122.3419	0.9778	116.0256
9	634	0.9940	-3.2300	1.0218	-122.2215	0.9960	117.3453
10	611	–	–	–	–	0.9738	115.7786
11	652	0.9825	-5.2441	–	–	–	–
12	675	0.9835	-5.5457	1.0553	-122.5180	0.9759	116.0401
13	Added	1.0133	-3.1735	1.0443	-121.8776	1.0068	117.3451

Table 6.9: Branch currents for the 13 node network without harmonic sources

Branch No	IEEE Branch Name	Phase B		Phase C		Phase A	
		A	Degree	A	Degree	A	Degree
1	0 - 632	558.3715	-28.5699	414.8486	-140.9089	586.5241	93.5957
2	632 - 645	0.0000	0.0000	143.0246	-142.6621	65.2060	57.8262
3	Added - 671	472.8982	-26.9428	195.8511	-132.9058	439.1296	100.9893
4	632 - 633	81.3261	-37.7380	61.1231	-159.0908	62.7034	80.4759
5	645 - 646	0.0000	0.0000	65.2069	-122.1742	65.2067	57.8257
6	671 - 684	63.0657	-39.1159	0.0000	0.0000	71.1500	121.6170
7	671 - 680	0.0018	90.6775	0.0017	-40.9411	0.0015	-150.4885
8	671 - 692	229.0881	-18.1609	69.6075	-55.1878	178.3650	109.4062
9	633 - 634	704.8295	-37.7385	529.7370	-159.0914	543.4344	80.4754
10	684 - 611	0.0000	0.0000	0.0000	0.0000	71.1499	121.6165
11	684 - 652	63.0748	-39.1282	0.0000	0.0000	0.0000	0.0000
12	692 - 675	205.3194	-5.1329	69.5968	-55.1915	124.0637	111.8011
13	632 - Added	478.2625	-27.0179	215.1023	-134.6520	475.4434	99.9164

appendix B.2.1, including bus voltages and branch currents at each iteration for each harmonic, loads currents, shunt capacitors currents and losses at each harmonic order for the first 5 harmonics calculated.

From Table 6.11 can be seen that the process is diverging for the 5th harmonic. Actually, it also diverges for all harmonic orders higher than 5. In appendix B.2.1 is

Table 6.10: Active power losses for the 13 node network without harmonic sources.

Branch No	IEEE Branch Name	Phase A (kW)	Phase B (kW)	Phase C (kW)
1	0 - 632	21.5174	-3.2502	41.4385
2	632 - 645	0.0000	2.5462	0.2202
3	Added - 671	8.1357	-4.7547	22.8756
4	632 - 633	0.3539	0.1477	0.3061
5	645 - 646	0.0000	0.2713	0.2699
6	671 - 684	0.2108	0.0000	0.3713
7	671 - 680	0.0000	0.0000	0.0000
8	671 - 692	0.0000	0.0000	-0.0000
9	633 - 634	2.5181	1.4224	1.4969
10	684 - 611	0.0000	0.0000	0.3823
11	684 - 652	0.8092	0.0000	0.0000
12	692 - 675	3.2173	0.3449	0.5731
13	632 - Added	2.3676	-1.4641	8.6554

shown the evaluation of the convergence criterion $Z_{line} * Y_{load} < 1$ [7] and can be seen that it is satisfied only for harmonic orders below the 5th.

Table 6.11: Bus voltages in p.u. at each harmonic order for the 4 node test feeder with harmonic sources, obtained with the method 1.

Bus No	Phase	Harmonic Order				
		1	2	3	4	5
1	A	1.0000e+00	0.0000e+00	0.0000e+00	0.0000e+00	0.0000e+00
	B	1.0000e+00	0.0000e+00	0.0000e+00	0.0000e+00	0.0000e+00
	C	1.0000e+00	0.0000e+00	0.0000e+00	0.0000e+00	0.0000e+00
2	A	9.9754e-01	0.0000e+00	4.0968e-04	0.0000e+00	2.2427e+37
	B	9.9504e-01	0.0000e+00	2.2469e-04	0.0000e+00	2.1412e+37
	C	9.9890e-01	0.0000e+00	1.3149e-05	0.0000e+00	2.0157e+37
3	A	9.8155e-01	0.0000e+00	1.4912e-03	0.0000e+00	8.1633e+37
	B	9.6469e-01	0.0000e+00	8.1787e-04	0.0000e+00	7.7940e+37
	C	9.8911e-01	0.0000e+00	4.7864e-05	0.0000e+00	7.3372e+37
4	A	9.7849e-01	0.0000e+00	2.0033e-03	0.0000e+00	1.0967e+38
	B	9.5862e-01	0.0000e+00	1.0987e-03	0.0000e+00	1.0470e+38
	C	9.8794e-01	0.0000e+00	6.4301e-05	0.0000e+00	9.8568e+37

Table 6.12: Branch currents in amperes at each harmonic order for the 4 node test feeder with harmonic sources, obtained with the method 1.

Branch No	Phase	Harmonic Order				
		1	2	3	4	5
1	A	8.9970e+01	0.0000e+00	1.7457e+00	0.0000e+00	2.0242e+39
	B	1.3012e+02	0.0000e+00	1.3233e+00	0.0000e+00	1.7348e+39
	C	9.9463e+01	0.0000e+00	3.7298e-01	0.0000e+00	1.7410e+39
2	A	8.9970e+01	0.0000e+00	1.7457e+00	0.0000e+00	2.0242e+39
	B	1.3012e+02	0.0000e+00	1.3233e+00	0.0000e+00	1.7348e+39
	C	9.9463e+01	0.0000e+00	3.7298e-01	0.0000e+00	1.7410e+39
3	A	2.6969e+02	0.0000e+00	5.2328e+00	0.0000e+00	6.0677e+39
	B	3.9006e+02	0.0000e+00	3.9667e+00	0.0000e+00	5.2002e+39
	C	2.9815e+02	0.0000e+00	1.1180e+00	0.0000e+00	5.2190e+39
4	A	2.6969e+02	0.0000e+00	5.2328e+00	0.0000e+00	6.0677e+39
	B	3.9006e+02	0.0000e+00	3.9667e+00	0.0000e+00	5.2002e+39
	C	2.9815e+02	0.0000e+00	1.1180e+00	0.0000e+00	5.2190e+39

Table 6.13: Active power losses for the 4 node test feeder with harmonic sources, obtained with the method 1.

Branch No	IEEE Branch Name	Phase A (kW)	Phase B (kW)	Phase C (kW)
1	0 - 1	0.0000	0.0000	0.0000
2	1 - 2	1.3532	2.7102	0.2186
3	2 - 3	5.6703	11.5432	3.1411
4	3 - 4	1.6915	3.3877	0.2733

6.4.3 Harmonic Analysis Method 2

The analysis was made for frequencies from the fundamental to the 7th harmonic. Most important results obtained applying the set of .m files to the 4 node test feeder are shown in the tables below. They were calculated for a tolerance of 10^{-5} for the maximum difference between bus voltages of two consecutive iterations and 30 maximum of iterations allowed for each harmonic order. More specific results are shown in appendix B.2.2, including bus voltages and branch currents at each iteration for each harmonic, loads currents, shunt capacitors currents and losses at each harmonic order for the first 5 harmonics calculated.

From Table 6.15 can be seen that the process is diverging for the 5th harmonic. Since the test network is the same used for the implementation of method 1, it was reasonable to expected the same diverging behavior for harmonic order higher than the 5th.

Table 6.14: Active power losses for the 4 node test feeder with harmonic sources, obtained with the method 2.

1	0 - 1	0.0000	0.0000	0.0000
2	1 - 2	1.3532	2.7102	0.2186
3	2 - 3	5.6703	11.5432	3.1411
4	3 - 4	1.6915	3.3877	0.2733

Table 6.15: Bus voltages in p.u. at each harmonic order for the 4 node test feeder with harmonic sources, obtained with the method 2.

Bus No	Phase	Harmonic Order				
		1	2	3	4	5
1	A	1.0000e+00	0.0000e+00	0.0000e+00	0.0000e+00	0.0000e+00
	B	1.0000e+00	0.0000e+00	0.0000e+00	0.0000e+00	0.0000e+00
	C	1.0000e+00	0.0000e+00	0.0000e+00	0.0000e+00	0.0000e+00
2	A	9.9754e-01	0.0000e+00	4.1026e-04	0.0000e+00	4.0213e+22
	B	9.9504e-01	0.0000e+00	2.2608e-04	0.0000e+00	4.6441e+22
	C	9.9890e-01	0.0000e+00	1.2040e-05	0.0000e+00	3.9402e+22
3	A	9.8155e-01	0.0000e+00	1.4934e-03	0.0000e+00	1.4637e+23
	B	9.6469e-01	0.0000e+00	8.2292e-04	0.0000e+00	1.6905e+23
	C	9.8911e-01	0.0000e+00	4.3826e-05	0.0000e+00	1.4342e+23
4	A	9.7849e-01	0.0000e+00	2.0062e-03	0.0000e+00	1.9664e+23
	B	9.5862e-01	0.0000e+00	1.1055e-03	0.0000e+00	2.2710e+23
	C	9.8794e-01	0.0000e+00	5.8876e-05	0.0000e+00	1.9268e+23

6.4.4 Fundamental Power Flow for a Weakly Meshed Single Phase Network

The bus voltages and branch currents obtained after applying the set of .m files to a weakly meshed single phase network without harmonic sources are shown in Tables 6.18 and 6.17, respectively. Table 6.18 also shows the comparison between the results obtained applying the developed set of .m files and those obtained with PowerWorld

Table 6.16: Branch currents in amperes at each harmonic order for the 4 node test feeder with harmonic sources, obtained with the method 2.

Branch No	Phase	Harmonic Order				
		1	2	3	4	5
1	A	8.9970e+01	0.0000e+00	1.7464e+00	0.0000e+00	2.8853e+24
	B	1.3012e+02	0.0000e+00	1.3253e+00	0.0000e+00	4.6585e+24
	C	9.9463e+01	0.0000e+00	3.7098e-01	0.0000e+00	3.3030e+24
2	A	8.9970e+01	0.0000e+00	1.7464e+00	0.0000e+00	2.8853e+24
	B	1.3012e+02	0.0000e+00	1.3253e+00	0.0000e+00	4.6585e+24
	C	9.9463e+01	0.0000e+00	3.7098e-01	0.0000e+00	3.3030e+24
3	A	2.6969e+02	0.0000e+00	5.2350e+00	0.0000e+00	8.6491e+24
	B	3.9006e+02	0.0000e+00	3.9726e+00	0.0000e+00	1.3964e+25
	C	2.9815e+02	0.0000e+00	1.1120e+00	0.0000e+00	9.9010e+24
4	A	2.6969e+02	0.0000e+00	5.2350e+00	0.0000e+00	8.6491e+24
	B	3.9006e+02	0.0000e+00	3.9726e+00	0.0000e+00	1.3964e+25
	C	2.9815e+02	0.0000e+00	1.1120e+00	0.0000e+00	9.9010e+24

Simulator. Voltages levels and current flows at each iteration can be seen in appendix B.3.

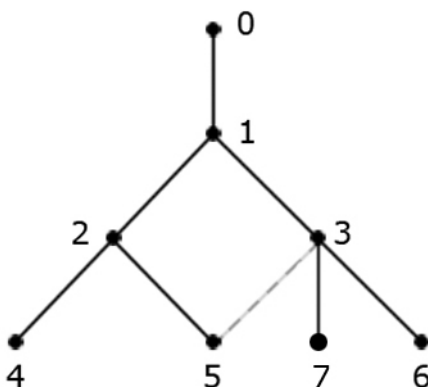


Figure 6.11: One line diagram of the single phase test system after the cut of the breakpoint.

In Table 6.18 node 7 is a virtual node, due to the breakpoint at node 5. Physically, these two nodes are the same.

It can be seen that the approach used for weakly meshed networks gives accurate

Table 6.17: Branch currents obtained with the application of BFS to a weakly meshed single phase network without harmonic sources.

Branch No	Branch Current	
	A	Degree
1	609.5747	-17.3006
2	495.5040	-16.9724
3	114.1304	-18.7497
4	273.8553	-13.9169
5	119.4288	-23.3517
6	59.2722	-23.4624
7	55.2889	-13.7607

Table 6.18: Bus voltages obtained with the application of BFS to a weakly meshed single phase network without harmonic sources and comparison with the PowerWorld's solution.

Bus No	Bus Voltage				Error (%)
	.m files		Power World		
	p.u.	Degree	p.u.	Degree	
1	1.0000	0.00	1.0000	0.00	0.00
2	0.9720	-0.11	0.9871	-0.07	1.53
3	0.9741	-0.06	0.9924	-0.03	1.84
4	0.9566	-0.10	0.9778	-0.14	2.17
5	0.9679	-0.10	0.9868	-0.06	1.91
6	0.9721	-0.05	0.9905	-0.06	1.85
7	0.9679	-0.10	0.9868	-0.06	1.91

results, extending the application range of the backward/forward sweep methods.

6.5 Comparison of the Methods

From Tables 6.11 and 6.15 can be seen that the results obtained with both of the methods are very similar, with a maximum variation of 8.4% for the voltages at phase C. All the other voltages have a difference of less than 1%.

The methods show the same convergence problem, described in section 3.1.1. Both

are diverging for harmonics higher than the 4th order, because the convergence sufficient condition $Z_{line} * Y_{load} < 1$ is not satisfied.

To compare the time consumed of each method, the harmonic order limit was set to the last one in which the convergence of the method is guaranteed, that is the 4th harmonic. Method 1 required 0.527 s and method 2 employed 0.467 s.

Another advantage that has method 2 against method 1, it is the fact that is much simpler to include the shunt parameters of the line into the calculation of the harmonic cases. Method 2 would require that each of the lines capacitors would be added as a load into the I_h vector, magnifying its dimensions as well as the dimension of all the other matrices (A_j , HA and all their derivatives).

Considering the results just mentioned, it can be concluded that method 2, which is more complicated to implement into a program and understand, has no advantages against the simpler method 1.

Chapter 7

Conclusions and Recommendations

The three sets of .m files developed as the main objective of this project reaffirm the accuracy of the choice of Matlab[®] as a straightforward environment to program versatile tools that have to deal with a lot of complex matrices and changing entrances, in this case the models of components which are constantly improving or the new components that have to be included in the analysis.

In all three cases, fundamental analysis for unbalanced radial networks, harmonic analysis for unbalanced radial networks, and harmonic analysis for unbalanced weakly meshed networks, the backward/forward sweep based method gave accurate results with a optimal level of effectiveness and simplicity, the two main characteristic of this method. On the other hand, it was also confirmed the main reason that is leaving aside this kind of method of the major part of the researches on the field. This is the fact that the convergence range of the method depends on the frequency response of this one. It was shown with a very simple example that the backward/forward sweep based method will diverge for frequencies higher than the first resonance point.

This last result challenges the affirmation made by Teng and Chang in [45], where the authors say that the reason why the backward forward sweep technique is not being applied to harmonic studies is the fact that the harmonic currents absorbed by the shunt capacitors installed in distribution feeders are unknown, then the proposed method in [45] is needed to calculate these currents. With the application of method 2 it was proved that the shunt capacitors currents can be calculated as any other load modeled with constant impedance, without the need to define, program and implement the complicated matrix defined in reference [45] because it does not bring any improvement to the convergence range of the BFS method. In fact, method 2 results to be less time consuming than method 1 (the one proposed by Teng and Chang), which can be advantageous when dealing with networks involving a high number of nodes, as in the case

of distribution networks.

The other problem that have the methods specifically designed to radial structured networks is that they cannot be applied directly to weakly meshed networks. Nevertheless, if the network is first transformed into an equivalent radial network and then the method based on the compensation currents procedure, the BFS-based methods can be perfectly applied. This is a very important result because even if the application of the weakly meshed network treatment includes one more iterative process, it is still simpler than other iterative methods including the very time-consuming calculation and decomposition of the Jacobian matrix.

The main difficulty in meeting the aim of this project was the almost inexistent detailed data of the test systems, fact that does not allow to compare properly the results obtained with some values already verified. In the case of the analysis for fundamental frequency, there are a lots of well known and designed test system that allows a person or a team conducting a research or developing a program, to compare the results and make the correct conclusions about the results. In this project was used the IEEE 13 Node Test Feeder [22] for the fundamental load flow test, which have a very specified input data and results, allowing to find faster and easier the errors made with the first attempts to program the BFS method. Like the IEEE 13 Node Test Feeder there are other test feeders with different characteristics, giving the possibility of choose the more convenient according to the research conducted. Instead, a test feeder with harmonic loads was not found. The only system which contains some input data was reference [23], but even this one does not have very specified the input data, i.e. the loads connection is not specified, and the results given are just the total harmonic distortion levels at each node, which is an index that does not allow to find fast and easily the errors of the program code or components modeling.

An alternative to the need of developing a well documented test feeder to perform harmonic analysis could be to compare the results obtained with the developed tool to those ones obtained with a commercial and already tested program. The problem whit this solution is the fact that usually this programs need a very expensive license and if they have a free demo or trial version, it is often limited in the number of phases or number of nodes. Which verifies the utility of this project of providing a trustable tool to performance harmonic analysis for unbalanced radial or weakly meshed networks.

From the results obtained, it is possible to conclude that given the advantages of the BFS-based methods, it is worth continuing tusing it in the limits of application showing in this work.

Appendix A

Test System

A.1 For Harmonic Analysis

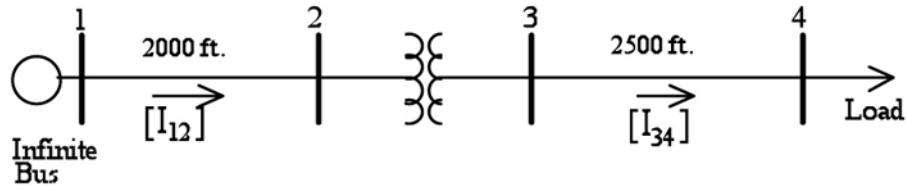


Figure A.1: IEEE 4 node test feeder.

Table A.1: Load specification for harmonic analysis test system.

Phase	Node	Model	Connection	P (kW)	Q (kvar)	Motive (%)	Passive (%)	Fluorescent (%)	ASD (%)	Other (%)
A	4	PQ	Y	600	300	0	90	10	0	0
		PQ	Y	800	500	0	95	5	0	0
		PQ	Y	700	200	0	90	0	0	10

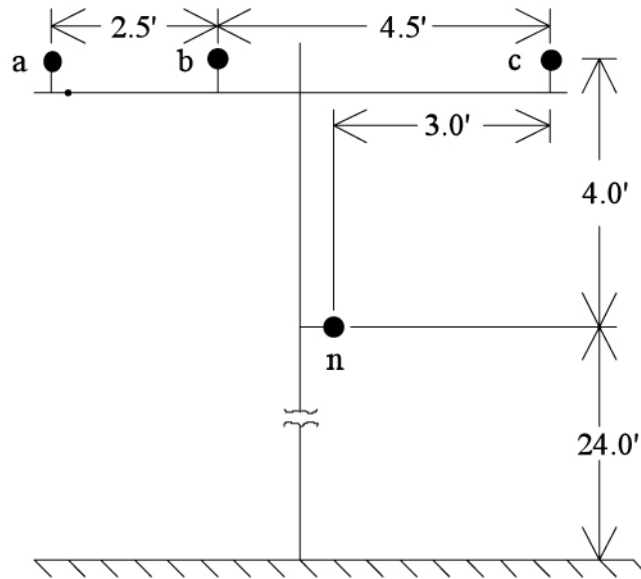


Figure A.2: Pole Configuration.

Table A.2: Shunt capacitors bank specification for harmonic analysis test system.

Node	Connection	Phase A (kvar)	Phase B (kvar)	Phase C (kvar)
4	Y	100	100	100

Table A.3: Transformer data for harmonic analysis test system.

Connection	kva	V_H (kV)	V_L (kV)	R (%)	X (%)
Ground Y- Ground Y	6 000	12.47	4.16	1.0	6.0

Table A.4: Lines specification for harmonic analysis test system.

Conductor	Geometric Mean Radius (ft.)	Resistance Ω /mile	Diameter inch
Phase	0.0244	0.306	0.721
Neutral	0.00814	0.592	0.563

Table A.5: Harmonic current magnitude as % of fundamental component and phase angles with respect to voltage.

Harmonic Order	ASD		Fluorescent		Non-Specific	
	Mag. (%)	Phase (°)	Mag. (%)	Phase (°)	Mag. (%)	Phase (°)
1	1.0000	-1.4500	1.0000	-107.0000	1.0000	105.5000
2	0.0000	0.0000	0.0000	0.0000	0.0000	0.0000
3	0.8460	-8.3400	0.1900	76.0000	0.0360	-44.4000
4	0.0000	0.0000	0.0000	0.0000	0.0000	0.0000
5	0.6830	-14.2300	0.1070	10.0000	0.0320	139.4000
6	0.0000	0.0000	0.0000	0	0.0000	0.0000
7	0.4780	-20.1300	0.0210	37.0000	0.0000	0.0000
8	0.0000	0.0000	0	0	0.0000	0.0000
9	0.2770	-29.0200	0.0140	31.0000	0.0000	0.0000
10	0	0.0000	0.0000	0	0.0000	0.0000
11	0.0020	-27.9100	0.0090	36.0000	0.0000	0.0000
12	0.0000	0	0	0	0.0000	0.0000
13	0.0610	158.2	0.01	47.0000	0.0000	0.0000
14	0	0	0	0	0.0000	0.0000
15	0.0420	122.3000	0.0050	20.0000	0.0000	0.0000

A.2 For Weakly Meshed Networks

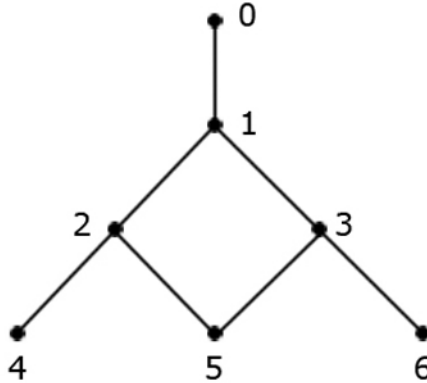


Figure A.3: Weakly Meshed Test System.

Table A.6: Load specification for the single phase weakly meshed test system.

Node	Model	P (kW)	Q (kvar)
2	PQ	230	73
4	PQ	420	15
4	I	200	140
5	PQ	380	140
6	PQ	127	55

Table A.7: Lines impedance data for the single phase weakly meshed test system.

Line	Nodes	Length (ft.)	z (Ω /mile)
1	0-1	100	0.00
2	1-2	500	1.3425+0.5124i
3	1-3	2000	1.3425+0.5124i
4	2-4	500	1.3425+0.5124i
5	2-5	300	1.3425+0.5124i
6	3-6	300	1.3425+0.5124i
7	3-5	1000	1.3425+0.5124i

Appendix B

Power Flow Results

B.1 Fundamental Power Flow Results

SHUNT CAPACITORS CURRENTS AT ITERATION # 8

Bus No	Bus Name IEEE	Phase A		Phase B		Phase C	
		pu	Degree	pu	Degree	pu	Degree
12	675	0.1919	83.4931	0.2051	-30.9181	0.1800	-155.4383
10	611	0.0000	0.0000	0.0000	0.0000	0.0898	-155.8143

LINEAR LOADS CURRENTS AT ITERATION # 8

Bus No	Bus Name IEEE	Phase A		Phase B		Phase C	
		pu	Degree	pu	Degree	pu	Degree
9	634	0.0462	-22.6835	0.0000	0.0000	0.0000	0.0000
2	645	0.0000	0.0000	0.1785	-138.0881	0.0000	0.0000
5	646	0.0000	0.0000	0.0000	0.0000	0.2576	98.9887
11	652	0.1455	-29.8336	0.0000	0.0000	0.0000	0.0000
3	671	0.4230	-26.4093	0.3996	-140.9036	0.4531	94.3554
12	675	0.5435	-27.7638	0.0890	-162.5136	0.3996	78.3015
8	692	0.0000	0.0000	0.0000	0.0000	0.1974	97.7585
10	611	0.0000	0.0000	0.0000	0.0000	0.1958	99.3592

BRANCH CURRENTS AT ITERATION # 8

Branch No	Branch IEEE	Phase A		Phase B		Phase C	
		A	Degree	A	Degree	A	Degree
1	0 - 632	459.7944	-17.9710	255.7270	-124.9499	585.5923	102.2241
2	632 - 645	0.0000	0.0000	74.3338	-138.0872	107.2399	98.9893
3	632 - 671	440.6151	-17.7664	184.1142	-119.6876	478.5639	102.9477
4	632 - 633	19.2497	-22.6812	0.0007	-34.4379	0.0007	-145.1013
5	645 - 646	0.0000	0.0000	0.0004	-22.6636	107.2400	98.9889
6	671 - 684	60.5561	-29.8063	0.0000	0.0000	80.5209	126.0376
7	671 - 680	0.0017	90.4491	0.0017	-40.1361	0.0014	-151.5404
8	671 - 692	210.9168	-7.0850	66.8275	-55.4039	218.0054	102.0536
9	633 - 634	166.8330	-22.6835	0.0000	0.0000	0.0000	0.0000
10	684 - 611	0.0000	0.0000	0.0000	0.0000	80.5208	126.0371
11	684 - 652	60.5625	-29.8202	0.0000	0.0000	0.0000	0.0000
12	692 - 675	210.9170	-7.0879	66.8173	-55.4079	136.1889	104.6400

BUS VOLTAGES AT ITERATION # 8

Bus No	Bus Name IEEE	Phase A		Phase B		Phase C	
		pu	Degree	pu	Degree	pu	Degree
1	632	0.9830	-3.0141	1.0074	-120.4868	0.9467	116.9770
2	645	NaN	NaN	1.0019	-120.5172	0.9411	116.7355
3	671	0.9663	-6.2388	1.0228	-120.7330	0.9022	114.5258
4	633	0.9822	-3.0521	1.0077	-120.4910	0.9466	116.9992
5	646	NaN	NaN	1.0016	-120.4467	0.9369	116.5976
6	684	0.9647	-6.2820	NaN	NaN	0.9001	114.3786
7	680	0.9663	-6.2388	1.0228	-120.7330	0.9022	114.5258
8	692	0.9663	-6.2388	1.0228	-120.7330	0.9022	114.5258
9	634	0.9775	-3.2983	1.0077	-120.4910	0.9466	116.9992
10	611	NaN	NaN	NaN	NaN	0.8982	114.1856

11	652	0.9592	-6.2668	NaN	NaN	NaN	NaN
12	675	0.9595	-6.5069	1.0253	-120.9181	0.8998	114.5616

BRANCH LOSSES

Branch No	Branch IEEE	Phase A		Phase B		Phase C	
		kW	Degree	kW	Degree	kW	Degree
1	0 - 632	1.6442	-----	-4.9457	-----	51.6501	-----
2	632 - 645	0.0000	-----	0.9017	-----	1.0660	-----
3	632 - 671	4.0414	-----	-6.8086	-----	39.7892	-----
4	632 - 633	0.0264	-----	0.0000	-----	-0.0000	-----
5	645 - 646	0.0000	-----	-0.0000	-----	0.8650	-----
6	671 - 684	0.1715	-----	0.0000	-----	0.4896	-----
7	671 - 680	0.0000	-----	0.0000	-----	0.0000	-----
8	671 - 692	0.0000	-----	0.0000	-----	-0.0000	-----
9	633 - 634	0.1411	-----	0.0000	-----	0.0000	-----
10	684 - 611	0.0000	-----	0.0000	-----	0.4897	-----
11	684 - 652	0.7461	-----	0.0000	-----	0.0000	-----
12	692 - 675	3.4278	-----	0.3160	-----	0.8300	-----

No of ITERATIONS MADE	7
-----------------------	---

APARENT POWER DELIVERED TO PHASE A BY THE FEEDER (kVA)	1104.3237
APARENT POWER DELIVERED TO PHASE B BY THE FEEDER (kVA)	614.1992
APARENT POWER DELIVERED TO PHASE C BY THE FEEDER (kVA)	1406.4622
TOTAL APARENT POWER DELIVERED BY THE FEEDER (kVA)	3112.4789

ACTIVE POWER DELIVERED TO PHASE A BY THE FEEDER (kW)	1050.4468
ACTIVE POWER DELIVERED TO PHASE B BY THE FEEDER (kW)	611.9085
ACTIVE POWER DELIVERED TO PHASE C BY THE FEEDER (kW)	1339.3144
TOTAL ACTIVE POWER DELIVERED BY THE FEEDER (kW)	3001.6698

REACTIVE POWER DELIVERED TO PHASE A BY THE FEEDER (kVAr)	340.7231
REACTIVE POWER DELIVERED TO PHASE B BY THE FEEDER (kVAr)	52.9964
REACTIVE POWER DELIVERED TO PHASE C BY THE FEEDER (kVAr)	429.3865
TOTAL REACTIVE POWER DELIVERED BY THE FEEDER (kVAr)	823.1060

APARENT POWER LOSSES IN PHASE A (kVA)	124.6073
APARENT POWER LOSSES IN PHASE B (kVA)	13.1440
APARENT POWER LOSSES IN PHASE C (kVA)	176.8718
TOTAL APARENT POWER LOSSES IN THE SYSTEM (kVA)	296.6929

ACTIVE POWER LOSSES IN PHASE A (kW)	10.1985
ACTIVE POWER LOSSES IN PHASE B (kW)	-10.5366
ACTIVE POWER LOSSES IN PHASE C (kW)	95.1795
TOTAL ACTIVE POWER LOSSES IN THE SYSTEM (kW)	94.8415

REACTIVE POWER LOSSES IN PHASE A (kVAr)	124.1893
---	----------










REACTIVE POWER LOSSES IN PHASE B (kVAr)	7.8578
REACTIVE POWER LOSSES IN PHASE C (kVAr)	149.0788
TOTAL REACTIVE LOSSES IN THE SYSTEM (kVAr)	281.1259

POWER FACTOR FOR PHASE A	0.9512
POWER FACTOR FOR PHASE B	0.9963
POWER FACTOR FOR PHASE C	0.9523
TOTAL POWER FACTOR	0.9644

>>

Profile Summary

Generated 23-Sep-2010 13:44:02 using cpu time.

Function Name	Calls	Total Time	Self Time*	Total Time Plot (dark band = self time)
fundamental	1	0.479 s	0.171 s	
results	6	0.205 s	0.164 s	
lineC	6	0.055 s	0.055 s	
angle	958	0.041 s	0.041 s	
cell2mat	25	0.021 s	0.021 s	
inputs	1	0.007 s	0.007 s	
distributedLOAD	1	0.007 s	0.007 s	
genZ	1	0.007 s	0.007 s	
genA	1	0.007 s	0.007 s	
configurations	1	0 s	0.000 s	

Self time is the time spent in a function excluding the time spent in its child functions. Self time also includes overhead resulting from the process of profiling.

B.2 Harmonic Power Flow Results

B.2.1 Method 1

SHUNT CAPACITORS CURRENTS AT HARMONIC ORDER # 1

Bus No	Bus Name IEEE	Phase A		Phase B		Phase C	
		pu	Degree	pu	Degree	pu	Degree
4	4	9.7849e-02	88.8086	9.5864e-02	-32.1917	9.8794e-02	-152.3799

LOADS CURRENTS AT HARMONIC ORDER # 1

Bus No	Bus Name IEEE	Phase A		Phase B		Phase C	
		pu	Degree	pu	Degree	pu	Degree
4	4	6.8557e-01	-27.7565	9.8410e-01	-154.1971	7.3690e-01	

101.6747

BUS VOLTAGES AT HARMONIC ORDER # 1

Bus No	Bus Name IEEE	Phase A		Phase B		Phase C	
		pu	Degree	pu	Degree	pu	Degree

1 120.0000 1 1.0000e+00 0.0000 1.0000e+00 -120.0000 1.0000e+00

2 119.7586 2 9.9754e-01 -0.0375 9.9504e-01 -120.1698 9.9890e-01

3 117.9278 3 9.8155e-01 -1.1400 9.6469e-01 -121.9589 9.8911e-01

4 117.6199 4 9.7849e-01 -1.1913 9.5862e-01 -122.1918 9.8794e-01

BRANCH CURRENTS AT HARMONIC ORDER # 1

Branch No	Branch IEEE	Phase A		Phase B		Phase C	
		A	Degree	A	Degree	A	Degree
1	0 - 1	269.6945	-19.9913	390.0566	-149.2191	298.1491	109.2977
2	1 - 2	89.9703	-19.9913	130.1231	-149.2191	99.4627	109.2977
3	2 - 3	269.6945	-19.9913	390.0566	-149.2191	298.1491	109.2977
4	3 - 4	269.6945	-19.9913	390.0566	-149.2191	298.1491	109.2977

BRANCH LOSSES AT HARMONIC ORDER # 1

Branch No	Branch IEEE	Phase A		Phase B		Phase C	
		kW	Degree	kW	Degree	kW	Degree
1	0 - 1	0.0000	-----	0.0000	-----	0.0000	-----
2	1 - 2	1.3532	-----	2.7102	-----	0.2186	-----
3	2 - 3	5.6703	-----	11.5432	-----	3.1411	-----
4	3 - 4	1.6915	-----	3.3877	-----	0.2733	-----

HARMONIC ORDER # 1

No of ITERATIONS MADE | 4 |

ACTIVE POWER LOSSES IN PHASE A (kW)	8.7150
ACTIVE POWER LOSSES IN PHASE B (kW)	17.6411
ACTIVE POWER LOSSES IN PHASE C (kW)	3.6330
TOTAL ACTIVE POWER LOSSES IN THE SYSTEM (kW)	29.9890

Harmonic Order # 2
 Convergence criterium: $Z1*Ys < 1$?

ZY =
 0.049874120370321 0.031514435853938 0.019738106147352
 0.022042583410433 0.069578149101420 0.021528565775664
 0.017268691035559 0.026926848126409 0.056405118399338

Convergence criterium reached. Method should convergence for armonic 2 will be possible

BRANCH CURRENTS AT HARMONIC ORDER # 2 (Iteration # 1)

Branch No	Branch IEEE	Phase A		Phase B		Phase C	
		A	Degree	A	Degree	A	Degree
1	0 - 1	0.0000	0.0000	0.0000	0.0000	0.0000	0.0000
2	1 - 2	0.0000	0.0000	0.0000	0.0000	0.0000	0.0000
3	2 - 3	0.0000	0.0000	0.0000	0.0000	0.0000	0.0000
4	3 - 4	0.0000	0.0000	0.0000	0.0000	0.0000	0.0000

BUS VOLTAGES AT ORDER # 2 (Iteration # 1)

Bus No	Bus Name IEEE	Phase A		Phase B		Phase C	
		V	Degree	V	Degree	V	Degree
1 0.0000	1	0.0000e+00	0.0000	0.0000e+00	0.0000	0.0000e+00	0.0000
2 0.0000	2	0.0000e+00	0.0000	0.0000e+00	0.0000	0.0000e+00	0.0000
3 0.0000	3	0.0000e+00	0.0000	0.0000e+00	0.0000	0.0000e+00	0.0000
4 0.0000	4	0.0000e+00	0.0000	0.0000e+00	0.0000	0.0000e+00	0.0000

SHUNT CAPACITORS CURRENTS AT HARMONIC ORDER # 2

Bus No	Bus Name IEEE	Phase A		Phase B		Phase C	
		pu	Degree	pu	Degree	pu	Degree
4	4	0.0000e+00	0.0000	0.0000e+00	0.0000	0.0000e+00	0.0000

LOADS CURRENTS AT HARMONIC ORDER # 2

Bus No	Bus Name IEEE	Phase A		Phase B		Phase C	
		pu	Degree	pu	Degree	pu	Degree
4 0.0000	4	0.0000e+00	0.0000	0.0000e+00	0.0000	0.0000e+00	0.0000

BUS VOLTAGES AT HARMONIC ORDER # 2

Bus No	Bus Name IEEE	Phase A		Phase B		Phase C	
		pu	Degree	pu	Degree	pu	Degree
1 0.0000	1	0.0000e+00	0.0000	0.0000e+00	0.0000	0.0000e+00	0.0000
2 0.0000	2	0.0000e+00	0.0000	0.0000e+00	0.0000	0.0000e+00	0.0000
3 0.0000	3	0.0000e+00	0.0000	0.0000e+00	0.0000	0.0000e+00	0.0000
4 0.0000	4	0.0000e+00	0.0000	0.0000e+00	0.0000	0.0000e+00	0.0000

BRANCH CURRENTS AT HARMONIC ORDER # 2

Branch No	Branch IEEE	Phase A		Phase B		Phase C	
		A	Degree	A	Degree	A	Degree
1	0 - 1	0.0000	0.0000	0.0000	0.0000	0.0000	0.0000
2	1 - 2	0.0000	0.0000	0.0000	0.0000	0.0000	0.0000
3	2 - 3	0.0000	0.0000	0.0000	0.0000	0.0000	0.0000
4	3 - 4	0.0000	0.0000	0.0000	0.0000	0.0000	0.0000

BRANCH LOSSES AT HARMONIC ORDER # 2

Branch No	Branch IEEE	Phase A		Phase B		Phase C	
		kW	Degree	kW	Degree	kW	Degree
1	0 - 1	0.0000	-----	0.0000	-----	0.0000	-----
2	1 - 2	0.0000	-----	0.0000	-----	0.0000	-----
3	2 - 3	0.0000	-----	0.0000	-----	0.0000	-----
4	3 - 4	0.0000	-----	0.0000	-----	0.0000	-----

HARMONIC ORDER # 2

No of ITERATIONS MADE | 1 |

ACTIVE POWER LOSSES IN PHASE A (kW)	0.0000
ACTIVE POWER LOSSES IN PHASE B (kW)	0.0000
ACTIVE POWER LOSSES IN PHASE C (kW)	0.0000
TOTAL ACTIVE POWER LOSSES IN THE SYSTEM (kW)	0.0000

Harmonic Order # 3
 Convergence criterium: Zl*Ys < 1 ?

ZY =
 0.150788339978876 0.095763974340612 0.059683473613435
 0.067582351620598 0.207092352740909 0.065525808593978
 0.051650932729401 0.080340917642355 0.171920200081123

Convergence crterium reached. Method should convergence for armonic 3 will be posible

BRANCH CURRENTS AT HARMONIC ORDER # 3 (Iteration # 1)

Branch No	Branch IEEE	Phase A		Phase B		Phase C	
		A	Degree	A	Degree	A	Degree
1	0 - 1	1.8567	-74.3769	1.3269	140.4166	0.3681	45.7021
2	1 - 2	1.8567	-74.3769	1.3269	140.4166	0.3681	45.7021
3	2 - 3	5.5656	-74.3769	3.9776	140.4166	1.1033	45.7021
4	3 - 4	5.5656	-74.3769	3.9776	140.4166	1.1033	45.7021

BUS VOLTAGES AT ORDER # 3 (Iteration # 1)

Bus No	Bus Name IEEE	Phase A		Phase B		Phase C	
		V	Degree	V	Degree	V	Degree
1 0.0000	1	0.0000e+00	0.0000	0.0000e+00	0.0000	0.0000e+00	
2 -168.0856	2	4.4995e-04	174.1237	2.2726e-04	68.1220	1.0999e-05	
3 -168.0856	3	1.6378e-03	174.1237	8.2723e-04	68.1220	4.0035e-05	
4 -168.0856	4	2.2003e-03	174.1237	1.1113e-03	68.1220	5.3783e-05	

BRANCH CURRENTS AT HARMONIC ORDER # 3 (Iteration # 2)

Branch No	Branch IEEE	Phase A		Phase B		Phase C	
		A	Degree	A	Degree	A	Degree
1	0 - 1	1.7581	-80.0667	1.3515	134.2220	0.3646	46.5233
2	1 - 2	1.7581	-80.0667	1.3515	134.2220	0.3646	46.5233
3	2 - 3	5.2700	-80.0667	4.0512	134.2220	1.0928	46.5233
4	3 - 4	5.2700	-80.0667	4.0512	134.2220	1.0928	46.5233

BUS VOLTAGES AT ORDER # 3 (Iteration # 2)

Bus No	Bus Name IEEE	Phase A		Phase B		Phase C	
		V	Degree	V	Degree	V	Degree
1 0.0000	1	0.0000e+00	0.0000	0.0000e+00	0.0000	0.0000e+00	
2 22.1465	2	4.0984e-04	166.9954	2.4452e-04	56.9461	1.6316e-05	
3 22.1465	3	1.4918e-03	166.9954	8.9005e-04	56.9461	5.9388e-05	
4 22.1465	4	2.0041e-03	166.9954	1.1957e-03	56.9461	7.9783e-05	

BRANCH CURRENTS AT HARMONIC ORDER # 3 (Iteration # 3)

Branch No	Branch IEEE	Phase A		Phase B		Phase C	
		A	Degree	A	Degree	A	Degree
1	0 - 1	1.7461	-79.1411	1.3230	133.5865	0.3768	45.2355

2	1 - 2	1.7461	-79.1411	1.3230	133.5865	0.3768	45.2355
3	2 - 3	5.2341	-79.1411	3.9659	133.5865	1.1295	45.2355
4	3 - 4	5.2341	-79.1411	3.9659	133.5865	1.1295	45.2355

BUS VOLTAGES AT ORDER # 3 (Iteration # 3)

Bus No	Bus Name IEEE	Phase A V	Phase A Degree	Phase B V	Phase B Degree	Phase C V	Phase C Degree
1 0.0000	1	0.0000e+00	0.0000	0.0000e+00	0.0000	0.0000e+00	
2 -21.8562	2	4.0542e-04	169.0987	2.2976e-04	55.6565	1.5035e-05	
3 -21.8562	3	1.4757e-03	169.0987	8.3631e-04	55.6565	5.4728e-05	
4 -21.8562	4	1.9825e-03	169.0987	1.1235e-03	55.6565	7.3522e-05	

SHUNT CAPACITORS CURRENTS AT HARMONIC ORDER # 3

Bus No	Bus Name IEEE	Phase A pu	Phase A Degree	Phase B pu	Phase B Degree	Phase C pu	Phase C Degree
4	4	1.9825e-04	-100.9013	1.1235e-04	145.6565	7.3522e-06	68.1438

LOADS CURRENTS AT HARMONIC ORDER # 3

Bus No	Bus Name IEEE	Phase A pu	Phase A Degree	Phase B pu	Phase B Degree	Phase C pu	Phase C Degree
4 45.1749	4	1.2387e-02	-78.8012	9.4153e-03	133.4435	2.7059e-03	

BUS VOLTAGES AT HARMONIC ORDER # 3

Bus No	Bus Name IEEE	Phase A pu	Phase A Degree	Phase B pu	Phase B Degree	Phase C pu	Phase C Degree
1 0.0000	1	0.0000e+00	0.0000	0.0000e+00	0.0000	0.0000e+00	
2 -21.8562	2	4.0542e-04	169.0987	2.2976e-04	55.6565	1.5035e-05	
3 -21.8562	3	1.4757e-03	169.0987	8.3631e-04	55.6565	5.4728e-05	
4 -21.8562	4	1.9825e-03	169.0987	1.1235e-03	55.6565	7.3522e-05	

BRANCH CURRENTS AT HARMONIC ORDER # 3

Branch No	Branch IEEE	Phase A		Phase B		Phase C	
		A	Degree	A	Degree	A	Degree
1	0 - 1	5.2341	-79.1411	3.9659	133.5865	1.1295	45.2355
2	1 - 2	1.7461	-79.1411	1.3230	133.5865	0.3768	45.2355
3	2 - 3	5.2341	-79.1411	3.9659	133.5865	1.1295	45.2355
4	3 - 4	5.2341	-79.1411	3.9659	133.5865	1.1295	45.2355

BRANCH LOSSES AT HARMONIC ORDER # 3

Branch No	Branch IEEE	Phase A		Phase B		Phase C	
		kW	Degree	kW	Degree	kW	Degree
1	0 - 1	0.0000	-----	-0.0000	-----	0.0000	-----
2	1 - 2	0.0019	-----	-0.0005	-----	-0.0000	-----
3	2 - 3	0.0050	-----	-0.0012	-----	-0.0000	-----
4	3 - 4	0.0024	-----	-0.0006	-----	-0.0000	-----

HARMONIC ORDER # 3

No of ITERATIONS MADE | 3 |

ACTIVE POWER LOSSES IN PHASE A (kW)	0.0092
ACTIVE POWER LOSSES IN PHASE B (kW)	-0.0022
ACTIVE POWER LOSSES IN PHASE C (kW)	-0.0001
TOTAL ACTIVE POWER LOSSES IN THE SYSTEM (kW)	0.0069

Harmonic Order # 4
Convergence criterium: $Z1*Ys < 1$?

ZY =

0.637616830025859	0.404116438251788	0.250356029223367
0.286147999742046	0.871832914120840	0.276402088367958
0.215819432220380	0.336430657496545	0.729515770761282

Convergence criterium reached. Method should convergence for armonic 4 will be possible

BRANCH CURRENTS AT HARMONIC ORDER # 4 (Iteration # 1)

Branch No	Branch IEEE	Phase A		Phase B		Phase C	
		A	Degree	A	Degree	A	Degree
1	0 - 1	0.0000	0.0000	0.0000	0.0000	0.0000	0.0000
2	1 - 2	0.0000	0.0000	0.0000	0.0000	0.0000	0.0000
3	2 - 3	0.0000	0.0000	0.0000	0.0000	0.0000	0.0000
4	3 - 4	0.0000	0.0000	0.0000	0.0000	0.0000	0.0000

BUS VOLTAGES AT ORDER # 4 (Iteration # 1)

Bus No	Bus Name IEEE	Phase A		Phase B		Phase C	
		V	Degree	V	Degree	V	Degree
1 0.0000	1	0.0000e+00	0.0000	0.0000e+00	0.0000	0.0000e+00	
2 0.0000	2	0.0000e+00	0.0000	0.0000e+00	0.0000	0.0000e+00	

3	3	0.0000e+00	0.0000	0.0000e+00	0.0000	0.0000e+00
0.0000						
4	4	0.0000e+00	0.0000	0.0000e+00	0.0000	0.0000e+00
0.0000						

SHUNT CAPACITORS CURRENTS AT HARMONIC ORDER # 4

Bus No	Bus Name IEEE	Phase A		Phase B		Phase C	
		pu	Degree	pu	Degree	pu	Degree
4	4	0.0000e+00	0.0000	0.0000e+00	0.0000	0.0000e+00	0.0000

LOADS CURRENTS AT HARMONIC ORDER # 4

Bus No	Bus Name IEEE	Phase A		Phase B		Phase C	
		pu	Degree	pu	Degree	pu	Degree
4	4	0.0000e+00	0.0000	0.0000e+00	0.0000	0.0000e+00	0.0000

BUS VOLTAGES AT HARMONIC ORDER # 4

Bus No	Bus Name IEEE	Phase A		Phase B		Phase C	
		pu	Degree	pu	Degree	pu	Degree
1	1	0.0000e+00	0.0000	0.0000e+00	0.0000	0.0000e+00	0.0000
0.0000							
2	2	0.0000e+00	0.0000	0.0000e+00	0.0000	0.0000e+00	0.0000
0.0000							
3	3	0.0000e+00	0.0000	0.0000e+00	0.0000	0.0000e+00	0.0000
0.0000							
4	4	0.0000e+00	0.0000	0.0000e+00	0.0000	0.0000e+00	0.0000
0.0000							

BRANCH CURRENTS AT HARMONIC ORDER # 4

Branch No	Branch IEEE	Phase A		Phase B		Phase C	
		A	Degree	A	Degree	A	Degree
1	0 - 1	0.0000	0.0000	0.0000	0.0000	0.0000	0.0000
2	1 - 2	0.0000	0.0000	0.0000	0.0000	0.0000	0.0000
3	2 - 3	0.0000	0.0000	0.0000	0.0000	0.0000	0.0000
4	3 - 4	0.0000	0.0000	0.0000	0.0000	0.0000	0.0000

BRANCH LOSSES AT HARMONIC ORDER # 4

Branch No	Branch IEEE	Phase A		Phase B		Phase C	
		kW	Degree	kW	Degree	kW	Degree
1	0 - 1	0.0000	-----	0.0000	-----	0.0000	-----
2	1 - 2	0.0000	-----	0.0000	-----	0.0000	-----
3	2 - 3	0.0000	-----	0.0000	-----	0.0000	-----

4 3 - 4 0.0000 ----- 0.0000 ----- 0.0000 -----

 HARMONIC ORDER # 4

No of ITERATIONS MADE	1
-----------------------	---

ACTIVE POWER LOSSES IN PHASE A (kW)	0.0000
ACTIVE POWER LOSSES IN PHASE B (kW)	0.0000
ACTIVE POWER LOSSES IN PHASE C (kW)	0.0000
TOTAL ACTIVE POWER LOSSES IN THE SYSTEM (kW)	0.0000

Harmonic Order # 5
 Convergence criterium: Zl*Ys < 1 ?

ZY =

3.414563871589917	2.157647297127712	1.337316128010484
1.530167251047231	4.661842319637738	1.478616300543190
1.150707338285221	1.793612286832283	3.914052552500547

Convergence criterium not reached. Method convergence for armonic 5 will be not guaranteed

BRANCH CURRENTS AT HARMONIC ORDER # 5 (Iteration # 1)

Branch No	Branch IEEE	Phase A		Phase B		Phase C	
		A	Degree	A	Degree	A	Degree
1	0 - 1	0.9284	135.0832	1.2648	-165.1033	2.8950	-172.8862
2	1 - 2	0.9284	135.0832	1.2648	-165.1033	2.8950	-172.8862
3	2 - 3	2.7829	135.0832	3.7915	-165.1033	8.6779	-172.8862
4	3 - 4	2.7829	135.0832	3.7915	-165.1033	8.6779	-172.8862

BUS VOLTAGES AT ORDER # 5 (Iteration # 1)

Bus No	Bus Name IEEE	Phase A		Phase B		Phase C	
		V	Degree	V	Degree	V	Degree
1 0.0000	1	0.0000e+00	0.0000	0.0000e+00	0.0000	0.0000e+00	0.0000e+00
2 93.0388	2	1.4643e-02	78.4156	1.6873e-02	92.1859	2.3257e-02	8.4657e-02
3 93.0388	3	5.3302e-02	78.4156	6.1419e-02	92.1859	8.4657e-02	1.1373e-01
4 93.0388	4	7.1606e-02	78.4156	8.2511e-02	92.1859	1.1373e-01	

 BRANCH CURRENTS AT HARMONIC ORDER # 5 (Iteration # 2)

Branch No	Branch IEEE	Phase A		Phase B		Phase C	
		A	Degree	A	Degree	A	Degree
1	0 - 1	43.0456	-88.9406	35.2188	-92.9074	26.7390	-101.8275
2	1 - 2	43.0456	-88.9406	35.2188	-92.9074	26.7390	-101.8275
3	2 - 3	129.0333	-88.9406	105.5718	-92.9074	80.1527	-101.8275
4	3 - 4	129.0333	-88.9406	105.5718	-92.9074	80.1527	-101.8275

BUS VOLTAGES AT ORDER # 5 (Iteration # 2)

Bus No	Bus Name IEEE	Phase A		Phase B		Phase C	
		V	Degree	V	Degree	V	Degree
1 0.0000	1	0.0000e+00	0.0000	0.0000e+00	0.0000	0.0000e+00	0.0000
2 172.4443	2	4.4729e-01	177.2638	4.1781e-01	175.7187	3.5562e-01	
3 172.4443	3	1.6281e+00	177.2638	1.5208e+00	175.7187	1.2945e+00	
4 172.4443	4	2.1872e+00	177.2638	2.0431e+00	175.7187	1.7390e+00	

BRANCH CURRENTS AT HARMONIC ORDER # 5 (Iteration # 3)

Branch No	Branch IEEE	Phase A		Phase B		Phase C	
		A	Degree	A	Degree	A	Degree
1	0 - 1	848.2718	-6.2685	730.9314	-3.8001	783.3929	-5.3804
2	1 - 2	848.2718	-6.2685	730.9314	-3.8001	783.3929	-5.3804
3	2 - 3	2542.7764	-6.2685	2191.0371	-3.8001	2348.2955	-5.3804
4	3 - 4	2542.7764	-6.2685	2191.0371	-3.8001	2348.2955	-5.3804

BUS VOLTAGES AT ORDER # 5 (Iteration # 3)

Bus No	Bus Name IEEE	Phase A		Phase B		Phase C	
		V	Degree	V	Degree	V	Degree
1 0.0000	1	0.0000e+00	0.0000	0.0000e+00	0.0000	0.0000e+00	0.0000
2 -96.5313	2	9.5232e+00	-96.7574	9.1220e+00	-96.0240	8.8006e+00	
3 -96.5313	3	3.4664e+01	-96.7574	3.3204e+01	-96.0240	3.2034e+01	
4 -96.5313	4	4.6568e+01	-96.7574	4.4606e+01	-96.0240	4.3035e+01	

BRANCH CURRENTS AT HARMONIC ORDER # 5 (Iteration # 4)

Branch No	Branch IEEE	Phase A		Phase B		Phase C	
		A	Degree	A	Degree	A	Degree
1	0 - 1	19629.8391	83.1173	16783.6245	84.5700	16636.5117	81.6806
2	1 - 2	19629.8391	83.1173	16783.6245	84.5700	16636.5117	81.6806
3	2 - 3	58842.3301	83.1173	50310.5282	84.5700	49869.5434	81.6806
4	3 - 4	58842.3301	83.1173	50310.5282	84.5700	49869.5434	81.6806

BUS VOLTAGES AT ORDER # 5 (Iteration # 4)

Bus No	Bus Name IEEE	Phase A		Phase B		Phase C	
		V	Degree	V	Degree	V	Degree
1 0.0000	1	0.0000e+00	0.0000	0.0000e+00	0.0000	0.0000e+00	
2 -8.6771	2	2.1665e+02	-7.9980	2.0657e+02	-7.6151	1.9360e+02	
3 -8.6771	3	7.8861e+02	-7.9980	7.5192e+02	-7.6151	7.0471e+02	
4 -8.6771	4	1.0594e+03	-7.9980	1.0101e+03	-7.6151	9.4672e+02	

BRANCH CURRENTS AT HARMONIC ORDER # 5 (Iteration # 5)

Branch No	Branch IEEE	Phase A		Phase B		Phase C	
		A	Degree	A	Degree	A	Degree
1	0 - 1	438593.1043	171.2787	375439.3969	172.8819	379339.9028	170.2778
2	1 - 2	438593.1043	171.2787	375439.3969	172.8819	379339.9028	170.2778
3	2 - 3	1314725.0025	171.2787	1125415.6921	172.8819	1137107.8335	170.2778
4	3 - 4	1314725.0025	171.2787	1125415.6921	172.8819	1137107.8335	170.2778

BUS VOLTAGES AT ORDER # 5 (Iteration # 5)

Bus No	Bus Name IEEE	Phase A		Phase B		Phase C	
		V	Degree	V	Degree	V	Degree
1 0.0000	1	0.0000e+00	0.0000	0.0000e+00	0.0000	0.0000e+00	
2 79.7561	2	4.8591e+03	80.2663	4.6372e+03	80.7033	4.3766e+03	
3 79.7561	3	1.7687e+04	80.2663	1.6879e+04	80.7033	1.5931e+04	
4 79.7561	4	2.3761e+04	80.2663	2.2676e+04	80.7033	2.1402e+04	

BRANCH CURRENTS AT HARMONIC ORDER # 5 (Iteration # 6)

Branch No	Branch IEEE	Phase A		Phase B		Phase C	
		A	Degree	A	Degree	A	Degree
1 -101.4334	0 - 1	9877325.5601	-100.3530	8453898.3395	-98.7737	8502671.7738	
2	1 - 2	9877325.5601	-100.3530	8453898.3395	-98.7737	8502671.7738	-101.4334
3 -101.4334	2 - 3	29608233.1092	-100.3530	25341373.1476	-98.7737	25487576.2066	
4 -101.4334	3 - 4	29608233.1092	-100.3530	25341373.1476	-98.7737	25487576.2066	

BUS VOLTAGES AT ORDER # 5 (Iteration # 6)

Bus No	Bus Name IEEE	Phase A		Phase B		Phase C	
		V	Degree	V	Degree	V	Degree
1 0.0000	1	0.0000e+00	0.0000	0.0000e+00	0.0000	0.0000e+00	0.0000e+00
2 168.0756	2	1.0934e+05	168.6168	1.0432e+05	169.0451	9.8298e+04	
3 168.0756	3	3.9798e+05	168.6168	3.7974e+05	169.0451	3.5781e+05	
4 168.0756	4	5.3465e+05	168.6168	5.1015e+05	169.0451	4.8068e+05	

BRANCH CURRENTS AT HARMONIC ORDER # 5 (Iteration # 7)

Branch No	Branch IEEE	Phase A		Phase B		Phase C	
		A	Degree	A	Degree	A	Degree
1 -13.0873	0 - 1	222044096.0315	-12.0209	190046645.5221	-10.4377	191351812.2552	
2 -13.0873	1 - 2	222044096.0315	-12.0209	190046645.5221	-10.4377	191351812.2552	
3 -13.0873	2 - 3	665598528.2482	-12.0209	569683093.6685	-10.4377	573595456.4478	
4 -13.0873	3 - 4	665598528.2482	-12.0209	569683093.6685	-10.4377	573595456.4478	

BUS VOLTAGES AT ORDER # 5 (Iteration # 7)

Bus No	Bus Name IEEE	Phase A		Phase B		Phase C	
		V	Degree	V	Degree	V	Degree
1 0.0000	1	0.0000e+00	0.0000	0.0000e+00	0.0000	0.0000e+00	
2 -103.5839	2	2.4584e+06	-103.0481	2.3458e+06	-102.6184	2.2111e+06	
3 -103.5839	3	8.9484e+06	-103.0481	8.5386e+06	-102.6184	8.0485e+06	
4 -103.5839	4	1.2021e+07	-103.0481	1.1471e+07	-102.6184	1.0812e+07	

BRANCH CURRENTS AT HARMONIC ORDER # 5 (Iteration # 8)

Branch No	Branch IEEE	Phase A		Phase B		Phase C	
		A	Degree	A	Degree	A	Degree
1 75.2487	0 - 1	4993620592.3913	76.3174	4274030402.4583	77.8999	4302273377.3951	
2 75.2487	1 - 2	4993620592.3913	76.3174	4274030402.4583	77.8999	4302273377.3951	
3 12896478128.8744	2 - 3	14968857881.5192	76.3174	12811817095.8305	77.8999		
4 12896478128.8744	3 - 4	14968857881.5192	76.3174	12811817095.8305	77.8999		

BUS VOLTAGES AT ORDER # 5 (Iteration # 8)

Bus No	Bus Name IEEE	Phase A		Phase B		Phase C	
		V	Degree	V	Degree	V	Degree
1 0.0000	1	0.0000e+00	0.0000	0.0000e+00	0.0000	0.0000e+00	0.0000e+00
2 -15.2470	2	5.5284e+07	-14.7103	5.2752e+07	-14.2808	4.9720e+07	
3 -15.2470	3	2.0124e+08	-14.7103	1.9202e+08	-14.2808	1.8098e+08	
4 -15.2470	4	2.7034e+08	-14.7103	2.5796e+08	-14.2808	2.4313e+08	

BRANCH CURRENTS AT HARMONIC ORDER # 5 (Iteration # 9)

Branch No	Branch IEEE	Phase A		Phase B		Phase C	
		A	Degree	A	Degree	A	Degree
1 96751968795.8695	0 - 1 163.5863	112292725925.8960	164.6547	96111006124.2533	166.2373		
2 96751968795.8695	1 - 2 163.5863	112292725925.8960	164.6547	96111006124.2533	166.2373		
3 290023329539.5417	2 - 3 163.5863	336608243340.3662	164.6547	288101982300.3458	166.2373		
4 290023329539.5417	3 - 4 163.5863	336608243340.3662	164.6547	288101982300.3458	166.2373		

BUS VOLTAGES AT ORDER # 5 (Iteration # 9)

Bus No	Bus Name IEEE	Phase A		Phase B		Phase C	
		V	Degree	V	Degree	V	Degree
1 0.0000	1	0.0000e+00	0.0000	0.0000e+00	0.0000	0.0000e+00	0.0000e+00
2 73.0905	2	1.2432e+09	73.6271	1.1863e+09	74.0566	1.1181e+09	
3 73.0905	3	4.5253e+09	73.6271	4.3180e+09	74.0566	4.0699e+09	
4 73.0905	4	6.0793e+09	73.6271	5.8008e+09	74.0566	5.4675e+09	

BRANCH CURRENTS AT HARMONIC ORDER # 5 (Iteration # 10)

Branch No	Branch IEEE	Phase A		Phase B		Phase C	
		A	Degree	A	Degree	A	Degree
1 2175700626279.1606	0 - 1 -108.0763	2525206540756.8628	-107.0079	2161317583903.2610	-105.4253		
2 2175700626279.1606	1 - 2 -108.0763	2525206540756.8628	-107.0079	2161317583903.2610	-105.4253		
3 6521871829255.0801	2 - 3 -108.0763	7569549414239.9219	-107.0079	6478757276748.4766	-105.4253		
4 6521871829255.0801	3 - 4 -108.0763	7569549414239.9219	-107.0079	6478757276748.4766	-105.4253		

BUS VOLTAGES AT ORDER # 5 (Iteration # 10)

Bus No	Bus Name IEEE	Phase A		Phase B		Phase C	
		V	Degree	V	Degree	V	Degree
1 0.0000	1	0.0000e+00	0.0000	0.0000e+00	0.0000	0.0000e+00	0.0000
2 161.4279	2	2.7957e+10	161.9645	2.6676e+10	162.3940	2.5143e+10	162.3940
3 161.4279	3	1.0176e+11	161.9645	9.7101e+10	162.3940	9.1522e+10	162.3940
4 161.4279	4	1.3671e+11	161.9645	1.3045e+11	162.3940	1.2295e+11	162.3940

BRANCH CURRENTS AT HARMONIC ORDER # 5 (Iteration # 11)

Branch No	Branch IEEE	Phase A		Phase B		Phase C	
		A	Degree	A	Degree	A	Degree
1 48926447836449.3516	0 - 1	56785843310086.2812	-18.6705	48602847149251.5234	-17.0879		
		-19.7389					
2 48926447836449.3516	1 - 2	56785843310086.2812	-18.6705	48602847149251.5234	-17.0879		
		-19.7389					
3 146661731855895.0312	2 - 3	170221025499225.0000	-18.6705	145691707680568.8750	-17.0879		
		-19.7389					
4 146661731855895.0312	3 - 4	170221025499225.0000	-18.6705	145691707680568.8750	-17.0879		
		-19.7389					

BUS VOLTAGES AT ORDER # 5 (Iteration # 11)

Bus No	Bus Name IEEE	Phase A		Phase B		Phase C	
		V	Degree	V	Degree	V	Degree
1 0.0000	1	0.0000e+00	0.0000	0.0000e+00	0.0000	0.0000e+00	0.0000
2 -110.2347	2	6.2868e+11	-109.6981	5.9988e+11	-109.2686	5.6541e+11	-109.2686
3 -110.2347	3	2.2884e+12	-109.6981	2.1836e+12	-109.2686	2.0581e+12	-109.2686
4 -110.2347	4	3.0743e+12	-109.6981	2.9334e+12	-109.2686	2.7649e+12	-109.2686

BRANCH CURRENTS AT HARMONIC ORDER # 5 (Iteration # 12)

Branch No	Branch IEEE	Phase A		Phase B		Phase C	
		A	Degree	A	Degree	A	Degree
1 1100238977736753.1250	0 - 1	1276978945234797.2500	69.6669	1092962799957181.1250	71.2495		
		68.5985					
2 1100238977736753.1250	1 - 2	1276978945234797.2500	69.6669	1092962799957181.1250	71.2495		
		68.5985					
3	2 - 3	3827867174778347.0000	69.6669	3276261085448569.0000	71.2495		

3298072127975315.5000 68.5985

4 3 - 4 3827867174778347.0000 69.6669 3276261085448569.0000 71.2495
3298072127975315.5000 68.5985

BUS VOLTAGES AT ORDER # 5 (Iteration # 12)

Bus No	Bus Name IEEE	Phase A		Phase B		Phase C	
		V	Degree	V	Degree	V	Degree
1 0.0000	1	0.0000e+00	0.0000	0.0000e+00	0.0000	0.0000e+00	0.0000
2 -21.8973	2	1.4138e+13	-21.3607	1.3490e+13	-20.9312	1.2715e+13	1.2715e+13
3 -21.8973	3	5.1461e+13	-21.3607	4.9104e+13	-20.9312	4.6282e+13	4.6282e+13
4 -21.8973	4	6.9133e+13	-21.3607	6.5966e+13	-20.9312	6.2175e+13	6.2175e+13

BRANCH CURRENTS AT HARMONIC ORDER # 5 (Iteration # 13)

Branch No	Branch IEEE	Phase A		Phase B		Phase C	
		A	Degree	A	Degree	A	Degree
1 24741763174077388.0000	0 - 1	28716220741019216.0000	156.9359	158.0043	24578134918124308.0000	159.5869	159.5869
2 24741763174077388.0000	1 - 2	28716220741019216.0000	156.9359	158.0043	24578134918124308.0000	159.5869	159.5869
3 74165814129986784.0000	2 - 3	86079632846276352.0000	156.9359	158.0043	73675322699281280.0000	159.5869	159.5869
4 74165814129986784.0000	3 - 4	86079632846276352.0000	156.9359	158.0043	73675322699281280.0000	159.5869	159.5869

BUS VOLTAGES AT ORDER # 5 (Iteration # 13)

Bus No	Bus Name IEEE	Phase A		Phase B		Phase C	
		V	Degree	V	Degree	V	Degree
1 0.0000	1	0.0000e+00	0.0000	0.0000e+00	0.0000	0.0000e+00	0.0000
2 66.4401	2	3.1792e+14	66.9767	3.0336e+14	67.4062	2.8593e+14	2.8593e+14
3 66.4401	3	1.1572e+15	66.9767	1.1042e+15	67.4062	1.0408e+15	1.0408e+15
4 66.4401	4	1.5546e+15	66.9767	1.4834e+15	67.4062	1.3982e+15	1.3982e+15

BRANCH CURRENTS AT HARMONIC ORDER # 5 (Iteration # 14)

Branch No	Branch IEEE	Phase A		Phase B		Phase C	
		A	Degree	A	Degree	A	Degree
1 556383446753472896.0000	0 - 1	645759575543776768.0000	-114.7267	-113.6583	552703858273990656.0000	-112.0757	-112.0757


```

2      1 - 2 645759575543776768.0000 -113.6583 552703858273990656.0000 -112.0757
556383446753472896.0000 -114.7267
-----
3      2 - 3 1935726419959350528.0000 -113.6583 1656782959778044160.0000 -112.0757
1667812880051876608.0000 -114.7267
-----
4      3 - 4 1935726419959350528.0000 -113.6583 1656782959778044160.0000 -112.0757
1667812880051876608.0000 -114.7267

```


BUS VOLTAGES AT ORDER # 5 (Iteration # 14)

Bus No	Bus Name IEEE	Phase A		Phase B		Phase C	
		V	Degree	V	Degree	V	Degree
1	1	0.0000e+00	0.0000	0.0000e+00	0.0000	0.0000e+00	0.0000
2	2	7.1493e+15	155.3141	6.8218e+15	155.7436	6.4298e+15	154.7775
3	3	2.6023e+16	155.3141	2.4831e+16	155.7436	2.3404e+16	154.7775
4	4	3.4960e+16	155.3141	3.3359e+16	155.7436	3.1442e+16	154.7775

BRANCH CURRENTS AT HARMONIC ORDER # 5 (Iteration # 15)

Branch No	Branch IEEE	Phase A		Phase B		Phase C	
		A	Degree	A	Degree	A	Degree
1	0 - 1	14521598354718298112.0000	-26.3893	-25.3209	12428996394163853312.0000	-23.7382	12511741709287168000.0000
2	1 - 2	14521598354718298112.0000	-26.3893	-25.3209	12428996394163853312.0000	-23.7382	12511741709287168000.0000
3	2 - 3	43529887375802212352.0000	-26.3893	-25.3209	37257111787313283072.0000	-23.7382	37505148825675718656.0000
4	3 - 4	43529887375802212352.0000	-26.3893	-25.3209	37257111787313283072.0000	-23.7382	37505148825675718656.0000

BUS VOLTAGES AT ORDER # 5 (Iteration # 15)

Bus No	Bus Name IEEE	Phase A		Phase B		Phase C	
		V	Degree	V	Degree	V	Degree
1	1	0.0000e+00	0.0000	0.0000e+00	0.0000	0.0000e+00	0.0000
2	2	1.6077e+17	-116.3485	1.5341e+17	-115.9190	1.4459e+17	-116.8851
3	3	5.8520e+17	-116.3485	5.5840e+17	-115.9190	5.2631e+17	-116.8851
4	4	7.8617e+17	-116.3485	7.5015e+17	-115.9190	7.0705e+17	-116.8851

BRANCH CURRENTS AT HARMONIC ORDER # 5 (Iteration # 16)

Branch No	Branch IEEE	A	Phase A Degree	A	Phase B Degree	A	Phase C Degree
-----------	-------------	---	----------------	---	----------------	---	----------------

1	0 - 1	326556240742975864832.0000	63.0165	279498595119200796672.0000	64.5992
281359340055334191104.0000		61.9481			
2	1 - 2	326556240742975864832.0000	63.0165	279498595119200796672.0000	64.5992
281359340055334191104.0000		61.9481			
3	2 - 3	978883731265603108864.0000	63.0165	837823913734719668224.0000	64.5992
843401675598561804288.0000		61.9481			
4	3 - 4	978883731265603108864.0000	63.0165	837823913734719668224.0000	64.5992
843401675598561804288.0000		61.9481			

BUS VOLTAGES AT ORDER # 5 (Iteration # 16)

Bus No	Bus Name IEEE	Phase A		Phase B		Phase C	
		V	Degree	V	Degree	V	Degree
1	1	0.0000e+00	0.0000	0.0000e+00	0.0000	0.0000e+00	0.0000
2	2	3.6153e+18	-28.0111	3.4497e+18	-27.5816	3.2515e+18	
3	3	1.3160e+19	-28.0111	1.2557e+19	-27.5816	1.1835e+19	
4	4	1.7679e+19	-28.0111	1.6869e+19	-27.5816	1.5900e+19	

BRANCH CURRENTS AT HARMONIC ORDER # 5 (Iteration # 17)

Branch No	Branch IEEE	Phase A		Phase B		Phase C	
		A	Degree	A	Degree	A	Degree
1	0 - 1	7343473885599322079232.0000	151.3539	6285259254612772257792.0000	152.9366	6327102989645000998912.0000	150.2855
2	1 - 2	7343473885599322079232.0000	151.3539	6285259254612772257792.0000	152.9366	6327102989645000998912.0000	150.2855
3	2 - 3	22012769075342199488512.0000	151.3539	18840668967553193738240.0000	152.9366	18966099586748357017600.0000	150.2855
4	3 - 4	22012769075342199488512.0000	151.3539	18840668967553193738240.0000	152.9366	18966099586748357017600.0000	150.2855

BUS VOLTAGES AT ORDER # 5 (Iteration # 17)

Bus No	Bus Name IEEE	Phase A		Phase B		Phase C	
		V	Degree	V	Degree	V	Degree
1	1	0.0000e+00	0.0000	0.0000e+00	0.0000	0.0000e+00	0.0000
2	2	8.1300e+19	60.3263	7.7576e+19	60.7558	7.3119e+19	
3	3	2.9593e+20	60.3263	2.8238e+20	60.7558	2.6615e+20	
4	4	3.9756e+20	60.3263	3.7935e+20	60.7558	3.5755e+20	

BRANCH CURRENTS AT HARMONIC ORDER # 5 (Iteration # 18)

Branch No	Branch IEEE	Phase A		Phase B		Phase C	
		A	Degree	A	Degree	A	Degree
1 -118.7260	0 - 1 142281511670877553426432.0000	165137278020312524390400.0000		-120.3087		141340545514613057257472.0000	
2 -118.7260	1 - 2 142281511670877553426432.0000	165137278020312524390400.0000		-120.3087		141340545514613057257472.0000	
3 -118.7260	2 - 3 426502512148039245758464.0000	495014869450311807795200.0000		-120.3087		423681875617121405239296.0000	
4 -118.7260	3 - 4 426502512148039245758464.0000	495014869450311807795200.0000		-120.3087		423681875617121405239296.0000	

BUS VOLTAGES AT ORDER # 5 (Iteration # 18)

Bus No	Bus Name IEEE	Phase A		Phase B		Phase C	
		V	Degree	V	Degree	V	Degree
1 0.0000	1	0.0000e+00	0.0000	0.0000e+00	0.0000	0.0000e+00	
2 148.1272	2	1.8283e+21	148.6637	1.7445e+21	149.0932	1.6443e+21	
3 148.1272	3	6.6548e+21	148.6637	6.3500e+21	149.0932	5.9851e+21	
4 148.1272	4	8.9401e+21	148.6637	8.5306e+21	149.0932	8.0404e+21	

BRANCH CURRENTS AT HARMONIC ORDER # 5 (Iteration # 19)

Branch No	Branch IEEE	Phase A		Phase B		Phase C	
		A	Degree	A	Degree	A	Degree
1 -30.3886	0 - 1 3199573106092387592044544.0000	3713544981004637763010560.0000		-31.9713		3178413013100739117973504.0000	
2 -30.3886	1 - 2 3199573106092387592044544.0000	3713544981004637763010560.0000		-31.9713		3178413013100739117973504.0000	
3 -30.3886	2 - 3 9591028036772131650928640.0000	11131708152194192159801344.0000		-31.9713		9527598623405340910157824.0000	
4 -30.3886	3 - 4 9591028036772131650928640.0000	11131708152194192159801344.0000		-31.9713		9527598623405340910157824.0000	

BUS VOLTAGES AT ORDER # 5 (Iteration # 19)

Bus No	Bus Name IEEE	Phase A		Phase B		Phase C	
		V	Degree	V	Degree	V	Degree
1 0.0000	1	0.0000e+00	0.0000	0.0000e+00	0.0000	0.0000e+00	
2 -123.5354	2	4.1113e+22	-122.9989	3.9230e+22	-122.5694	3.6976e+22	
3 -123.5354	3	1.4965e+23	-122.9989	1.4280e+23	-122.5694	1.3459e+23	
4 -123.5354	4	2.0104e+23	-122.9989	1.9183e+23	-122.5694	1.8081e+23	

BRANCH CURRENTS AT HARMONIC ORDER # 5 (Iteration # 20)

Branch No	Branch IEEE	Phase A		Phase B		Phase C	
		A	Degree	A	Degree	A	Degree
1 57.9488	0 - 1 71950796282704504385699840.0000	83508802442270944278872064.0000	56.3661	71474956072624267917787136.0000	55.2977		
2 57.9488	1 - 2 71950796282704504385699840.0000	83508802442270944278872064.0000	56.3661	71474956072624267917787136.0000	55.2977		
3 57.9488	2 - 3 215679430203203154020925440.0000	250325665013249661953114112.0000	56.3661	214253053419621314486861824.0000	55.2977		
4 57.9488	3 - 4 215679430203203154020925440.0000	250325665013249661953114112.0000	56.3661	214253053419621314486861824.0000	55.2977		

BUS VOLTAGES AT ORDER # 5 (Iteration # 20)

Bus No	Bus Name IEEE	Phase A		Phase B		Phase C	
		V	Degree	V	Degree	V	Degree
1 0.0000	1	0.0000e+00	0.0000	0.0000e+00	0.0000	0.0000e+00	
2 -35.1980	2	9.2453e+23	-34.6615	8.8219e+23	-34.2320	8.3149e+23	
3 -35.1980	3	3.3653e+24	-34.6615	3.2112e+24	-34.2320	3.0266e+24	
4 -35.1980	4	4.5210e+24	-34.6615	4.3139e+24	-34.2320	4.0660e+24	

BRANCH CURRENTS AT HARMONIC ORDER # 5 (Iteration # 21)

Branch No	Branch IEEE	Phase A		Phase B		Phase C	
		A	Degree	A	Degree	A	Degree
1 146.2862	0 - 1 1618002437850416873149038592.0000	1877914532071572322190884864.0000	144.7036	1607301922222407986804948992.0000	143.6351		
2 146.2862	1 - 2 1618002437850416873149038592.0000	1877914532071572322190884864.0000	144.7036	1607301922222407986804948992.0000	143.6351		
3 146.2862	2 - 3 4850117884614110500205101056.0000	5629229378589545686189998080.0000	144.7036	4818042060123420378529792000.0000	143.6351		
4 146.2862	3 - 4 4850117884614110500205101056.0000	5629229378589545686189998080.0000	144.7036	4818042060123420378529792000.0000	143.6351		

BUS VOLTAGES AT ORDER # 5 (Iteration # 21)

Bus No	Bus Name IEEE	Phase A		Phase B		Phase C	
		V	Degree	V	Degree	V	Degree
1 0.0000	1	0.0000e+00	0.0000	0.0000e+00	0.0000	0.0000e+00	
2 53.1394	2	2.0791e+25	53.6759	1.9838e+25	54.1054	1.8698e+25	
3 53.1394	3	7.5678e+25	53.6759	7.2211e+25	54.1054	6.8062e+25	

-----<

4 4 1.0167e+26 53.6759 9.7009e+25 54.1054 9.1435e+25<

53.1394 -----<

*****<

BRANCH CURRENTS AT HARMONIC ORDER # 5 (Iteration # 22)

-----<
| Branch No | Branch IEEE | Phase A A | Phase A Degree | Phase B A | Phase B Degree | Phase C A | Phase C Degree | -----<

1 0 - 1 42229835497938655566874279936.0000 -126.9590 36144400936126544704239042560.0000<
-125.3764 36385030105867366448555360256.0000 -128.0275 -----<

2 1 - 2 42229835497938655566874279936.0000 -126.9590<
36144400936126544704239042560.0000 -125.3764 36385030105867366448555360256.0000 -128.0275 -----<

3 2 - 3 126587992466176690832545939456.0000 -126.9590<
108346317229206251240649916416.0000 -125.3764 109067626302924520049627627520.0000 -128.0275 -----<

4 3 - 4 126587992466176690832545939456.0000 -126.9590<
108346317229206251240649916416.0000 -125.3764 109067626302924520049627627520.0000 -128.0275 -----<

*****<

**** -----<

BUS VOLTAGES AT ORDER # 5 (Iteration # 22)

-----<
| Bus No | Bus Name IEEE | Phase A V | Phase A Degree | Phase B V | Phase B Degree | Phase C V | Phase C Degree | -----<

1 1 0.0000e+00 0.0000 0.0000e+00 0.0000 0.0000e+00 0.0000 -----<

2 2 4.6753e+26 142.0133 4.4612e+26 142.4428 4.2048e+26 141.4768 -----<

3 3 1.7018e+27 142.0133 1.6239e+27 142.4428 1.5305e+27 141.4768 -----<

4 4 2.2862e+27 142.0133 2.1815e+27 142.4428 2.0561e+27 141.4768 -----<

*****<

BRANCH CURRENTS AT HARMONIC ORDER # 5 (Iteration # 23)

-----<
| Branch No | Branch IEEE | Phase A A | Phase A Degree | Phase B A | Phase B Degree | Phase C A | Phase C Degree | -----<

1 0 - 1 949648653187395663400875851776.0000 -38.6216<
812801690192073787382599516160.0000 -37.0390 818212868432989110249560473600.0000<
-39.6901 -----<

2 1 - 2 949648653187395663400875851776.0000 -38.6216<
812801690192073787382599516160.0000 -37.0390 818212868432989110249560473600.0000 -39.6901 -----<

3 2 - 3 2846663150299717314462028398592.0000 -38.6216<
2436451220359413532725631516672.0000 -37.0390 2452671747442157365648613703680.0000 -39.6901 -----<

4 3 - 4 2846663150299717314462028398592.0000 -38.6216<
2436451220359413532725631516672.0000 -37.0390 2452671747442157365648613703680.0000 -39.6901 -----<

*****<

**** -----<

BUS VOLTAGES AT ORDER # 5 (Iteration # 23)

-----<
| Bus No | Bus Name IEEE | Phase A V | Phase A Degree | Phase B V | Phase B Degree | Phase C V | Phase C Degree | -----<

1 1 0.0000e+00 0.0000 0.0000e+00 0.0000 0.0000e+00 0.0000 -----<

2 2 1.0514e+28 -129.6493 1.0032e+28 -129.2197 9.4556e+27 -----<

-130.1858

3	3	3.8270e+28	-129.6493	3.6517e+28	-129.2197	3.4418e+28
---	---	------------	-----------	------------	-----------	------------

-130.1858

4	4	5.1412e+28	-129.6493	4.9057e+28	-129.2197	4.6238e+28
---	---	------------	-----------	------------	-----------	------------

-130.1858

BRANCH CURRENTS AT HARMONIC ORDER # 5 (Iteration # 24)

Branch No	Branch IEEE	Phase A		Phase B		Phase C	
		A	Degree	A	Degree	A	Degree
1	0 - 1	21355341640974951984209055449088.0000	49.7158	49088.0000	49.7158	18399663161508583732083683229696.0000	48.6473

2	1 - 2	21355341640974951984209055449088.0000	49.7158	49088.0000	49.7158	18399663161508583732083683229696.0000	48.6473
---	-------	---------------------------------------	---------	------------	---------	---------------------------------------	---------

3	2 - 3	64014689967057130571544695668736.0000	49.7158	49088.0000	49.7158	55154759525002889282047394709504.0000	48.6473
---	-------	---------------------------------------	---------	------------	---------	---------------------------------------	---------

4	3 - 4	64014689967057130571544695668736.0000	49.7158	49088.0000	49.7158	55154759525002889282047394709504.0000	48.6473
---	-------	---------------------------------------	---------	------------	---------	---------------------------------------	---------

BUS VOLTAGES AT ORDER # 5 (Iteration # 24)

Bus No	Bus Name IEEE	Phase A		Phase B		Phase C	
		V	Degree	V	Degree	V	Degree

1	1	0.0000e+00	0.0000	0.0000e+00	0.0000	0.0000e+00	0.0000
---	---	------------	--------	------------	--------	------------	--------

2	2	2.3643e+29	-41.3119	2.2560e+29	-40.8823	2.1263e+29	48.6484
---	---	------------	----------	------------	----------	------------	---------

3	3	8.6059e+29	-41.3119	8.2117e+29	-40.8823	7.7399e+29	48.6484
---	---	------------	----------	------------	----------	------------	---------

4	4	1.1561e+30	-41.3119	1.1032e+30	-40.8823	1.0398e+30	48.6484
---	---	------------	----------	------------	----------	------------	---------

BRANCH CURRENTS AT HARMONIC ORDER # 5 (Iteration # 25)

Branch No	Branch IEEE	Phase A		Phase B		Phase C	
		A	Degree	A	Degree	A	Degree
1	0 - 1	480230888626094606250882732392448.0000	138.0532	480230888626094606250882732392448.0000	138.0532	413764702949922149835018233446400.0000	136.9847

2	1 - 2	480230888626094606250882732392448.0000	138.0532	480230888626094606250882732392448.0000	138.0532	413764702949922149835018233446400.0000	136.9847
---	-------	--	----------	--	----------	--	----------

3	2 - 3	1439538264703702018190532071653376.0000	138.0532	1439538264703702018190532071653376.0000	138.0532	1240299482159983115828124899606528.0000	136.9847
---	-------	---	----------	---	----------	---	----------

4	3 - 4	1439538264703702018190532071653376.0000	138.0532	1439538264703702018190532071653376.0000	138.0532	1240299482159983115828124899606528.0000	136.9847
---	-------	---	----------	---	----------	---	----------

BUS VOLTAGES AT ORDER # 5 (Iteration # 25)

Bus No	Bus Name IEEE	Phase A		Phase B		Phase C	
--------	---------------	---------	--	---------	--	---------	--

No	IEEE	V	Degree	V	Degree	V	Degree
1 0.0000	1	0.0000e+00	0.0000	0.0000e+00	0.0000	0.0000e+00	0.0000
2 46.4890	2	5.3167e+30	47.0256	5.0731e+30	47.4551	4.7816e+30	47.4551
3 46.4890	3	1.9353e+31	47.0256	1.8466e+31	47.4551	1.7405e+31	47.4551
4 46.4890	4	2.5999e+31	47.0256	2.4808e+31	47.4551	2.3382e+31	47.4551

BRANCH CURRENTS AT HARMONIC ORDER # 5 (Iteration # 26)

Branch No	Branch IEEE	Phase A		Phase B		Phase C	
		A	Degree	A	Degree	A	Degree
1 9243049927977829006059671270719488.0000 -134.6778	0 - 1	10799251553443182907441604036919296.0000	-133.6094	-132.0268	9304584975521925986129622188687360.0000	-133.6094	-134.6778
2 9243049927977829006059671270719488.0000 -134.6778	1 - 2	10799251553443182907441604036919296.0000	-133.6094	-132.0268	9304584975521925986129622188687360.0000	-133.6094	-134.6778
3 27706930913914312088794113710751744.0000 -134.6778	2 - 3	32371794921018388283643497581379584.0000	-133.6094	-132.0268	27891388135759238627928174569193472.0000	-133.6094	-134.6778
4 27706930913914312088794113710751744.0000 -134.6778	3 - 4	32371794921018388283643497581379584.0000	-133.6094	-132.0268	27891388135759238627928174569193472.0000	-133.6094	-134.6778

BUS VOLTAGES AT ORDER # 5 (Iteration # 26)

Bus No	Bus Name	Phase A		Phase B		Phase C	
		V	Degree	V	Degree	V	Degree
1 0.0000	1	0.0000e+00	0.0000	0.0000e+00	0.0000	0.0000e+00	0.0000
2 134.8264	2	1.1956e+32	135.3630	1.1408e+32	135.7925	1.0753e+32	135.7925
3 134.8264	3	4.3520e+32	135.3630	4.1526e+32	135.7925	3.9140e+32	135.7925
4 134.8264	4	5.8465e+32	135.3630	5.5787e+32	135.7925	5.2581e+32	135.7925

BRANCH CURRENTS AT HARMONIC ORDER # 5 (Iteration # 27)

Branch No	Branch IEEE	Phase A		Phase B		Phase C	
		A	Degree	A	Degree	A	Degree
1 207854229407940616074731991871782912.0000 -46.3404	0 - 1	242849506095281026603792051891863552.0000	-45.2720	-43.6894	209238006406715056946648529017765888.0000	-45.2720	-46.3404
2 207854229407940616074731991871782912.0000 -46.3404	1 - 2	242849506095281026603792051891863552.0000	-45.2720	-43.6894	209238006406715056946648529017765888.0000	-45.2720	-46.3404
3 623063038633898966287152193975877632.0000 -46.3404	2 - 3	727964745434652577222811116283887616.0000	-45.2720	-43.6894	627211043243205988935229022016634880.0000	-45.2720	-46.3404
4	3 - 4	727964745434652577222811116283887616.0000	-45.2720	-43.6894	627211043243205988935229022016634880.0000	-45.2720	-46.3404

623063038633898966287152193975877632.0000 -43.6894 627211043243205988935229022016634880.0000K
-46.3404

*****K

BUS VOLTAGES AT ORDER # 5 (Iteration # 27)

Bus No	Bus Name IEEE	Phase A		Phase B		Phase C	
		V	Degree	V	Degree	V	Degree
1 0.0000	1	0.0000e+00	0.0000	0.0000e+00	0.0000	0.0000e+00	0.0000e+00
2 -136.8362	2	2.6886e+33	-136.2996	2.5655e+33	-135.8701	2.4180e+33	2.4180e+33
3 -136.8362	3	9.7865e+33	-136.2996	9.3383e+33	-135.8701	8.8017e+33	8.8017e+33
4 -136.8362	4	1.3147e+34	-136.2996	1.2545e+34	-135.8701	1.1824e+34	1.1824e+34

BRANCH CURRENTS AT HARMONIC ORDER # 5 (Iteration # 28)

Branch No	Branch IEEE	Phase A		Phase B		Phase C	
		A	Degree	A	Degree	A	Degree
1 4674147713082918192210048363452694528.0000 41.9970	0 - 1	5461108329485883977217830030082572288.0000	43.0654	44.6480	4705265569633934641075522183662403584.0000	41.9970	43.0654
2 4674147713082918192210048363452694528.0000 4705265569633934641075522183662403584.0000	1 - 2	5461108329485883977217830030082572288.0000	43.0654	44.6480	4705265569633934641075522183662403584.0000	41.9970	43.0654
3 14011207207246153621508159780784439296.0000 14104485974359413476670821982172872704.0000	2 - 3	16370197324204078769842180703081463808.0000	43.0654	44.6480	4705265569633934641075522183662403584.0000	41.9970	43.0654
4 14011207207246153621508159780784439296.0000 14104485974359413476670821982172872704.0000	3 - 4	16370197324204078769842180703081463808.0000	43.0654	44.6480	4705265569633934641075522183662403584.0000	41.9970	43.0654

*****K

BUS VOLTAGES AT ORDER # 5 (Iteration # 28)

Bus No	Bus Name IEEE	Phase A		Phase B		Phase C	
		V	Degree	V	Degree	V	Degree
1 0.0000	1	0.0000e+00	0.0000	0.0000e+00	0.0000	0.0000e+00	0.0000e+00
2 -48.4988	2	6.0460e+34	-47.9622	5.7691e+34	-47.5327	5.4376e+34	5.4376e+34
3 -48.4988	3	2.2008e+35	-47.9622	2.1000e+35	-47.5327	1.9793e+35	1.9793e+35
4 -48.4988	4	2.9565e+35	-47.9622	2.8211e+35	-47.5327	2.6590e+35	2.6590e+35

BRANCH CURRENTS AT HARMONIC ORDER # 5 (Iteration # 29)

Branch No	Branch IEEE	Phase A		Phase B		Phase C	
		A	Degree	A	Degree	A	Degree
1	0 - 1	122807349563556017574728055367172882432.0000	131.4028				

105110475288137856217999050237320101888.0000 132.9854
105810241939258104912825104293567660032.0000 130.3344

2 1 - 2 122807349563556017574728055367172882432.0000 131.4028
105110475288137856217999050237320101888.0000 132.9854
105810241939258104912825104293567660032.0000 130.3344

3 2 - 3 368126838715755641196367382406259277824.0000 131.4028
315078756452663262696984945370056359936.0000 132.9854
317176374274651118709665798110278844416.0000 130.3344

4 3 - 4 368126838715755641196367382406259277824.0000 131.4028
315078756452663262696984945370056359936.0000 132.9854
317176374274651118709665798110278844416.0000 130.3344

BUS VOLTAGES AT ORDER # 5 (Iteration # 29)

Bus No	Bus Name IEEE	Phase A V	Phase A Degree	Phase B V	Phase B Degree	Phase C V	Phase C Degree
1	1	0.0000e+00	0.0000	0.0000e+00	0.0000	0.0000e+00	0.0000
2	2	1.3596e+36	40.3752	1.2973e+36	40.8047	1.2228e+36	40.8047
3	3	4.9490e+36	40.3752	4.7223e+36	40.8047	4.4509e+36	40.8047
4	4	6.6485e+36	40.3752	6.3440e+36	40.8047	5.9794e+36	40.8047

BRANCH CURRENTS AT HARMONIC ORDER # 5 (Iteration # 30)

Branch No	Branch IEEE	Phase A A	Phase A Degree	Phase B A	Phase B Degree	Phase C A	Phase C Degree
1	0 - 1	2761645475039541454000780497382151290880.0000	-140.2598	2363684824160422751259705422020832395264.0000	-138.6772	2379420913348226402519485955510483550208.0000	-141.3282
2	1 - 2	2761645475039541454000780497382151290880.0000	-140.2598	2363684824160422751259705422020832395264.0000	-138.6772	2379420913348226402519485955510483550208.0000	-141.3282
3	2 - 3	8278297854265162812789385499597521027072.0000	-140.2598	7085372537807805751397878399815632551936.0000	-138.6772	7132542978233745571429083628629955444736.0000	-141.3282
4	3 - 4	8278297854265162812789385499597521027072.0000	-140.2598	7085372537807805751397878399815632551936.0000	-138.6772	7132542978233745571429083628629955444736.0000	-141.3282

BUS VOLTAGES AT ORDER # 5 (Iteration # 30)

Bus No	Bus Name IEEE	Phase A V	Phase A Degree	Phase B V	Phase B Degree	Phase C V	Phase C Degree
1	1	0.0000e+00	0.0000	0.0000e+00	0.0000	0.0000e+00	0.0000
2	2	3.0574e+37	128.7126	2.9174e+37	129.1421	2.7498e+37	129.1421
3	3	1.1129e+38	128.7126	1.0619e+38	129.1421	1.0009e+38	129.1421

4 4 1.4951e+38 128.7126 1.4266e+38 129.1421 1.3446e+38
 128.1760

 WARNING: maximum number of iteration have been reached.
 It is possible that the iterative process is diverging.
 It is possible that the system is in resonance at 5 harmonic order.

SHUNT CAPACITORS CURRENTS AT HARMONIC ORDER # 5

Bus No	Bus Name IEEE	Phase A		Phase B		Phase C	
		pu	Degree	pu	Degree	pu	Degree
4	4	2.4918e+37	-141.2874	2.3777e+37	-140.8579	2.2411e+37	-141.8240

LOADS CURRENTS AT HARMONIC ORDER # 5

Bus No	Bus Name IEEE	Phase A		Phase B		Phase C	
		pu	Degree	pu	Degree	pu	Degree
4	4	5.0513e+36	34.6646	6.8025e+36	33.6797	5.2825e+36	36.5681

BUS VOLTAGES AT HARMONIC ORDER # 5

Bus No	Bus Name IEEE	Phase A		Phase B		Phase C	
		pu	Degree	pu	Degree	pu	Degree
1	1	0.0000e+00	0.0000	0.0000e+00	0.0000	0.0000e+00	0.0000
2	2	3.0574e+37	128.7126	2.9174e+37	129.1421	2.7498e+37	128.1760
3	3	1.1129e+38	128.7126	1.0619e+38	129.1421	1.0009e+38	128.1760
4	4	1.4951e+38	128.7126	1.4266e+38	129.1421	1.3446e+38	128.1760

BRANCH CURRENTS AT HARMONIC ORDER # 5

Branch No	Branch IEEE	Phase A		Phase B		Phase C	
		A	Degree	A	Degree	A	Degree
1	0 - 1	8278297854265162812789385499597521027072.0000	-140.2598	7085372537807805751397878399815632551936.0000	-138.6772	7132542978233745571429083628629955444736.0000	-141.3282
2	1 - 2	2761645475039541454000780497382151290880.0000	-140.2598	2363684824160422751259705422020832395264.0000	-138.6772	2379420913348226402519485955510483550208.0000	-141.3282
3	2 - 3	8278297854265162812789385499597521027072.0000	-140.2598	7085372537807805751397878399815632551936.0000	-138.6772	7132542978233745571429083628629955444736.0000	-141.3282
4	3 - 4	8278297854265162812789385499597521027072.0000	-140.2598	7085372537807805751397878399815632551936.0000	-138.6772	7132542978233745571429083628629955444736.0000	-141.3282

BRANCH LOSSES AT HARMONIC ORDER # 5

Branch No	Branch IEEE	Phase A		Phase B		Phase C	
		kW	Degree	kW	Degree	kW	Degree

```

1      0 - 1      -0.0000 ----- -0.0000 ----- -0.0000 -----
-----
2      1 - 2      10902371368987885148556932572932678832984431757566886577964449773276626944000.0000 ✓
----- 18891606047267817131177945510916519311710668097553876647844499490747141062656.0000 ----- ✓
4075753993139192521453435573979837686374718182774198792715855095884939264000.0000 -----
-----
3      2 - 3      28782260322024900471865998668703971611041134818448220772441033704671805440000.0000 ✓
----- 49873839805190758886245371962334801608886113628129795842712371374849863450624.0000 ----- ✓
10759990507455470192565923267095728672657315919459426877731483833742655488000.0000 -----
-----
4      3 - 4      13627964211234604949892239184187726224163088305011313497687035209517059014656.0000 ✓
----- 23614507559084609113229961730627819401467008664519491067303252301357560889344.0000 ----- ✓
5094692491423790186295773158437923248197378168433083846071344466449970233344.0000 -----
-----

```

HARMONIC ORDER # 5

```

| No of ITERATIONS MADE | 30 |
-----

```

```

| ACTIVE POWER LOSSES IN PHASE A (kW) | ✓
53312595902247388963377126166834101126226562539863818325889524904672656097280.0000 |
-----
| ACTIVE POWER LOSSES IN PHASE B (kW) | ✓
92379953411543188344529367721859691405987975072528368602266110732540236005376.0000 |
-----
| ACTIVE POWER LOSSES IN PHASE C (kW) | ✓
19930436992018451293377087740523214065267319929504106994315689613284729683968.0000 |
-----
| TOTAL ACTIVE POWER LOSSES IN THE SYSTEM (kW) | ✓
165622986305809041456787935701139210933178596271197114100095275512840304197632.0000 |
-----

```

WARNING: maximun number of iteration have been reached.
It is possible that the iterative process is diverging.
It is possible that the system is in resonace at 5 harmonic order.

BRANCH CURRENTS MAGNITUDES IN AMPERES FOR EACH HARMONIC

Branch No	Phase	Harmonic Order				
		1	2	3	4	5
1	A	8.9970e+01	0.0000e+00	1.7461e+00	0.0000e+00	2.7616e+39
	B	1.3012e+02	0.0000e+00	1.3230e+00	0.0000e+00	2.3637e+39
	C	9.9463e+01	0.0000e+00	3.7679e-01	0.0000e+00	2.3794e+39
2	A	8.9970e+01	0.0000e+00	1.7461e+00	0.0000e+00	2.7616e+39
	B	1.3012e+02	0.0000e+00	1.3230e+00	0.0000e+00	2.3637e+39
	C	9.9463e+01	0.0000e+00	3.7679e-01	0.0000e+00	2.3794e+39
3	A	2.6969e+02	0.0000e+00	5.2341e+00	0.0000e+00	8.2783e+39
	B	3.9006e+02	0.0000e+00	3.9659e+00	0.0000e+00	7.0854e+39
	C	2.9815e+02	0.0000e+00	1.1295e+00	0.0000e+00	7.1325e+39
4	A	2.6969e+02	0.0000e+00	5.2341e+00	0.0000e+00	8.2783e+39
	B	3.9006e+02	0.0000e+00	3.9659e+00	0.0000e+00	7.0854e+39
	C	2.9815e+02	0.0000e+00	1.1295e+00	0.0000e+00	7.1325e+39

BRANCH LOSSES

Branch No	Branch IEEE	Phase A		Phase B		Phase C	
		kW	Degree	kW	Degree	kW	Degree
1	0 - 1	0.0000	-----	0.0000	-----	0.0000	-----
2	1 - 2	1.3532	-----	2.7102	-----	0.2186	-----
3	2 - 3	5.6703	-----	11.5432	-----	3.1411	-----
4	3 - 4	1.6915	-----	3.3877	-----	0.2733	-----

BUS VOLTAGES MAGNITUDES IN P.U. FOR EACH HARMONIC

Bus No	Phase	Harmonic Order				
		1	2	3	4	5
1	A	1.0000e+00	0.0000e+00	0.0000e+00	0.0000e+00	0.0000e+00
	B	1.0000e+00	0.0000e+00	0.0000e+00	0.0000e+00	0.0000e+00
	C	1.0000e+00	0.0000e+00	0.0000e+00	0.0000e+00	0.0000e+00
2	A	9.9754e-01	0.0000e+00	4.0542e-04	0.0000e+00	3.0574e+37
	B	9.9504e-01	0.0000e+00	2.2976e-04	0.0000e+00	2.9174e+37
	C	9.9890e-01	0.0000e+00	1.5035e-05	0.0000e+00	2.7498e+37
	A	9.8155e-01	0.0000e+00	1.4757e-03	0.0000e+00	1.1129e+38

3	B	9.6469e-01	0.0000e+00	8.3631e-04	0.0000e+00	1.0619e+38
	C	9.8911e-01	0.0000e+00	5.4728e-05	0.0000e+00	1.0009e+38
4	A	9.7849e-01	0.0000e+00	1.9825e-03	0.0000e+00	1.4951e+38
	B	9.5862e-01	0.0000e+00	1.1235e-03	0.0000e+00	1.4266e+38
	C	9.8794e-01	0.0000e+00	7.3522e-05	0.0000e+00	1.3446e+38

THD AT EACH NODE

Bus No	THD (%)		
	Phase A	Phase B	Phase C
1	0.0000e+00	0.0000e+00	0.0000e+00
2	3.0650e+39	2.9319e+39	2.7528e+39
3	1.1338e+40	1.1008e+40	1.0119e+40
4	1.5280e+40	1.4882e+40	1.3611e+40

WARNING:

Method reached the maximum number of for harmonic order # 5.
 It is possible that the iterative process is diverging for that harmonic order.
 It is possible that the system is in resonance at 5 harmonic order.

Results showing bellow are without taking account of the harmonic orders: 5 ;

THD AT EACH NODE

Bus No	THD (%)		
	Phase A	Phase B	Phase C
1	0.0000e+00	0.0000e+00	0.0000e+00
2	4.0642e-02	2.3090e-02	1.5052e-03
3	1.5035e-01	8.6692e-02	5.5331e-03
4	2.0261e-01	1.1720e-01	7.4420e-03

>>

Profile Summary

Generated 07-Oct-2010 10:34:34 using *cpu* time.

Function Name	Calls	Total Time	Self Time *	Total Time Plot (dark band = self time)
method1	1	0.527 s	0.214 s	
fundamental_hPQ	1	0.128 s	0.057 s	
results_it	9	0.107 s	0.078 s	
genHA	9	0.036 s	0.021 s	
angle	309	0.036 s	0.036 s	
results_h	4	0.028 s	0.021 s	
genZ_h	1	0.021 s	0.021 s	
cell2mat	71	0.021 s	0.021 s	
total_res	1	0.021 s	0.021 s	
inputs_c	1	0.007 s	0.007 s	
carson	1	0.007 s	0.007 s	
kron	4	0.007 s	0.007 s	
genA_h	1	0.007 s	0.007 s	
HlineC	4	0.007 s	0.007 s	
configurations_h	1	0 s	0.000 s	
input_LINES	1	0 s	0.000 s	
HZSaux	9	0 s	0.000 s	
mat2cell	3	0 s	0.000 s	
pinv	5	0 s	0.000 s	

Self time is the time spent in a function excluding the time spent in its child functions. Self time also includes overhead resulting from the process of profiling.

B.2.2 Method 2

SHUNT CAPACITORS CURRENTS AT HARMONIC ORDER # 1

Bus No	Bus Name IEEE	Phase A		Phase B		Phase C	
		pu	Degree	pu	Degree	pu	Degree
4	4	9.7849e-02	88.8086	9.5864e-02	-32.1917	9.8794e-02	-152.3799

LOADS CURRENTS AT HARMONIC ORDER # 1

Bus No	Bus Name IEEE	Phase A		Phase B		Phase C	
		pu	Degree	pu	Degree	pu	Degree
4	4	6.8557e-01	-27.7565	9.8410e-01	-154.1971	7.3690e-01	

BUS VOLTAGES AT HARMONIC ORDER # 1

Bus No	Bus Name IEEE	Phase A		Phase B		Phase C	
		pu	Degree	pu	Degree	pu	Degree
1	1	1.0000e+00	0.0000	1.0000e+00	-120.0000	1.0000e+00	
2	2	9.9754e-01	-0.0375	9.9504e-01	-120.1698	9.9890e-01	
3	3	9.8155e-01	-1.1400	9.6469e-01	-121.9589	9.8911e-01	
4	4	9.7849e-01	-1.1913	9.5862e-01	-122.1918	9.8794e-01	

BRANCH CURRENTS AT HARMONIC ORDER # 1

Branch No	Branch IEEE	Phase A		Phase B		Phase C	
		A	Degree	A	Degree	A	Degree
1	0 - 1	269.6945	-19.9913	390.0566	-149.2191	298.1491	109.2977
2	1 - 2	89.9703	-19.9913	130.1231	-149.2191	99.4627	109.2977
3	2 - 3	269.6945	-19.9913	390.0566	-149.2191	298.1491	109.2977
4	3 - 4	269.6945	-19.9913	390.0566	-149.2191	298.1491	109.2977

BRANCH LOSSES AT HARMONIC ORDER # 1

Branch No	Branch IEEE	Phase A		Phase B		Phase C	
		kW	Degree	kW	Degree	kW	Degree
1	0 - 1	0.0000	-----	0.0000	-----	0.0000	-----
2	1 - 2	1.3532	-----	2.7102	-----	0.2186	-----
3	2 - 3	5.6703	-----	11.5432	-----	3.1411	-----
4	3 - 4	1.6915	-----	3.3877	-----	0.2733	-----

HARMONIC ORDER # 1

No of ITERATIONS MADE | 4 |

BRANCH LOSSES AT HARMONIC ORDER # 2

Branch No	Branch IEEE	Phase A		Phase B		Phase C	
		kW	Degree	kW	Degree	kW	Degree
1	0 - 1	0.0000	-----	0.0000	-----	0.0000	-----
2	1 - 2	0.0000	-----	0.0000	-----	0.0000	-----
3	2 - 3	0.0000	-----	0.0000	-----	0.0000	-----
4	3 - 4	0.0000	-----	0.0000	-----	0.0000	-----

HARMONIC ORDER # 2

No of ITERATIONS MADE | 1 |

ACTIVE POWER LOSSES IN PHASE A (kW)	0.0000
ACTIVE POWER LOSSES IN PHASE B (kW)	0.0000
ACTIVE POWER LOSSES IN PHASE C (kW)	0.0000
TOTAL ACTIVE POWER LOSSES IN THE SYSTEM (kW)	0.0000

Harmonic Order # 3
Convergence criterium: Z1*Ys < 1 ?

ZY =

0.150788339978876	0.095763974340612	0.059683473613435
0.067582351620598	0.207092352740909	0.065525808593978
0.051650932729401	0.080340917642355	0.171920200081123

Convergence criterium reached. Method should convergence for armonic 3 will be posible

SHUNT CAPACITORS CURRENTS AT HARMONIC ORDER # 3

Bus No	Bus Name IEEE	Phase A		Phase B		Phase C	
		pu	Degree	pu	Degree	pu	Degree
4	4	2.0200e-04	-102.6392	1.1834e-04	147.6053	6.5372e-06	113.5875

LOADS CURRENTS AT HARMONIC ORDER # 3

Bus No	Bus Name IEEE	Phase A		Phase B		Phase C	
		pu	Degree	pu	Degree	pu	Degree
4	4	1.2389e-02	-78.8630	9.4276e-03	133.5158	2.6969e-03	45.3092

BUS VOLTAGES AT HARMONIC ORDER # 3

Bus No	Bus Name IEEE	Phase A		Phase B		Phase C	
		pu	Degree	pu	Degree	pu	Degree
1	1	0.0000e+00	0.0000	0.0000e+00	0.0000	0.0000e+00	0.0000
2	2	4.0571e-04	168.8591	2.3137e-04	55.8565	1.4673e-05	-16.2037
3	3	1.4768e-03	168.8591	8.4220e-04	55.8565	5.3409e-05	

-16.2037

4 4 1.9839e-03 168.8591 1.1314e-03 55.8565 7.1751e-05

-16.2037

BRANCH CURRENTS AT HARMONIC ORDER # 3

Branch No	Branch IEEE	Phase A		Phase B		Phase C	
		A	Degree	A	Degree	A	Degree
1	0 - 1	5.2352	-79.2342	3.9731	133.6888	1.1239	45.4381
2	1 - 2	1.7465	-79.2342	1.3254	133.6888	0.3749	45.4381
3	2 - 3	5.2352	-79.2342	3.9731	133.6888	1.1239	45.4381
4	3 - 4	5.2352	-79.2342	3.9731	133.6888	1.1239	45.4381

BRANCH LOSSES AT HARMONIC ORDER # 3

Branch No	Branch IEEE	Phase A		Phase B		Phase C	
		kW	Degree	kW	Degree	kW	Degree
1	0 - 1	0.0000	-----	-0.0000	-----	0.0000	-----
2	1 - 2	0.0019	-----	-0.0005	-----	-0.0000	-----
3	2 - 3	0.0050	-----	-0.0012	-----	-0.0000	-----
4	3 - 4	0.0024	-----	-0.0006	-----	-0.0000	-----

HARMONIC ORDER # 3

No of ITERATIONS MADE | 3 |

ACTIVE POWER LOSSES IN PHASE A (kW)	0.0093
ACTIVE POWER LOSSES IN PHASE B (kW)	-0.0023
ACTIVE POWER LOSSES IN PHASE C (kW)	0.0000
TOTAL ACTIVE POWER LOSSES IN THE SYSTEM (kW)	0.0070

Harmonic Order # 4
Convergence criterium: Zl*Ys < 1 ?

ZY =

0.637616830025859	0.404116438251788	0.250356029223367
0.286147999742046	0.871832914120840	0.276402088367958
0.215819432220380	0.336430657496545	0.729515770761282

Convergence criterium reached. Method should convergence for armonic 4 will be possible

SHUNT CAPACITORS CURRENTS AT HARMONIC ORDER # 4

Bus No	Bus Name IEEE	Phase A		Phase B		Phase C	
		pu	Degree	pu	Degree	pu	Degree
4	4	0.0000e+00	0.0000	0.0000e+00	0.0000	0.0000e+00	0.0000

LOADS CURRENTS AT HARMONIC ORDER # 4

Bus No	Bus Name IEEE	Phase A		Phase B		Phase C	
		pu	Degree	pu	Degree	pu	Degree
4	4	0.0000e+00	0.0000	0.0000e+00	0.0000	0.0000e+00	0.0000

0.0000

BUS VOLTAGES AT HARMONIC ORDER # 4

Bus No	Bus Name IEEE	Phase A		Phase B		Phase C	
		pu	Degree	pu	Degree	pu	Degree
1 0.0000	1	0.0000e+00	0.0000	0.0000e+00	0.0000	0.0000e+00	0.0000
2 0.0000	2	0.0000e+00	0.0000	0.0000e+00	0.0000	0.0000e+00	0.0000
3 0.0000	3	0.0000e+00	0.0000	0.0000e+00	0.0000	0.0000e+00	0.0000
4 0.0000	4	0.0000e+00	0.0000	0.0000e+00	0.0000	0.0000e+00	0.0000

BRANCH CURRENTS AT HARMONIC ORDER # 4

Branch No	Branch IEEE	Phase A		Phase B		Phase C	
		A	Degree	A	Degree	A	Degree
1	0 - 1	0.0000	0.0000	0.0000	0.0000	0.0000	0.0000
2	1 - 2	0.0000	0.0000	0.0000	0.0000	0.0000	0.0000
3	2 - 3	0.0000	0.0000	0.0000	0.0000	0.0000	0.0000
4	3 - 4	0.0000	0.0000	0.0000	0.0000	0.0000	0.0000

BRANCH LOSSES AT HARMONIC ORDER # 4

Branch No	Branch IEEE	Phase A		Phase B		Phase C	
		kW	Degree	kW	Degree	kW	Degree
1	0 - 1	0.0000	-----	0.0000	-----	0.0000	-----
2	1 - 2	0.0000	-----	0.0000	-----	0.0000	-----
3	2 - 3	0.0000	-----	0.0000	-----	0.0000	-----
4	3 - 4	0.0000	-----	0.0000	-----	0.0000	-----

HARMONIC ORDER # 4

No of ITERATIONS MADE | 1 |

ACTIVE POWER LOSSES IN PHASE A (kW)	0.0000
ACTIVE POWER LOSSES IN PHASE B (kW)	0.0000
ACTIVE POWER LOSSES IN PHASE C (kW)	0.0000
TOTAL ACTIVE POWER LOSSES IN THE SYSTEM (kW)	0.0000

Harmonic Order # 5
 Convergence criterium: Z1*Ys < 1 ?

ZY =

3.414563871589917	2.157647297127712	1.337316128010484
1.530167251047231	4.661842319637738	1.478616300543190
1.150707338285221	1.793612286832283	3.914052552500547

Convergence criterium not reached. Method convergence for armonic 5 will be not guaranteed
 WARNING: maximun number of iteration have been reached.
 It is possible that the iterative process is diverging.
 It is possible that the system is in resonace at 5 harmonic order.

SHUNT CAPACITORS CURRENTS AT HARMONIC ORDER # 5

Bus No	Bus Name IEEE	Phase A		Phase B		Phase C	
		pu	Degree	pu	Degree	pu	Degree
4	4	4.4657e+21	97.0974	5.1623e+21	95.0885	4.3737e+21	97.9863

LOADS CURRENTS AT HARMONIC ORDER # 5

Bus No	Bus Name IEEE	Phase A		Phase B		Phase C	
		pu	Degree	pu	Degree	pu	Degree
4	4	2.0357e+22	1.3868	3.3213e+22	-2.0365	2.3183e+22	4.7159

BUS VOLTAGES AT HARMONIC ORDER # 5

Bus No	Bus Name IEEE	Phase A		Phase B		Phase C	
		pu	Degree	pu	Degree	pu	Degree
1	1	0.0000e+00	0.0000	0.0000e+00	0.0000	0.0000e+00	0.0000
2	2	3.9467e+22	-79.4369	4.5623e+22	-81.4459	3.8653e+22	-78.5480
3	3	1.4366e+23	-79.4369	1.6607e+23	-81.4459	1.4070e+23	-78.5480
4	4	1.9299e+23	-79.4369	2.2310e+23	-81.4459	1.8901e+23	-78.5480

BRANCH CURRENTS AT HARMONIC ORDER # 5

Branch No	Branch IEEE	Phase A		Phase B		Phase C	
		A	Degree	A	Degree	A	Degree
1	0 - 1	8494895974431228631711744.0000	13.9661	13728541519499055591325696.0000	15.4959	6.9008	9720166977624446647402496.0000
2	1 - 2	2833902746883232687456256.0000	13.9661	4579850258309227948802048.0000	15.4959	6.9008	3242653939608475727298560.0000
3	2 - 3	8494895974431228631711744.0000	13.9661	13728541519499055591325696.0000	15.4959	6.9008	9720166977624446647402496.0000
4	3 - 4	8494895974431228631711744.0000	13.9661	13728541519499055591325696.0000	15.4959	6.9008	9720166977624446647402496.0000

BRANCH LOSSES AT HARMONIC ORDER # 5

Branch No	Branch IEEE	Phase A		Phase B		Phase C	
		kW	Degree	kW	Degree	kW	Degree
1	0 - 1	0.0000	-----	0.0000	-----	0.0000	-----
2	1 - 2	47797794437659545514724407014202332690306301952.0000	-----	43403171690899615140642631256957399640324440064.0000	-----	63636659880609095350484466796006952705705639936.0000	-----
3	2 - 3	126186176911625419214757368457905025073511661568.0000	-----	114584372897304927126533034316786604970854055936.0000	-----	168000781547205516490477741879811542054076416000.0000	-----
4	3 - 4	59747243047074426822803107854835309876070055936.0000	-----	54253964613624534137610491809949567510844014592.0000	-----	79545824850761270311358765693115374139282030592.0000	-----

HARMONIC ORDER # 5

No of ITERATIONS MADE | 30 |

ACTIVE POWER LOSSES IN PHASE A (kW) | 233731214396359401693489685152777879613513662464.0000 |
 ACTIVE POWER LOSSES IN PHASE B (kW) | -212241509201829096687195761035363996069273796608.0000 |
 ACTIVE POWER LOSSES IN PHASE C (kW) | 0.0000 |
 TOTAL ACTIVE POWER LOSSES IN THE SYSTEM (kW) | 21489705194530305006293924117413883544239865856.0000 |

WARNING: maximum number of iteration have been reached.
 It is possible that the iterative process is diverging.
 It is possible that the system is in resonance at 5 harmonic order.

BRANCH CURRENTS MAGNITUDES IN AMPERES FOR EACH HARMONIC

Branch No	Phase	Harmonic Order				
		1	2	3	4	5
1	A	8.9970e+01	0.0000e+00	1.7465e+00	0.0000e+00	2.8339e+24
	B	1.3012e+02	0.0000e+00	1.3254e+00	0.0000e+00	4.5799e+24
	C	9.9463e+01	0.0000e+00	3.7493e-01	0.0000e+00	3.2427e+24
2	A	8.9970e+01	0.0000e+00	1.7465e+00	0.0000e+00	2.8339e+24
	B	1.3012e+02	0.0000e+00	1.3254e+00	0.0000e+00	4.5799e+24
	C	9.9463e+01	0.0000e+00	3.7493e-01	0.0000e+00	3.2427e+24
3	A	2.6969e+02	0.0000e+00	5.2352e+00	0.0000e+00	8.4949e+24
	B	3.9006e+02	0.0000e+00	3.9731e+00	0.0000e+00	1.3729e+25
	C	2.9815e+02	0.0000e+00	1.1239e+00	0.0000e+00	9.7202e+24
4	A	2.6969e+02	0.0000e+00	5.2352e+00	0.0000e+00	8.4949e+24
	B	3.9006e+02	0.0000e+00	3.9731e+00	0.0000e+00	1.3729e+25
	C	2.9815e+02	0.0000e+00	1.1239e+00	0.0000e+00	9.7202e+24

BRANCH LOSSES

Branch No	Branch IEEE	Phase A		Phase B		Phase C	
		kW	Degree	kW	Degree	kW	Degree
1	0 - 1	0.0000	-----	0.0000	-----	0.0000	-----
2	1 - 2	1.3532	-----	2.7102	-----	0.2186	-----
3	2 - 3	5.6703	-----	11.5432	-----	3.1411	-----
4	3 - 4	1.6915	-----	3.3877	-----	0.2733	-----

BUS VOLTAGES MAGNITUDES IN P.U. FOR EACH HARMONIC

Bus No	Phase	Harmonic Order				
		1	2	3	4	5
1	A	1.0000e+00	0.0000e+00	0.0000e+00	0.0000e+00	0.0000e+00
	B	1.0000e+00	0.0000e+00	0.0000e+00	0.0000e+00	0.0000e+00
	C	1.0000e+00	0.0000e+00	0.0000e+00	0.0000e+00	0.0000e+00
2	A	9.9754e-01	0.0000e+00	4.0571e-04	0.0000e+00	3.9467e+22
	B	9.9504e-01	0.0000e+00	2.3137e-04	0.0000e+00	4.5623e+22
	C	9.9890e-01	0.0000e+00	1.4673e-05	0.0000e+00	3.8653e+22
3	A	9.8155e-01	0.0000e+00	1.4768e-03	0.0000e+00	1.4366e+23
	B	9.6469e-01	0.0000e+00	8.4220e-04	0.0000e+00	1.6607e+23
	C	9.8911e-01	0.0000e+00	5.3409e-05	0.0000e+00	1.4070e+23
4	A	9.7849e-01	0.0000e+00	1.9839e-03	0.0000e+00	1.9299e+23
	B	9.5862e-01	0.0000e+00	1.1314e-03	0.0000e+00	2.2310e+23
	C	9.8794e-01	0.0000e+00	7.1751e-05	0.0000e+00	1.8901e+23

THD AT EACH NODE

Bus No	THD (%)		
	Phase A	Phase B	Phase C

1	0.0000e+00	0.0000e+00	0.0000e+00
2	3.9564e+24	4.5851e+24	3.8696e+24
3	1.4636e+25	1.7215e+25	1.4225e+25
4	1.9723e+25	2.3273e+25	1.9132e+25

WARNING:

Method reached the maximum number of for harmonic order # 5.
It is possible that the iterative process is diverging for that harmonic order.
It is possible that the system is in resonance at 5 harmonic order.

Results showing bellow are without taking account of the harmonic orders: 5 ;

THD AT EACH NODE

Bus No	THD (%)		
	Phase A	Phase B	Phase C
1	0.0000e+00	0.0000e+00	0.0000e+00
2	4.0671e-02	2.3253e-02	1.4689e-03
3	1.5045e-01	8.7303e-02	5.3997e-03
4	2.0275e-01	1.1803e-01	7.2627e-03

>>

Profile Summary

Generated 07-Oct-2010 10:34:34 using *cpu* time.

Function Name	Calls	Total Time	Self Time *	Total Time Plot (dark band = self time)
method1	1	0.527 s	0.214 s	
fundamental_hPQ	1	0.128 s	0.057 s	
results_it	9	0.107 s	0.078 s	
genHA	9	0.036 s	0.021 s	
angle	309	0.036 s	0.036 s	
results_h	4	0.028 s	0.021 s	
genZ_h	1	0.021 s	0.021 s	
cell2mat	71	0.021 s	0.021 s	
total_res	1	0.021 s	0.021 s	
inputs_c	1	0.007 s	0.007 s	
carson	1	0.007 s	0.007 s	
kron	4	0.007 s	0.007 s	
genA_h	1	0.007 s	0.007 s	
HlineC	4	0.007 s	0.007 s	
configurations_h	1	0 s	0.000 s	
input_LINES	1	0 s	0.000 s	
HZSaux	9	0 s	0.000 s	
mat2cell	3	0 s	0.000 s	
pinv	5	0 s	0.000 s	

Self time is the time spent in a function excluding the time spent in its child functions. Self time also includes overhead resulting from the process of profiling.

B.3 Fundamental Power Flow Results for Weakly Meshed Network

BSF Iteration= 5 / Meshed Iteration= 1

LOADS CURRENTS

Bus No	pu	Phase A Degree
2	2.4778e-01	-17.7408
4	4.3847e-01	-2.2913
4	2.4413e-01	-35.2379
5	2.0855e-01	-20.3587
6	1.4349e-01	-23.3909
7	2.1169e-01	-20.2120
7	0.0000e+00	0.0000
5	0.0000e+00	0.0000

BRANCH CURRENTS

Branch No	A	Phase A Degree
1	610.2867	-17.3093
2	463.0173	-15.9902
3	147.7955	-21.4638
4	273.5017	-13.9503
5	86.8296	-20.3551
6	59.7429	-23.3857
7	88.1313	-20.2002

BUS VOLTAGES

Bus No	pu	Phase A Degree
1	1.0000e+00	0.0000
2	9.7387e-01	-0.1318
3	9.6651e-01	0.0199
4	9.5849e-01	-0.2459
5	9.7091e-01	-0.1339
6	9.6448e-01	0.0252
7	9.5652e-01	0.0129

BSF Iteration= 5 / Meshed Iteration= 2

LOADS CURRENTS

Bus No	pu	Phase A Degree
2	2.4828e-01	-17.7228
4	4.3937e-01	-2.2739
4	2.4413e-01	-35.2205
5	2.0922e-01	-20.3293
6	1.4232e-01	-23.4648

7	2.0910e-01	-20.3238
7	8.1450e-02	149.3185
5	8.1450e-02	-30.6815

BRANCH CURRENTS

Branch No	A	Phase A Degree
1	609.5506	-17.2997
2	496.7391	-16.9568
3	112.8759	-18.8336
4	273.8684	-13.9171
5	120.6209	-23.2226
6	59.2549	-23.4596
7	54.0412	-13.8259

BUS VOLTAGES

Bus No	pu	Phase A Degree
1	1.0000e+00	0.0000
2	9.7192e-01	-0.1138
3	9.7444e-01	-0.0540
4	9.5653e-01	-0.2285
5	9.6783e-01	-0.1044
6	9.7242e-01	-0.0488
7	9.6836e-01	-0.0989

BSF Iteration= 4 / Meshed Iteration= 3

LOADS CURRENTS

Bus No	pu	Phase A Degree
2	2.4826e-01	-17.7221
4	4.3933e-01	-2.2732
4	2.4413e-01	-35.2198
5	2.0919e-01	-20.3281
6	1.4237e-01	-23.4676
7	2.0919e-01	-20.3279
7	7.8615e-02	148.5790
5	7.8615e-02	-31.4210

BRANCH CURRENTS

Branch No	A	Phase A Degree
1	609.5755	-17.3006
2	495.4582	-16.9713
3	114.1773	-18.7539

4	273.8548	-13.9170
5	119.3829	-23.3493
6	59.2728	-23.4623
7	55.3343	-13.7736

BUS VOLTAGES

Bus No	pu	Phase A Degree
1	1.0000e+00	0.0000
2	9.7200e-01	-0.1131
3	9.7414e-01	-0.0567
4	9.5660e-01	-0.2278
5	9.6794e-01	-0.1033
6	9.7213e-01	-0.0515
7	9.6792e-01	-0.1031

BSF Iteration= 3 / Meshed Iteration= 4

LOADS CURRENTS

Bus No	pu	Phase A Degree
2	2.4826e-01	-17.7221
4	4.3934e-01	-2.2731
4	2.4413e-01	-35.2197
5	2.0919e-01	-20.3281
6	1.4236e-01	-23.4677
7	2.0919e-01	-20.3281
7	7.8725e-02	148.5815
5	7.8725e-02	-31.4185

BRANCH CURRENTS

Branch No	A	Phase A Degree
1	609.5747	-17.3006
2	495.5040	-16.9724
3	114.1304	-18.7497
4	273.8553	-13.9169
5	119.4288	-23.3517
6	59.2722	-23.4624
7	55.2889	-13.7607

BUS VOLTAGES

Bus No	pu	Phase A Degree
1	1.0000e+00	0.0000
2	9.7199e-01	-0.1131
3	9.7415e-01	-0.0568

```
4      9.5660e-01    -0.2277
-----
5      9.6794e-01    -0.1032
-----
6      9.7214e-01    -0.0516
-----
7      9.6794e-01    -0.1032
-----
```

```
*****
HARMONIC ORDER # 1
*****
```

```
-----
|No of ITERATIONS OF THE MESHED CYCLE           |    4 |
-----
|No of ITERATIONS OF THE  BFS CYCLE  FOR EACH MESHED CYCLE |
|                                                    |    4 |
-----
|                                                    |    4 |
-----
|                                                    |    3 |
-----
|                                                    |    2 |
-----
```

>>

Bibliography

- [1] J. Arrillaga, C. P. Arnold, and B. J. Harker, *Computer Modelling of Electrical Power Systems*. London: John Wiley & Sons, 1983.
- [2] J. Arrillaga, E. Acha, T. Densem, and P. Bodger, "Ineffectiveness of transmission line transpositions at harmonic frequencies," *Generation, Transmission and Distribution, IEE Proceedings C*, vol. 133, p. 99, march 1986.
- [3] J. Arrillaga and N. R. Watson, *Power System Harmonics*. John Wiley & Sons, 2nd ed., 2003.
- [4] J. Arrillaga, B. C. Smith, N. R. Watson, and A. R. Wood, *Power System Harmonic Analysis*. John Wiley & Sons, 1997.
- [5] G. Bathurst, N. Watson, and J. Arrillaga, "A harmonic domain solution for systems with multiple high-power ac/dc converters," *Generation, Transmission and Distribution, IEE Proceedings-*, vol. 148, pp. 312 –318, jul. 2001.
- [6] J. Bergeal and L. Moller, "Influence of load characteristic on the propagation of disturbances," *Proceedings of CIRED Conference*, 1981.
- [7] E. Bompard, E. Carpaneto, G. Chicco, and R. Napoli, "Convergence of the backward/forward sweep method for the load-flow analysis of radial distribution systems," *International Journal of Electrical Power & Energy Systems*, vol. 22, no. 7, pp. 521 – 530, 2000.
- [8] J. R. Carson, "Wave propagation in overhead wires with ground return," *Bell Systems Technical Journal*, vol. 5, pp. 539–554, 1926.
- [9] M.-S. Chen and W. Dillon, "Power system modeling," *Proceedings of the IEEE*, vol. 62, pp. 901–915, July 1974.
- [10] T.-H. Chen, M.-S. Chen, K.-J. Hwang, P. Kotas, and E. Chebli, "Distribution system power flow analysis—a rigid approach," *Power Delivery, IEEE Transactions on*, vol. 6, pp. 1146 –1152, jul 1991.
- [11] Y. Chen, Q. Chang, L. Qian, and N. Ma, "Studies on the sequence circuits of harmonics in three-phase power system," vol. 2, pp. 1243 –1248 vol.2, 2000.
- [12] C. S. Cheng and D. Shirmohammadi, "A three-phase power flow method for real-time distribution system analysis," *IEEE Transactions on Power Systems*, vol. 10, May 1995.

- [13] R. Chu and J. Burns, "Impact of cycloconverter harmonics," *Industry Applications, IEEE Transactions on*, vol. 25, pp. 427–435, may. 1989.
- [14] J. C. Das, *Power System Analysis. Short-Circuit Load Flow and Harmonics*. New York: Marcel Bekker, Inc., 2002.
- [15] R. C. Dugan, M. F. McGranahan, S. Santoso, and H. Wayne Beaty, *Electrical Power System Quality*. McGraw-Hill, 2nd ed., 2002.
- [16] P. Famuori and W. Cawthorne, "Power system harmonics," *Wiley Encyclopedia of Electrical and Electronics Engineering*, December 1999.
- [17] J. B. J. Fourier, *Théorie Analytique de la Chaleur*. 1822.
- [18] R. Galloway, W. Shorrocks, and L. Wedepohl, "Calculation of electrical parameters for short and long polyphase transmission lines," *Electrical Engineers, Proceedings of the Institution of*, vol. 111, pp. 2051–2059, december 1964.
- [19] S. Goswami and S. Basu, "Direct solution of distribution systems," *Generation, Transmission and Distribution, IEE Proceedings C*, vol. 138, pp. 78–88, jan 1991.
- [20] E. Gunther and M. McGranaghan, "Power measurements in distorted and unbalanced conditions-an overview of ieee trial-use standard 1459-2000," vol. 2, pp. 930–934 vol.2, jul. 2002.
- [21] T. F. on Harmonics Modeling and I. P. H. W. G. Simulation, "Characteristics and modeling of harmonic sources-power electronic devices," *IEEE Transactions on Power Delivery*, vol. 16, pp. 791–800, October 2001.
- [22] IEEE Distribution Planning Working Group Report, "Radial distribution test system," *IEEE Transactions on Power Systems*, vol. 6, pp. 975–985, August 1991.
- [23] IEEE Task Force on Harmonics Modeling and Simulation, "Modeling and simulation of the propagation of harmonics in electric power networks - part II : Sample systems and examples," *IEEE Transactions on Power Delivery*, vol. 11, p. 466, 474 1996.
- [24] IEEE Task Force on Harmonics Modeling and Simulation, "Modeling and simulation of the propagation of harmonics in modeling and simulation of the propagation of harmonics in electric power networks - part I: Concepts, models, and simulation techniques," *IEEE Transactions on Power Delivery*, vol. 11, pp. 452–464, January 1996.
- [25] W. H. Kerrsting, *Distribution System Modeling and Analysis*. CRC Press, 2nd ed., 2007.
- [26] W. H. Kerrsting, "The modeling and application of step voltage regulators," *Power Systems Conference and Exposition. IEEE/PES*, pp. 1–8, April 2009.
- [27] G. Kron, *Tensor Analysis of networks*. London: McDonal, 1965.
- [28] C. E. Lin, Y. W. Huang, and C. L. Huang, "Distribution system load flow calculation with microcomputer implementation," *Electric Power Systems Research*, vol. 2, pp. 139–145, October 1987.

- [29] J. Lundquist and M. Bollen, "Harmonic active power flow in low and medium voltage distribution systems," *Power Engineering Society Winter Meeting, 2000. IEEE*, vol. 4, pp. 2858–2863, 2000.
- [30] S. Mishra, "A simple algorithm for unbalanced radial distribution system load flow," in *TENCON 2008 - 2008 IEEE Region 10 Conference*, pp. 1–6, 19-21 2008.
- [31] J. A. Oliver, *Adjustable Speed Drives: Application Guide*. EPRI, Palo Alto, CS. Tech. Rep. TR-1011 140, December 1992.
- [32] D. Penido, L. Araujo, J. Pereira, P. Garcia, and S. Carneiro, "Four wire newton-rapshon power flow based on the current injection method," *Power Systems Conference and Exposition, 2004. IEEE PES*, vol. 1, pp. 239–242, October 2004.
- [33] J. A. Pesonen, "Harmonics, characteristic parameters, method of study, estimates of existing values in the network," *Electra*, vol. 77, pp. 35–54, 1981.
- [34] D. J. Pileggi, N. H. Chandra, and A. E. Emanuel, "Prediction of harmonic voltages in distribution systems," *IEEE Transactions on Power Apparatus and Systems*, vol. PAS-100, pp. 1307–1315, March 1981.
- [35] A. Ralston and P. Rabinowitz, *A first course in numerical analysis*. McGraw-Hill, 2nd ed., 1978.
- [36] P. Ribeiro, "Guidelines on distribution system and load representation for harmonic studies," in *Harmonics in Power Systems., ICHPS V International Conference on*, pp. 272–280, 22-25 1992.
- [37] P. F. Ribeiro, "Tutorial on power systems harmonics modeling and simulation," January 1999.
- [38] A. Semlyen, J. F. Eggleston, and J. Arrillaga, "Admittance matrix model of a synchronous machine for harmonic analysis," *IEEE Transactions on Power Systems*, vol. PWRS-2, pp. 833–839, November 1987.
- [39] V. Sharma, R. J. Fleming, and L. Niekamp, "An iterative approach for analysis of harmonic penetration in the power transmission networks," in *IEEE/PES 1991 Winter Meeting*, (New York), pp. 1698–1706, February 1991.
- [40] D. Shirmohammadi, H. Hong, A. Semlyen, and G. Luo, "A compensation-based power flow method for weakly meshed distribution and transmission networks," *Power Systems, IEEE Transactions on*, vol. 3, pp. 753–762, may 1988.
- [41] B. C. Smith, J. Arrillaga, A. R. Wood, and N. R. Watson, "A review of iterative harmonic analysis for ac-dc power systems," *Proceedings of the 7th International Conference on Harmonics and Quality of Power (ICHQP VII)*, October 1996.
- [42] W. Song, G. T. Heydt, and W. M. Grady, "The integration of hvdc subsystems into the harmonic power flow algorithm," *Power Engineering Review, IEEE*, vol. PER-4, pp. 31–31, aug. 1984.
- [43] R. P. Stratford, "Analysis and control of harmonic current in systems with static power converters," *IEEE Transactions on Industry Applications*, vol. IA-17,

- pp. 71–78, January/February 1981.
- [44] J.-H. Teng and C.-Y. Chang, “A fast harmonic load flow method for industrial distribution systems,”
 - [45] J.-H. Teng and C.-Y. Chang, “Backward/forward sweep-based harmonic analysis method for distribution systems,” *IEEE Transactions on Power Delivery*, vol. 22, July 2007.
 - [46] W. Tinney, “Compensation methods for network solutions by optimally ordered triangular factorization,” *Power Apparatus and Systems, IEEE Transactions on*, vol. PAS-91, pp. 123–127, Jan. 1972.
 - [47] M. Valcárcel and J. G. Mayordomo, “Harmonic power flow for unbalanced systems,” *IEEE Transactions on Power Delivery*, vol. 8, October 1993.
 - [48] D. Xia and G. Heydt, “Harmonic power flow studies part i - formulation and solution,” *IEEE Transactions on Power Apparatus and Systems*, vol. PAS-101, pp. 1257–1265, Jun. 1982.
 - [49] W. Xu, J. Marti, and H. Dommel, “A multiphase harmonic load flow solution technique,” *Power Systems, IEEE Transactions on*, vol. 6, pp. 174–182, Feb. 1991.
 - [50] W. Xu, J. E. Drakos, Y. Mansour, and A. Chang, “A three-phase converter model for harmonic analysis of hvdc systems,” *IEEE Transactions on Power Delivery*, vol. 9, pp. 1724–1731, July 1994.
 - [51] W. Xu, H. W. Dommel, M. Brent Hughes, G. W. K. Chang, and L. Tan, “Modelling of adjustable speed drives for power system harmonic analysis,” *IEEE Transactions on Power Delivery*, vol. 14, pp. 595–601, April 1999.
 - [52] F. Zhang and C. Cheng, “A modified newton method for radial distribution system power flow analysis,” *Power Systems, IEEE Transactions on*, vol. 12, pp. 389–397, Feb. 1997.
 - [53] X.-P. Zhang and H. Chen, “Asymmetrical three-phase load-flow study based on symmetrical component theory,” *IEE Proc.-Gener. Transm. Distrib.*, vol. 141, May 1994.
 - [54] R. Zimmerman and H.-D. Chiang, “Fast decoupled power flow for unbalanced radial distribution systems,” *Power Systems, IEEE Transactions on*, vol. 10, pp. 2045–2052, Nov. 1995.
 - [55] *Direct Current Transmission*, vol. I. Wiley & Sons, 1971.
 - [56] Cooper Power Systems, Inc., P.O. Box 2850, Pittsburgh, PA 15230, *How Step-Voltage Regulators Operate*, February 1993.
 - [57] “IEEE recommended practices and requirements for harmonic control in electrical power systems,” *IEEE Std 519-1992*, p. 0_1, 1993.
 - [58] *Power Electronics-Converters, Applications and Design*. John Wiley & Sons, 1995.